

Human serum glycome in health and disease

Inaugural-Dissertation
to obtain the academic degree
Doctor rerum naturalium (Dr. rer. nat.)

submitted to the Department of Biology, Chemistry and Pharmacy
of Freie Universität Berlin

by
TEREZA DĚDOVÁ

from Náchod
(Czech Republic)

2018

This work was performed between Sep-2014 and Oct-2018 under supervision of Prof. Dr. Véronique Blanchard at the Institute of Laboratory Medicine, Clinical Chemistry and Pathobiochemistry, Charité - Universitätsmedizin Berlin.

1st Reviewer: Prof. Dr. Véronique Blanchard

2nd Reviewer: Prof. Dr. Rudolf Tauber

date of defence: 29.03.2019

*I would like
to dedicate this thesis
to Adam*

“When you can’t run anymore you crawl. And when you can’t do that, well... yeah, you know the rest.”

— Joss Whedon

Acknowledgment

Firstly, I would like to thank Prof. Dr. Véronique Blanchard and Prof. Dr. Rudolf Tauber for their scientific support and guidance in the last few years.

Secondly, I would like to thank my colleagues, office-mates and friends for making the days better, brighter and louder. Namely, I would like to thank Dominique Petzold and Detlef Grunow for sharing their know-how and their help at the beginning of my studies. I want to thank Karina Biskup and Marta Wieczorek for many scientific and non-scientific discussions and for greatly improving my knowledge of polish language, to Christian Schwedler I owe thanks for his translations to German and for bearing with the rest of us at times we discussed a bit too loudly. Additionally, I want to thank all people who even only briefly came through our lab and enriched the environment.

I want to thank my family for supporting me my whole life: 'Děkuji vám za bezmeznou podporu po celý můj život. Ať už budu kdekoli, nikdy na vás nezapomenu.' My friends Martina Kosinová and Jana Štirandová I thank for being there for me regardless of the distance between us.

My last and biggest thanks and all my love belongs to my partner, my life companion, my sun and stars, Adam Streck. Thank you for carrying me.

Zusammenfassung

Die Glykosylierung ist eine wichtige posttranslationale Modifikation von löslichen- und membrangebundenen Proteinen. N-Glykane nehmen eine bedeutende Rolle in der Proteinfaltung, Proteinstabilität und -funktionen ein und haben entscheidenden Einfluss auf Prozesse wie Zellerkennung, Zell-Zell-Wechselwirkungen, Zell-Zell-Kommunikation und Adhesion. Änderungen in der Glykosylierung wurde in vielen pathologischen Prozessen, wie Entzündungen und Malignomen beobachtet, was zu Studien der N-Glykananalyse als potentiell diagnostische oder prognostische Biomarker geführt hat. Obwohl in diesem Zusammenhang mehrere Biomarker vorgeschlagen wurden, wurde der Einfluss prä-analytischer Bedingungen bezüglich der Ergebnisse unzureichend betrachtet. Ein Ziel dieser Arbeit war zu untersuchen, wie prä-analytische Variablen, beispielsweise die Gerinnungszeit, Ergebnisse beeinflussen können und zu falschen Schlussfolgerungen führen. Wir erwarteten, dass die Aktivität von Exoglykosidasen, wie Sialidasen und Mannosidasen, von der Lagerungszeit und Lagerungstemperatur bis zur Bearbeitung der Proben abhängig ist. Weiterhin wurde untersucht, ob sich die Komposition des Serum- und Plasmaglykoms, nach lytischer Freisetzung der Glykoproteine aus leukozytischen intrazellulären Organellen, ändert. Eine weitere potentielle Fehlerquelle können von der Erythrozytenoberfläche abgelöste Glykoproteine sein. Die N-Glykane von Serum- und Plasma-Glykoproteinen wurden enzymatisch mit PNGase F freigesetzt und volumenanteilig geteilt. Ein Teil wurde permethyliert und mit MALDI-TOF-MS analysiert, der andere Teil chemisch desialyliert, mit APTS derivatisiert und mittels CE-LIF gemessen. Die statistische Analyse wurde mit SPSS durchgeführt. Die Ergebnisse dieser Studie wurden als Empfehlung von prä-analytischen Bedingungen für die Glykomanalyse von humanem Serum und Plasma publiziert. Darüber hinaus werden nützliche Informationen für zukünftige Untersuchungen von glykanbasierten Biomarkern im gesunden Körper und bei Krankheiten bereitgestellt. Unsere Untersuchungen zeigten, dass hämolysierte Proben zu falschen Ergebnissen führen, sodass für den zweiten Teil dieser Arbeit ausschließlich nicht-hämolysierte Proben verwendet wurden.

Die Sialylierung ist von fundamentaler Bedeutung für das Verständnis der Ursachen und den pathologischen Änderungen des Serumglykoms. In humanem Blut und

Gewebe sind Sialinsäuren entweder α -2,3 oder α -2,6 mit den Galaktosen verknüpft. Da sie die am meisten exponierten Monosaccharide gegenüber der Umgebung sind, spielen sie eine Schlüsselrolle in vielen biologischen Prozessen, einschließlich der Karzinogenese. Bisherige Untersuchungen zeigten, dass eine Zunahme der Sialinsäuren im Serum-N-Glykom mit dem Ovarialkarzinom korreliert, jedoch wurden die Bindungstypen der Sialinsäuren von Serum-Glykoproteinen nicht untersucht. Die Arbeitsgruppe von Prof. Blanchard identifizierte kürzlich charakteristische Änderungen im Serumglykom, welche zu einem Wert (GLYCOV) kombiniert wurden und eine bessere diagnostische Leistung, für das epitheliale Ovarialkarzinom gegenüber dem routinemäßigen Serummarker CA125, selbst für Patientinnen im Frühstadium, zeigte. Der GLYCOV beinhaltet sieben sialylierte N-Glykane, jedoch wurden deren Bindungstypen bezüglich der Sialinsäuren bis jetzt nicht untersucht. In diesem Zusammenhang sollten aus einem Patienteninnenkollektiv mit epitheliale Ovarialkarzinom weitere Informationen hinsichtlich der Sialylierungsmuster generiert werden. Zunächst musste aus einer Vielzahl bislang veröffentlichter Methoden, eine geeignete Derivatisierung ausgewählt werden. Dazu wurden mehrere Methoden für ihre Verwendung der Ovarialkarzinom-Proben getestet und ausgewertet. Im Anschluss wurde die ausgewählte Methode verwendet, um die Sialylierung im Serum von Ovarialkarzinom-Patientinnen zu untersuchen.

Die Studie umfasste mehr als 100 Patientinnen mit allen FIGO Stadien (I, II, III und IV) sowie alterskorrelierten gesunden Kontrollen. Die N-Glykane von Serum-Glykoproteinen wurden mit PNGase F freigesetzt und mit 1-Hydroxybenzotriazol sowie 1-Ethyl-3-(3-(dimethylaminopropyl)carbodiimid als Aktivatoren der Amidierung derivatisiert. α -2,6-verknüpfte Sialinsäuren wurden mit Dimethylamin zu einem pH-stabilen Produkt amidiert, wohingegen α -2,3-verknüpfte Sialinsäuren mit der benachbarten Galaktose laktonisiert und anschließend mit Ammonium amidiert wurden. Die Analyse erfolgte mittels MALDI-TOF-MS und die statistische Auswertung wurde mit SPSS und MedCalc durchgeführt. Dabei sollten die Ergebnisse hinsichtlich der Verknüpfung von Sialinsäuren für eine verbesserte Diagnostik des Ovarialkarzinoms abgeschätzt und evaluiert werden. Die beobachteten Unterschiede des Sialylierungsverhältnisses von α -2,3/ α -2,6-Sialylierung ermöglichte, in Kombination mit dem routinemäßig verwendeten Ovarialkarzinom Biomarker CA125, eine verbesserte

Diagnostik mit einer Sensitivität von 89.6 % und Spezifität von 100%. Unter alleiniger Verwendung von CA125 konnte eine Sensitivität von 84.4% und Spezifität von 97% erzielt werden.

Abstract

Glycosylation is an important post-translational modification of both soluble and membrane-bound proteins. N-Glycans have a significant role in protein folding, protein stability and functions, as well as cell recognition, cell-cell interactions, cell-cell communication and adhesion. Changes in glycosylation were observed in many pathological processes, for example inflammation and malignancies, which had led to studies of N-glycans as potential diagnostic or prognostic biomarkers. While several biomarkers have been suggested, there has been a lack of studies on how preanalytical conditions influence the results of glycomic studies. One aim of this thesis was to investigate how preanalytical variables such as time of coagulation can influence the results and bring to inaccurate conclusions. I expected that the activity of exoglycosidases such as sialidases and mannosidases depend on the time and temperature at which the samples are stored before being processed. In addition, it was investigated how the composition of the serum/plasma glycome is modified when glycoproteins from intracellular cell organelles are released from leukocytes that are undergoing lysis. Another potential source of errors could be the shedding of cell surface glycoproteins from erythrocytes. Glycoproteins from serum/plasma released by PNGase F digestion and part of the N-glycan pool was permethylated and analyzed by MALDI-TOF-MS and the rest of the pool was chemically desialylated, derivatized with APTS and measured by CE-LIF. Statistical analysis was performed with SPSS. The results of experiments were published as recommendations for the preanalytical conditions for glycome analysis in human serum and plasma. This study provided useful information to the future use of glycan-based biomarkers in health and disease and for the second part of this study. The investigation showed that samples, which are hemolysed, might provide inaccurate results, thus only non-hemolysed samples were used for the second part of this thesis.

Sialylation is of fundamental importance for understanding the causes and pathological alterations of the serum glycome. In human blood and tissues, sialic acids are either α -2,3- or α -2,6-linked to galactoses. As they are the most exposed monosaccharides to the outer environment, they play a key role in many biological processes including cancerogenesis. To date, although increases of sialic acids in the serum glycome have been

correlated with ovarian cancer, the type of sialic acid linkage on serum glycoproteins has not been investigated. The group of Prof. Dr. rer. nat. Blanchard recently identified characteristic changes of the serum glycome that were combined in a score named GLYCOV that could diagnose primary epithelial ovarian cancer in a better way than CA125 the routine serum marker even for early stage patients. GLYCOV contains seven sialylated N-glycans but the type of sialic acid linkage has not been investigated yet. The second aim of this thesis was to obtain information about sialylation patterns from a cohort of more than 100 ovarian cancer patients regarding sialic acid linkages. Firstly, a suitable derivatisation had to be selected from a wide range of previously published methods. Multiple methods were tested and evaluated for their use with ovarian cancer samples. Secondly, the selected method was applied to investigate the type of sialylation in the serum of epithelial ovarian cancer.

A cohort of more than 100 patients including FIGO stages I, II, III and IV as well as age-matched controls was enrolled in this study. Glycoproteins from serum were released by PNGase F digestion and the N-glycan pool was derivatized using 1-hydroxybenzotriazole and 1-ethyl-3-(3-(dimethylamino)propyl)-carbodiimide as activators for amidation. α -2,6-Linked sialic acids were amidated with dimethylamine forming pH stable products, while the α -2,3-linked sialic acids were lactonized with the neighboring galactose and subsequently amidated with ammonia and measured by MALDI-TOF-MS. Statistical analysis was performed with SPSS and MedCalc to evaluate if the information regarding sialylation linkage enables improvement in ovarian cancer diagnostic. The observed differences in α -2,3/ α -2,6-sialylation ratio in combination with routinely used ovarian cancer biomarker CA125 enabled improved ovarian cancer diagnostic with sensitivity and specificity of 89.6% and 100%, respectively. CA125 alone showed sensitivity of 84.4% and specificity of 97%.

Publication list

Publications included in this thesis:

Dědová T, Grunow D, Kappert K, Flach D, Tauber R, Blanchard V. **The effect of blood sampling and preanalytical processing on human N-glycome.** *PLoS One*. 2018 Jul 11;13(7):e0200507. DOI: <https://doi.org/10.1371/journal.pone.0200507>

Dědová T, Braicu, E.I., Sehouli, J., Tauber R, Blanchard V. **Sialic acid linkages in ovarian cancer.** *Manuscript in preparation.*

Publications not included in this thesis:

Montacir H, Freyer N, Knöspel F, Urbaniak T, Dedova T, Berger M, Damm G, Tauber R, Zeilinger K, Blanchard V. **The Cell - Surface N - Glycome of Human Embryonic Stem Cells and Differentiated Hepatic Cells thereof.** *ChemBioChem*. 2017 Jul 4;18(13):1234-41. DOI: <https://doi.org/10.1002/cbic.201700001>

Abbreviations

2-AB	2-aminobenzamide
α -2,3-SiaLacNAc	3'-Sialyl-N-acetyllactosamine
α -2,6-SiaLacNAc	6'-Sialyl-N-acetyllactosamine
A	α -2,3-linked sialic acid - amidated
ACN	acetonitrile
APTS	8-aminopyrene-1,3,6-trisulfonic acid
CA125	cancer antigen 125
CE	capillary electrophoresis
CFG	Consortium for Functional Glycomics
CHCA	α -cyano-4-hydroxycinnamic acid
CID	collision-induced dissociation
CRT	calreticulin
D	α -2,6-linked sialic acid - dimethylamidated
DCC	N,N'-Dicyclohexylcarbodiimide
DH	dextran hydrolysate
DHB	2,5-dihydroxybenzoic acid
DMA	dimethylamine
DMSO	dimethylsulfoxide
DMT-MM	4-(4,6-dimethoxy-1,3,5-triazin-2-yl)-4-methylmorpholinium chloride
Dol	dolichol pyrophosphate
DTE	dithioerythritol
EDT	1-ethyl-3-(3-(dimethylamino)propyl)-carbodiimide
EDTA	ethylenediaminetetraacetic acid
Endo H	endoglycosidase H
EOF	electroosmotic flow
ER	endoplasmic reticulum
EtOH	ethanol
Fuc, F	fucose
FucT	fucosyltransferase
Gal, G	galactose
GalNAc	N-acetylgalactosamine
Glc	glucose
GlcNAc	N-acetylglucosamine
GLYCOV	glycan-based biomarker for ovarian cancer developed in the group of Prof. Blanchard
H	hexose
HE4	human epididymis protein 4
HILIC	hydrophilic interaction liquid chromatography
HOBt	1-hydroxybenzotriazole
HPLC	high-performance liquid chromatography
IAA	iodoacetamide
L	α -2,3-linked sialic acid - lactonised
LC	liquid chromatography

LFA	<i>Limax flavus</i> agglutinin
LIF	laser-induced fluorescence
MAA	<i>Maacki amurensis</i> agglutinin
MAG	myelin-associated glycoprotein
MALDI	matrix-assisted laser desorption/ionisation
Man, M	mannose
MetOH	methanol
MS	mass spectrometry
N	N-acetylhexosamine
Neu5Ac, S	N-acetylneuraminic acid
Neu5Gc	N-glycolylneuraminic acid
OST	oligosaccharyltransferase
PGC	porous graphitised carbon
PNA	peanut agglutinin
PNGase	peptide-N4-(acetyl- β -glucosaminy) asparagine amidase
PTM	post-translational modification
SDS	sodium dodecyl sulphate
SNA	<i>Sambucus nigra</i> lectin
SPE	solid-phase extraction
ST3Gal	α 3-sialyltransferase
ST6Gal	α 6-sialyltransferase
ST8Sia	α 8-sialyltransferase
STn	Sialyl-Thomsen-nouveau antigen
TACA	tumour-associated carbohydrate antigen
T _{JT}	Jonckheere-Terpstra test
TOF	time-of-flight

Table of content

CHAPTER 1 GENERAL INTRODUCTION	15
Glycosylation	16
Biosynthesis of <i>N</i> -Glycans	18
Sialic acids	20
Sialic acids in immunity	23
N-Linked glycosylation in cancer	24
CHAPTER 2 GLYCOANALYTICAL METHODS AND MATERIALS	28
N-Glycan release	29
Reductive amination.....	30
Purification methods	31
Permethylation.....	32
Analytical methods	32
Data analysis	35
Materials and equipment.....	37
CHAPTER 3 SCIENTIFIC GOAL	40
CHAPTER 4 THE EFFECT OF PREANALYTICAL CONDITIONS ON RESULTS OF N-GLYCAN ANALYSIS	43
Background.....	44
Materials and methods.....	46
Results	50
Discussion.....	63
CHAPTER 5 COMPARISON OF METHODS TO DETERMINE SIALIC ACID LINKAGES	65
Background.....	66
Materials and methods.....	71
Results	73

Conclusion.....	83
CHAPTER 6 SIALIC ACID-LINKAGES IN OVARIAN CANCER	84
Background.....	85
Materials and methods.....	87
Results	90
Discussion.....	109
CHAPTER 7 GENERAL CONCLUSION	112
LIST OF REFERENCES	115
APPENDIX	130

Chapter 1

General introduction

Glycosylation

Glycosylation is one of the many observed co- and post-translational modifications (PTM) of proteins and lipids, such as phosphorylation, sulfation, acetylation and others, however, due to the number of enzymes involved in glycan production and lack of templates, glycosylation is among the more complicated PTMs [1, 2]. On the protein level, glycosylation plays an important role in protein folding, protein stability and functions [2]. For example, a large glycan content protects proteins from protease activity due to steric hindrance or gain of negative charge [3]. On the cellular level, glycans are densely coating the cell surface forming “glycocalyx”, which is involved in processes such as cell recognition, cell-cell interactions, cell-cell communication and adhesion [3]. These glycans are involved in immune processes [4-9], such as T-cells interactions with an infected cell [10].

N-Linked glycosylation occurs at Asn residues of a sequon Asn-X-Ser/Thr via an *N*-glycosidic bond, where X is any amino acid except from Pro [11]. However, various amino acids at the X position result in various efficiencies of core glycosylation [12]. Additionally, it was reported that the amino acid following this sequence (sometimes referred to as Y) plays also a role in the efficiency of core glycosylation [13, 14].

Only one acidic monosaccharide *N*-acetylneuraminic acid (Neu5Ac) and six neutral monosaccharides: hexoses glucose (Glc), galactose (Gal), and mannose (Man); *N*-acetylhexoses *N*-acetylglucosamine (GlcNAc) and *N*-acetylgalactosamine (GalNAc); and deoxyhexose fucose (Fuc) are used in humans to synthesise diverse *N*-glycans and *O*-Glycans. A second acidic monosaccharide *N*-glycolylneuraminic acid (Neu5Gc) is observed in mammalian *N*-glycans and in some cancers [15]. Monosaccharides commonly observed in mammalian *N*-glycans together with their notations as proposed by Consortium for Functional Glycomics (CFG) are shown in Figure 1 [16].

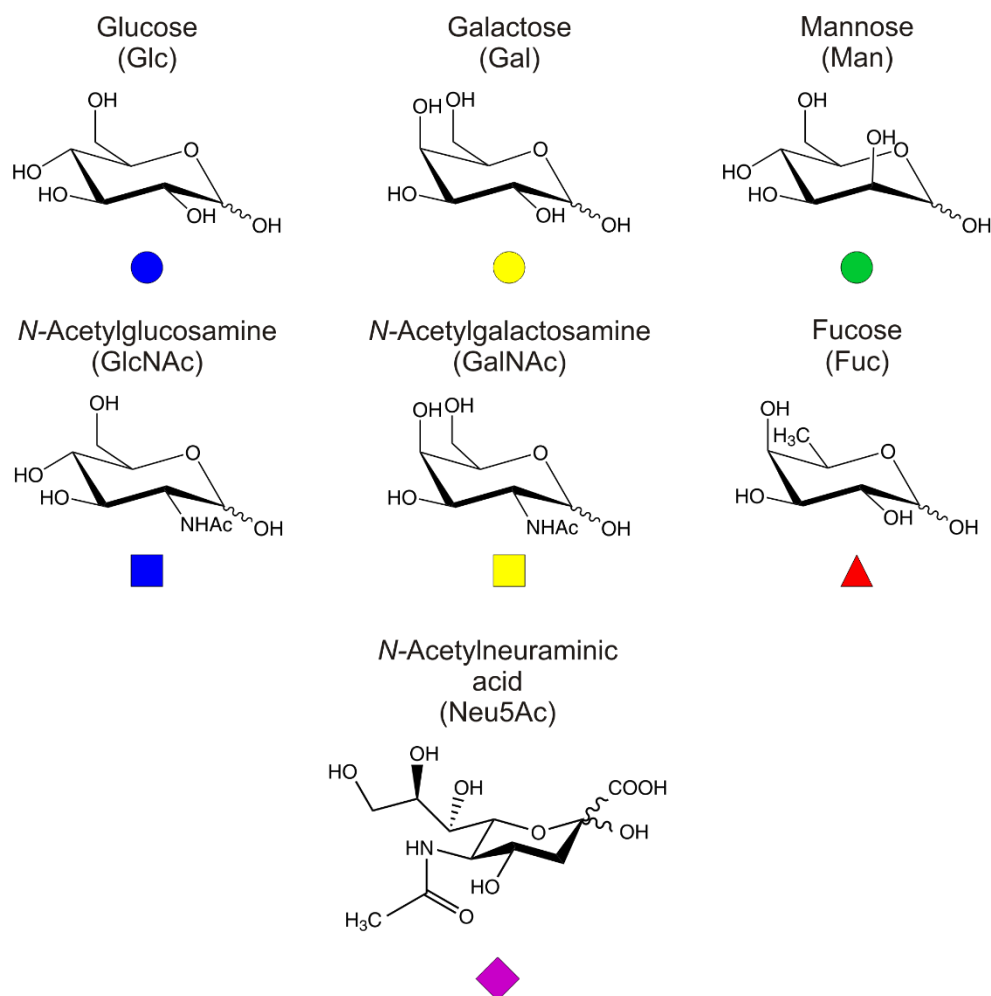


Figure 1 Monosaccharides and their corresponding CFG notations.

All glycans have the same core structure, consisting of two GlcNAc residues and three mannose residues ($\text{Man}_3\text{GlcNAc}_2$). Additional residues are attached to this core structure, forming three *N*-glycan types (Figure 2). When only mannose residues are added to the core, high-mannose glycans are formed. Complex-type *N*-glycans result from the addition of GlcNAc residues, giving antennae. And finally, hybrid *N*-glycans are formed when one arm contains only mannose residues and the second arm contains one or two antenna(e) [11].

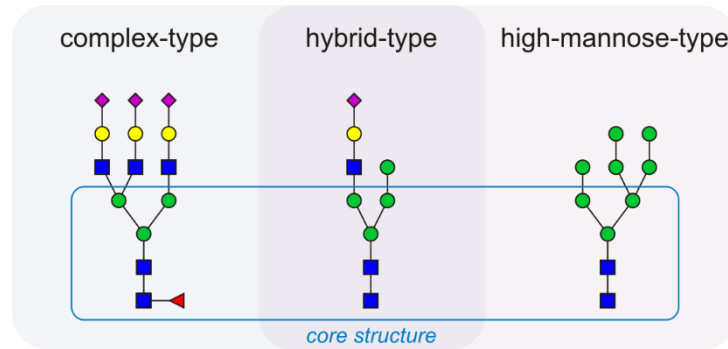


Figure 2 *N*-glycan types.

Biosynthesis of *N*-Glycans

The first seven steps of *N*-glycan biosynthesis (Figure 3) occur on the cytoplasmic side of the endoplasmic reticulum (ER) membrane. Monosaccharides first need to be activated into sugar nucleotide donors. The biosynthesis of *N*-glycans begins with the synthesis of dolichol pyrophosphate *N*-acetylglucosamine (Dol-P-P-GlcNAc) by reaction of UDP-GlcNAc with Dol-P catalysed by enzyme GlcNAc-1-phosphotransferase and is crucial in early embryogenesis [17]. The second GlcNAc residue is transferred by GlcNAc-transferase followed by five additions of mannose residues catalysed by enzymes Man-transferases. The resulting Man₅GlcNAc₂-P-P-Dol is then transferred to the lumen of the ER by a Man₅-GlcNAc₂-P-P-Dol flippase [18].

This Man₅GlcNAc₂-P-P-Dol is further extended in the lumen of ER by stepwise addition of four more Man residues transferred from Man-P-Dol and three Glc residues from Glc-P-Dol donors, producing an oligosaccharide made of 14 monosaccharides, namely the *N*-glycan precursor Glc₃-Man₉GlcNAc₂-P-P-Dol. There are three additional flippases involved in the *N*-glycan biosynthetic pathway – two transferring Dol-P bound monosaccharides to the lumen of ER (Man-P-Dol flippase and Glc-P-Dol flippase) and Dol-P-P flippase, which returns Dol-P back to the cytosolic side, where it can further participate in new biosynthetic cycles [18]. The Dol-bound monosaccharides are synthesized on the cytoplasmic side of the ER from Dol-P and either GDP-Man or UDP-Glc, these are then flipped and used in the ER lumen by their respective glycosyltransferases.

The *N*-glycan precursor $\text{Glc}_3\text{-Man}_9\text{GlcNAc}_2\text{-P-P-Dol}$ can be then transferred to a Asn-X-Ser/Thr sequon of a newly synthesised protein by the enzyme complex oligosaccharyltransferase (OST). Subsequently, the first two Glc residues are trimmed by α -glucosidase I and α -glucosidase II. At this point, the lectin chaperones calnexin and calreticulin (CRT) in complex with ERp57 interact with the nascent glycoprotein and initiate protein folding in a “calnexin cycle”. Incompletely folded glycoproteins are re-glucosylated and re-enter the cycle. Properly folded glycoproteins are trimmed again in the ER by α -glucosidase II and α -mannosidase, removing the last Glc and the Man residue of the middle arm, respectively.

This $\text{Man}_8\text{GlcNAc}_2$ -protein is transferred to the Golgi apparatus, where α -mannosidases IA-IC remove three Man residues, forming Man_5NAc_2 -protein, which serves in the *medial*-Golgi as a precursor structure for the synthesis of complex and hybrid *N*-glycans. Thereafter, a GlcNAc residue is added to the α 1-3 mannose of the precursor structure by the enzyme *N*-acetylglucosaminyltransferase-I (GlcNAcT-I) and $\text{GlcNAcMan}_3\text{GlcNAc}_2$ is then formed by cleavage of the remaining two Man residues at α 1-3 and α 1-6 positions, which is catalysed by α -mannosidase II.

Hybrid *N*-glycans are the result of incomplete processing by this enzyme. The production of complex-type *N*-glycans continues with an addition of a second GlcNAc to the α 1-6-linked core Man, and further branching can be achieved by activities of GlcNAc-T-IV and GlcNAc-T-V, resulting in tri- and tetraantennary *N*-glycans. Additionally, so-called bisecting *N*-glycans are formed by an activity of the enzyme GlcNAc-T-III, which adds GlcNAc to the first Man of the core.

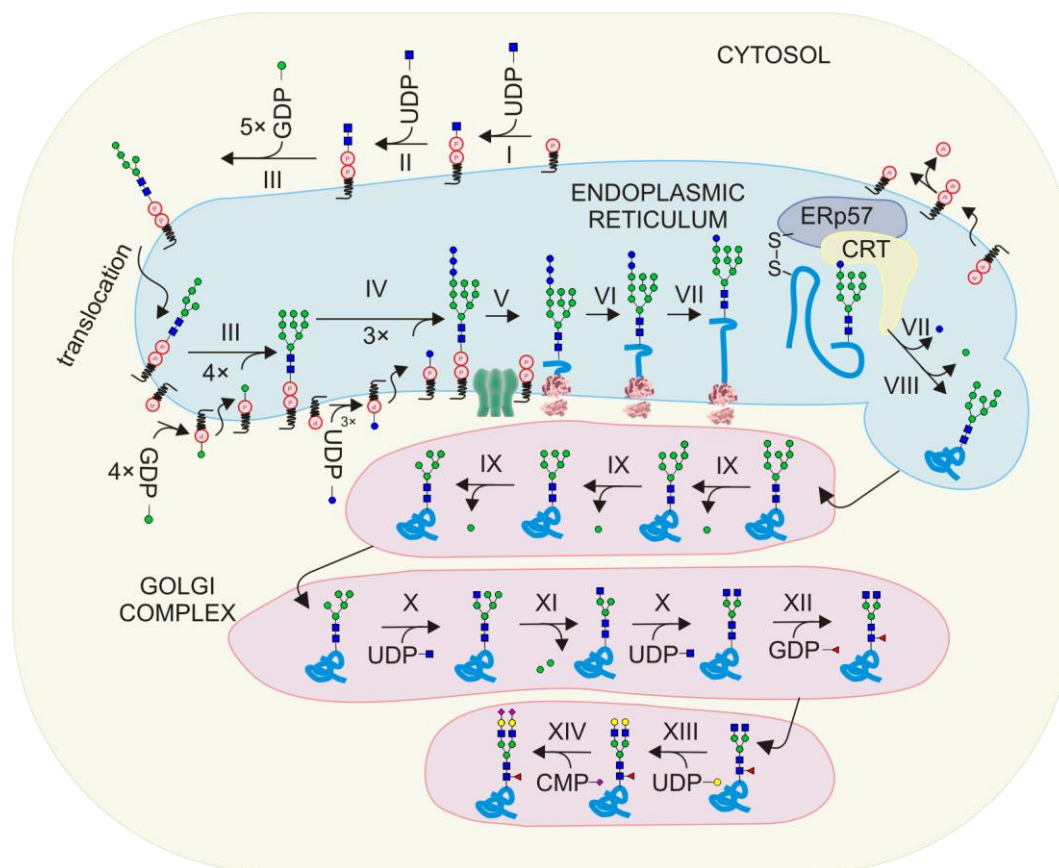


Figure 3 N-Glycan biosynthesis pathway occurring in the endoplasmic reticulum and in the Golgi complex. I - GlcNAc-1-phosphotransferase, II - GlcNAc-transferase, III - Man-transferase, IV - Glc-transferase, V - Oligosaccharyl transferase, VI - α -Glucosidase I, VII - α -Glucosidase II, VIII - ER α -Mannosidase, IX - Golgi α -Mannosidase I, X - GlcNAc-transferase I, XI - Golgi α -Mannosidase II, XII - Fuc-transferase, XIII - Gal-transferase, XIV - Sia-transferase.

In the *trans*-Golgi, N-glycans can be further elongated and capped by activity of galactosyltransferases and sialyltransferases, which add to the glycan heterogeneity. Specific sialyltransferases will be addressed in more detail in the next chapter.

Sialic acids

The term sialic acids covers a family of over 50 monosaccharides most commonly found on the non-reducing termini of glycan chains, which are diverse both in structure and linkage [19, 20]. The most common sialic acid is N-acetyl-neuraminic acid (Neu5Ac) – a 9-carbon acidic sugar with a N-acetyl group at the C-5 position. This C-5 position can naturally be hydroxylated instead, creating 2-keto-3-deoxynononic acid (Kdn).

Alternatively, in *N*-glycolylneuraminic acid (Neu5Gc) the 5-*N*-acetyl group is hydroxylated (Figure 4).

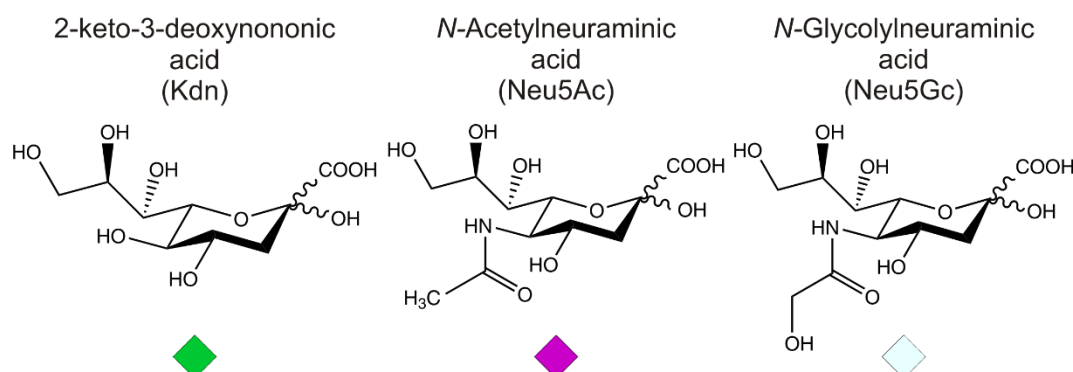


Figure 4 Chemical structures and CFG notations of sialic acids.

Other modifications, such as *O*-acetylation, *O*-sulfation, *O*-methylation and others are possible on positions C-4, C-7, C-8 and C-9, leading to great diversity. Most commonly, the C-2 position forms α linkages between sialic acid and other carbohydrates in reactions catalysed by enzymes called sialyltransferases, which will be introduced later in this chapter.

CMP-Sialic acid biosynthesis

As briefly mentioned before, the glycan biosynthetic pathway requires all monosaccharides to be activated to form of a sugar nucleotide. In the case of sialic acids, cytidine triphosphate serves as activator and resulting CMP-NeuAc is used as a donor for sialyltransferase reactions in the Golgi apparatus. The *de novo* production of CMP-Neu5Ac (Figure 5), the most common sialic acid, is initiated by production of *N*-acetylmannosamine (ManNAc) from UDP-*N*-acetylglucosamine (UDP-GlcNAc) [21]. Bacteria can convert ManNAc to Neu5Ac in a condensation reaction with phosphoenolpyruvate, which is catalysed by NeuNAc synthase [22].

In mammals, the produced ManNAc is firstly phosphorylated by ManNAc kinase to give ManNAc-6-phosphate (ManNAc-6-P), which then reacts with phosphoenolpyruvate, similarly to the bacterial pathway, to form *N*-acetylneuraminic acid-9-phosphate (NeuAc-9-P), in a reaction catalysed by NeuAc-9-P synthase [23]. In the next step, NeuAc-9-

P is dephosphorylated by NeuAc-9-P phosphatase to Neu5Ac. In the last step CMP-sialic acid synthetase catalyses the reaction of CTP with Neu5Ac forming CMP-Neu5Ac, which then diffuses from the nucleus to the cytoplasm, from where it is specifically transported by CMP-sialic acid transporter (CST) into the lumen of the Golgi apparatus, where Neu5Ac is added to nascent carbohydrate chains.

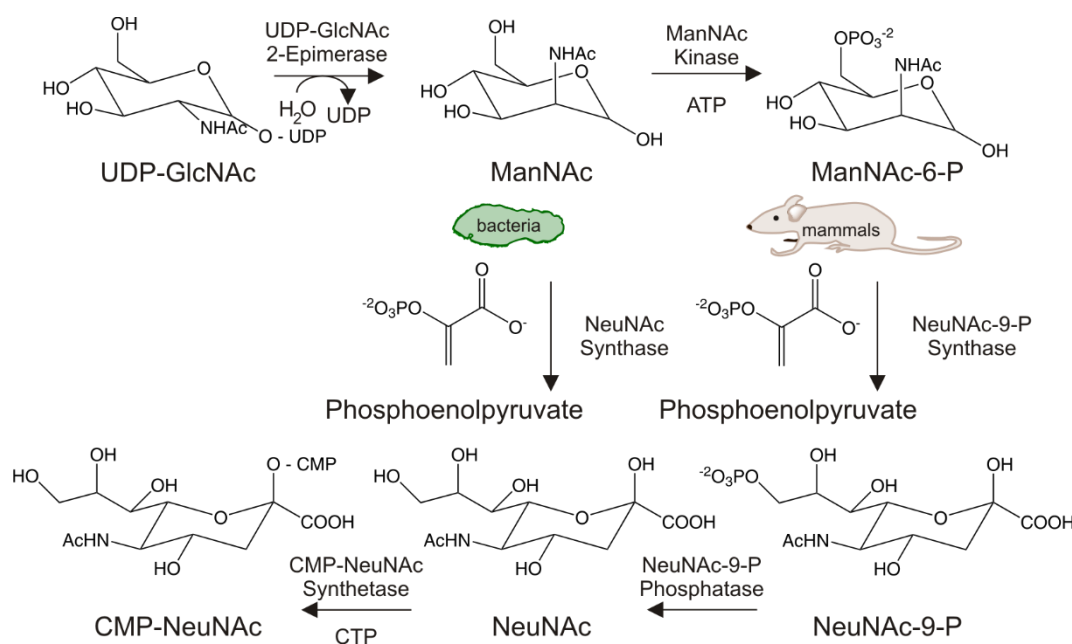


Figure 5 Sialic acid synthesis in bacteria and mammals.

Human sialyltransferases

CMP-Sialic acid transfer to a terminal Gal (or less often GalNAc residue) is mediated by enzymes named sialyltransferases. Mammalian sialyltransferases are Golgi membrane-bound proteins of type II; The mammalian sialyltransferase family has more than 20 members, which are generally linkage and substrate specific [24]. The α 6-sialyltransferases (ST6Gal I, II) and α 3-sialyltransferases (ST3Gal I-VI) facilitate the transfer of CMP-sialic acid to a terminal Gal with an α -2,6-linkage and α -2,3-linkage, respectively. Alternatively, α -2,6-linkage of sialic acids to GalNAc by ST6GalNAc I-V was described in O-glycans and gangliosides [24-26]. Production of polysialic acids is mediated by α 8-sialyltransferases (ST8Sia I-V), which specifically elongate the previously α -2,3-linked Neu5Ac to Gal (Figure 6).

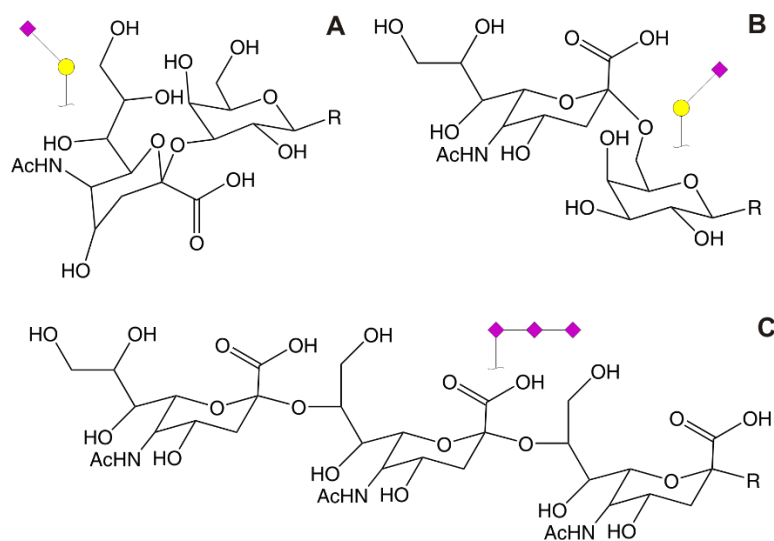


Figure 6 Chemical structures and CFG notations of A) α -2,3-linked Neu5Ac to Gal, B) α -2,6-linked Neu5Ac to Gal and C) poly- α -2,8-Neu5Ac.

Sialic acids in immunity

Due to their universal occurrence on the surface of cells and their negative charge, sialic acids alter cell biophysical properties, for example contributing to the hydrophilicity and negative charge repulsion between cells [6]. Sialic acids, located at the termini of N-glycans, are recognisable by various receptors and glycan binding proteins, such as *siglecs* (sialic acid-recognising Ig-superfamily lectins), these interactions then mediate inter- and intra-cellular communications, especially by cells of the hematopoietic system [5, 27]. Siglecs contribute to the interactions of both innate and adaptive immunity system [28]. The first four discovered siglecs were sialoadhesin (Siglec-1; CD169), which was found on macrophages to form rosettes with sheep erythrocytes [29] and having similar sequence as other members of immunoglobulin superfamily CD22 (Siglec-2) [30], CD33 (Siglec-3) [31], and myelin-associated glycoprotein (MAG; Siglec-4) [32]. All these molecules recognise sialic acid; however, their specificities differ [33]. For example, CD22 recognises the α -2,6-linked sialic acid, but does not show binding to α -2,3-linked sialic acids, whereas oligo- and polysialic acids are specifically recognised by Siglec-7 and Siglec-11 [28].

The complement system has a very important role in pathogen recognition and opsonization and consists of three pathways – the classical pathway, the lectin pathway and

the alternative pathway [34]. Sialic acids contribute to the regulation of complement system in multiple ways. Firstly, sialic acids on the surface of cells interact with the regulatory protein factor H, thus recognise cells as “self” and protect the cell surface from the alternative complement pathway [6, 35]. The complement factor H recognises α -2,3-linked sialic acids [36] and is itself mostly α -2,6-sialylated [37]. Secondly, sialic acids also contribute to the innate immune system by inhibition of complement C3 activation [38]. On the other hand, the lectin pathway is initiated when ficolins (oligomeric lectins) recognise sialic acids on pathogen surfaces [34, 39].

N-Linked glycosylation in cancer

Altered glycosylation has been observed in cancer, such as increased branching, fucosylation and sialylation [40, 41]. Increased branching has been associated with metastasis [42] and in breast and colon cancer correlated with the disease stage [43]. Fucosylation, which results from the activity of eleven different transferases, has been thoroughly studied in the context of cancer [44, 45]. Fucosyltransferases can connect fucose to nascent glycans via four different types of linkages: α -1,2 (FucT1 and 2), α -1,3 and α -1,4 (FucT3-7 and 9) and core α -1,6 (FucT8) [44]. Miyoshi *et al.* [45] reported increased expression of α 1-6FucT in multiple cell lines, namely lung, gastric and colon cancer. Kyselova *et al.* [46] observed increased sialylation and fucosylation together with a decrease of smaller *N*-glycan structures during breast cancer progression. Increase of antennarity and fucosylation has been also observed by Biskup *et al.* in ovarian cancer serum [47, 48] and ascites [49]. On the other hand, high-mannose structures were decreased in both ovarian cancer sera and ascites [47-49]. Interestingly, De Leoz *et al.* observed increased high-mannosylation in breast cancer in mouse and human sera when only neutral *N*-glycans were measured [50].

Sialylation in cancer

As already mentioned, sialic acids are widely expressed on physiologically normal cells and proteins. However, in carcinogenesis, mechanisms causing abnormal sialylation were described [51]. Firstly, increased expression and/or changed activity of sialyltransferases were reported in carcinomas. For example, increased expression of

ST6Gal-I was reported for acute myeloid leukaemia [52], some brain tumours [53], breast carcinoma [54], cervical carcinoma [55], choriocarcinoma [56], colorectal carcinoma [57] and ovarian cancer [58, 59]. For example, pro-apoptotic galectin functions are negatively regulated by α -2,6-linked sialic acids [60].

Addition of sialic acids leads to non-specific charge repulsion effects, preventing cell-cell interactions [60]. In ovarian cancer cells, ST6Gal-I overexpression induces invasive phenotype due to increased sialylation of β_1 integrins, which leads to increasing cell motility [61]. Additionally, ST6Gal-I contributes to the resistance of tumour cells to treatment [62, 63]. Britain *et al.* reported that increased α -2,6-sialylation of receptor tyrosine kinase EGFR by ST6Gal-I inhibits Gefitinib-mediated apoptosis, therefore leads to increased tumour cell survival [62]. Cui *et al.* published that higher expression of ST6Gal-I in cancer stem-like cells in colorectal carcinoma resulted in poorer 5-year survival rates of patients due to contributions to chemo-resistance [63].

Changes in expression of not only sialyltransferases but also other glycosyltransferases lead to the production of abnormal structures known as tumour-associated carbohydrate antigens (TACA) [5]. Reports have linked the occurrence of certain TACAs to increased metastatic potential, for example SLe^x and SLe^a, which serve as antigen for E-selectins and promote adhesion to vascular endothelium [64, 65]. Production of SLe^{x/a} is a result of combined increased expression of FucT and ST3Gal and was described for example in breast cancer [66]. Ricardo *et al.* [67] reported higher expression of SLe^a and SLe^x on mucins MUC16 and MUC1 in serous ovarian tumours.

Sialyl-Thomsen-nouveau antigen (STn), described on O-glycans as sialylated Tn (Ser/Thr-GalNAc), is correlated with increased cancer invasion and metastasis [68]; and relationship has been found between its expression and resistance to adjuvant chemotherapy [69]. The sialylated glycosphingolipid ganglioside GD2 and its precursor GD3 were overexpressed in breast cancer and other cancers, however, their function is not clear [70].

In the last decade, TACAs were widely investigated for their potential in development of cancer vaccines and cancer immunotherapies [71-74]. Unfortunately, the immune response to TACAs is T-cell-independent and thus approaches to improve their

immunogenicity were implemented. One promising option, tested in a clinical phase 1 study, is to use TACAs bound to peptides [73].

Thirdly, even though humans are not able to synthesise Neu5Gc due to exon deletion in the CMAH gene encoding CMP-Neu5Ac-hydroxylase, Neu5Gc acquired from dietary sources can be processed and presented on cell surfaces. This process is not observed in normal human tissues but does occur in cancer cells [75]. It was reported that the main source of dietary Neu5Gc is red meat, namely beef and pork, but also in goat's milk cheese as well as caviar [76] and that chronic inflammation might be enhanced in Neu5Gc-positive tumours in the presence of anti-Neu5Gc antibodies [77]. In humans, organ accumulated Neu5Gc and long-term inflammation exposure lead to increased cancer incidence in the colon, prostate and ovary [76].

Ovarian cancer markers

Serum tumour markers are used not only for screening and differential diagnosis, but also serve as prognostic markers and are used to monitor treatment response and recurrence. The most commonly used tumour marker for ovarian cancer is a glycoprotein, specifically a peptide epitope of mucin 16 (MUC16) also known as cancer antigen 125 (CA125) [78]. CA125 is detected using monoclonal antibody OC125 as capture antibody in combination with detection antibody. The clinically used cut-off value is 30-35 U/ml [78]. The CA125 marker shows a specificity of 94-98.5%, but has rather low sensitivity (50-62% for early stage epithelial ovarian cancer) [79]. This limits its use for screening in asymptomatic women. Elevation of CA125 concentration (CA125 >35 U/ml) was observed in other malignancies, for example liver, pancreas, biliary tract, lung, endometrial and other [79]. Additionally, other non-malignant conditions such as cirrhosis, endometriosis, acute and chronic salpingitis, acute and chronic pancreatitis, and more show elevated concentrations of CA125 [79].

Another clinically used ovarian cancer marker is human epididymis protein 4 (HE4), which shows better sensitivity than CA125 in terms of distinguishing benign disease from malignant tumour [80]. It was reported that the combination of CA125, HE4 and so-called

Symptom index [81], which is a survey-based index evaluating patients physical symptoms in the past year, has a sensitivity of 84% and a specificity of 98.5% [82].

Biskup *et al.* [47, 48] introduced a glycan-based biomarker for ovarian cancer (GLYCOV) in 2013. In the first discovery study [47], the biomarker, based on the ratio between relative intensities of seven sialylated structures and four high-mannose structures, was established from a cohort of 63 primary ovarian cancer patients and 33 age-matched healthy controls. The GLYCOV score diagnosed ovarian cancer patients with the same sensitivity as CA125 (97%), but showed a greater specificity of 98.4%, while CA125 had a specificity of 88.9%. In the second study [48] the GLYCOV score was used to recognise a cohort of 20 early stage ovarian cancer patients from 20 patients with benign ovarian diseases and 33 healthy controls. It was again superior to CA125 in distinguishing early stage ovarian cancer from benign diseases.

Chapter 2

Glycoanalytical methods and materials

N-Glycan release

It is possible to analyse the N-glycome on the glycopeptide level with the use of liquid chromatography mass spectrometry (LC-MS) or matrix-assisted laser desorption/ionisation time of flight mass spectrometry (MALDI-TOF-MS). However, to easily analyse N-glycans from various sources, these are initially cleaved from intact or reduced protein by either chemical or enzymatic methods. Hydrazinolysis as a method to release glycans from glycoproteins was introduced in 1993 by Patel *et al.* [83]. Anhydrous hydrazine is used to non-specifically cleave N- and O-glycans from glycoproteins, which also de-acetylates N-acetyl groups on N-glycans. As a result, they consequently need to be re-N-acetylated with the use of acetic anhydride in NaHCO₃. Both N- and O-glycans can be also cleaved by oxidative release with the use of NaClO [84]. Moreover, this method enables also the release of glycosphingolipid-derived glycans (GSL-glycans). However, authors warn that this method can cause partial degradation of primary amines and sulfhydryl groups.

Enzymatic release

The biggest advantage of enzymatic N-glycan release is its specificity. The enzymatic N-glycan release is often performed on previously denatured protein, to enable sufficient access to the glycosylation site. These methods include treatment with anionic detergent (for example sodium dodecyl sulphate; SDS) at higher temperature (>50°C) followed by non-ionic, non-denaturing detergent (such as IGEPAL® CA-630) [85]. Another option is the disruption of disulphide bridges with the use of reducing agent, for example dithioerythritol (DTE) and subsequent alkylation, which stabilises the unfolded glycoprotein. Enzymatic digestions, compared to chemical release, are substrate-specific. While by chemical digestion O-glycans are also released, enzymes cleave specifically N-glycans, while O-glycans remain intact. Additionally, this enables the release of various glycan types and therefore can lead to a better identification of diverse structures having the same mass. For example, the enzyme endoglycosidase H (Endo H) cleaves specifically high-mannose and hybrid-type N-glycans [86]. The most commonly used endoglycosidase peptide-N4-(acetyl-β-glucosaminyl)

asparagine amidase F (PNGase F) facilitates the cleavage of all three *N*-glycan types unless the core is α -1,3-fucosylated, in which case PNGase A can be used [87].

PNGase F is secreted by *Flavobacterium meningosepticum*, which specifically cleaves the glycosidic bond between the Asn side chain and the first GlcNAc, thus producing ammonia and a free *N*-glycan, and then converts Asn to Asp (Figure 7). This conversion can be also used for the analysis of glycosylation sites by protein sequencing before and after PNGase F treatment.

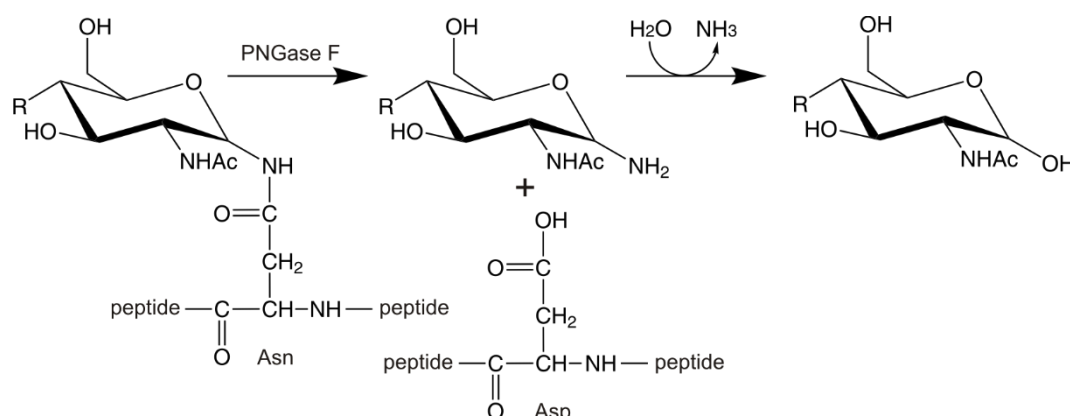


Figure 7 PNGase F-mediated enzymatic release.

Reductive amination

To detect glycans with methods such as capillary electrophoresis equipped with laser induced fluorescent detection (CE-LIF), it is necessary to label analytes with a fluorescent label, such as 8-aminopyrene-1,3,6-trisulfonic acid (APTS) [88] and 2-aminobenzamide (2-AB) [89]. Released *N*-glycans are labelled by reductive amination at their reducing end. In other words, the primary amine of the APTS forms a Schiff's base by condensation with the aldehyde group of the *N*-glycan, followed by reduction with sodium cyanoborohydride (Figure 8). The resulting labelled *N*-glycan gains a triple-negative charge from the APTS label, which is utilised during electrophoretic separation.

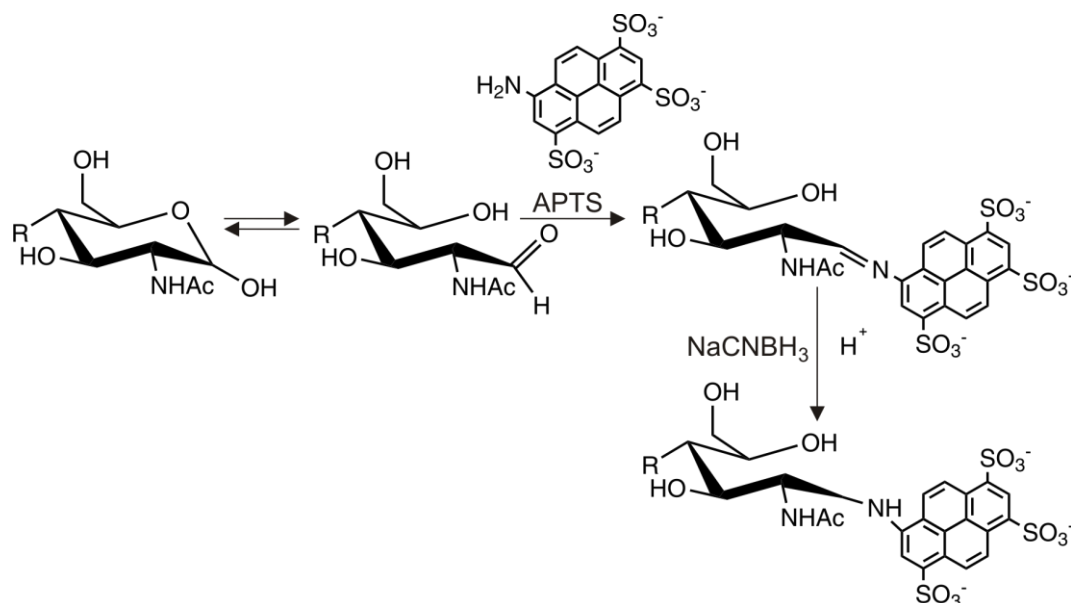


Figure 8 APTS labelling of free *N*-glycans by reductive amination.

Purification methods

Purification methods are of high importance in glycoanalytical techniques, since impurities such as excess of reagents or salts can disturb or completely hinder detection. Firstly, after *N*-glycan release, free *N*-glycans must be separated from proteins and/or peptides. Solid-phase extraction (SPE) is often used for this purpose. Reversed-phase chromatography utilising C18 as stationary phase is often applied for the separation of hydrophilic *N*-glycans from hydrophobic proteins [90]. While proteins adsorb to the C18 stationary phase, *N*-glycans do not interact.

Porous graphitised carbon (PGC) columns are then used for the subsequent desalting of *N*-glycan samples, which interact with the column surface, while salts and excess of reagents are washed away [90]. Elution of *N*-glycans is then performed by increasing the concentration of organic solvent with addition of acid for the recovery of charged *N*-glycans. PGC can be also used to purify glycans than underwent reductive amination, for instance via APTS or 2-AB labelling.

Hydrophilic interaction liquid chromatography (HILIC) is another widely used purification technique. HILIC consists of hydrophilic stationary phases, such as Sepharose, cotton [85, 91] or hydrophobic polypropylene [92] used with reversed-phase eluents (often

acetonitrile). It is increasingly used in glycoanalytical studies due to its cost-effectivity and easy transfer to a high-throughput setup. Any other polar surfaces can serve as stationary phases, for example amide, cationic and zwitterionic bonded phases [93].

Permethylation

In order to analyse negatively charged glycans by MALDI-TOF-MS without loss of sialic acids, some form of stabilisation is required. One of the most used reactions is permethylation, which converts all hydroxyl groups into methyl esters [90, 94]. Permethylation is a two-step reaction. Firstly, in the presence of sodium hydroxide in dimethylsulfoxide (DMSO), alcohols are transformed to alcoholates, which are subsequently methylated with methyl iodide. This derivatisation leads to +14.02 Da mass increase per hydroxyl/amine group (Table 1). The permethylation reaction not only stabilises sialic acids, but also improves ionisation.

Table 1 Residue masses of native and permethylated monosaccharides as part of oligosaccharides.

Monosaccharide	Native	Permethylated
Deoxyhexose (F; Fuc)	146.078	174.089
Hexose (H; Gal, Man)	162.053	204.099
N-Acetylhexosamine (N; GlcNAc)	203.079	245.126
N-Acetylneuraminic acid (S; Neu5Ac)	291.095	361.173
N-Glycolylneuraminic acid (Neu5Gc)	307.090	391.184

Analytical methods

MALDI-TOF-MS

For MALDI-TOF-MS experiments, a sample is co-crystallised with a matrix, which is a low molecular weight substance able to absorb the laser wavelength and transfer the excess of energy to the sample, which then becomes ionised [95]. Some of the most used matrices in glycobiology are 2,5-dihydroxybenzoic acid (DHB), super DHB (sDHB; a 9:1 mixture of DHB and 2-hydroxy-5-methoxybenzoic acid) and α -cyano-4-hydroxycinnamic

acid (CHCA). MALDI-TOF-MS analyses require low amount of sample and can tolerate impurities, such as salts to a certain content [96].

MALDI is so-called “soft” ionisation technique, which means that it produces molecular ions without unwanted fragmentation. During the ionisation, singly charged molecule ions are observed, such as $[M+Na]^+$, $[M+H]^+$ and $[M+K]^+$. Uniform adducts can be achieved by addition of low concentrations of salts to the matrix. During the time-of-flight (TOF) separation, ions are accelerated in an electric field, giving ions the same kinetic energy [97]. Ions travel at different velocities proportionally to their masses, thus molecules with lower mass travel at higher velocities, causing them to reach the detector faster than larger molecules (Figure 9) [97].

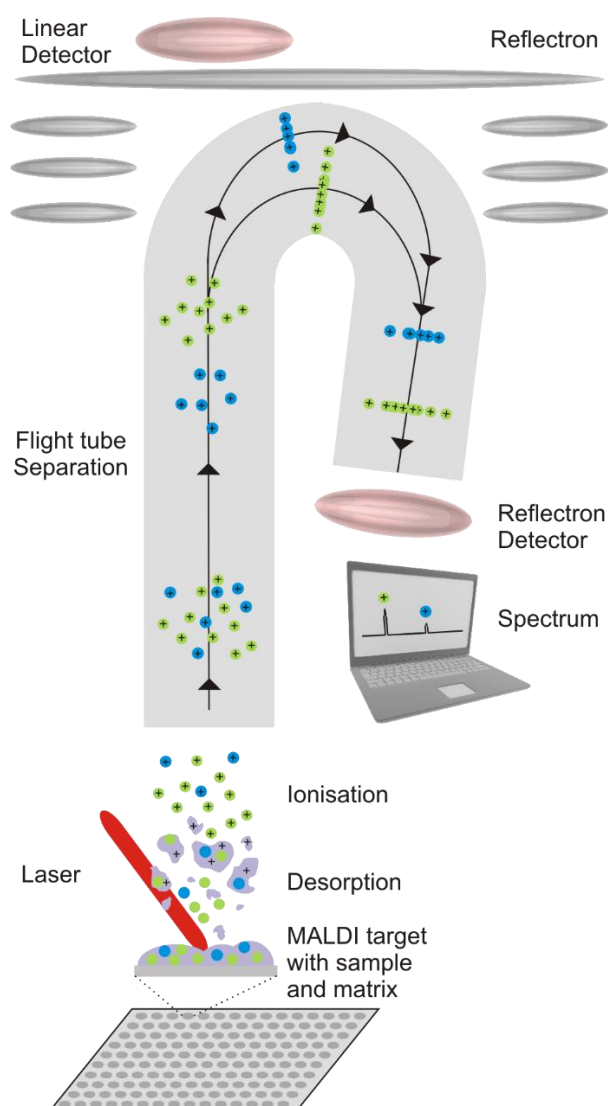


Figure 9 Schematics of the MALDI-TOF-MS instrument and measurement procedure.

In tandem mass spectrometry (MS/MS) a high-energy collision-induced dissociation (CID) is used to produce fragments, which is a useful tool for the differentiation between glycan isomers having the same mass [98, 99].

Capillary electrophoresis

Electrophoresis is an analytical separation technique, which allows an efficient separation of molecules due to their different charge and size in an electric field [100]. Electrophoretic separations of *N*-glycans are used less frequently than techniques such as high-performance liquid chromatography (HPLC), nevertheless provide similar information in terms of isomeric separations and offer some advantages compared to HPLC techniques, for instance high sensitivity even when lower volumes of sample are used, and generally shorter analysis times. The separation itself is performed in a capillary of small inner diameter (from 20 to 100 μm) and the outer diameter of 350–400 μm , whose both ends are placed in vials of buffer solution together with electrodes connected to a high voltage power supply (Figure 10).

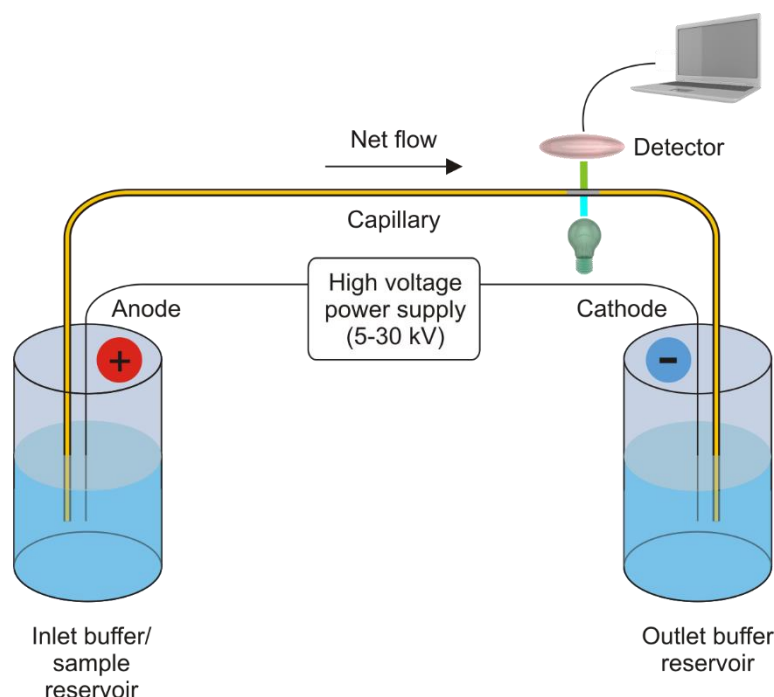


Figure 10 Scheme of capillary electrophoretic apparatus and its components.

In capillary electrophoresis (CE), electrophoretic separations can be influenced by the composition of the sample/analyte itself, of the buffer, by the strength of electric field and by the capillary wall. The analyte is separated based on its size and shape, net charge and mass. The mobility of the ion is proportional to its charge and disproportional to the half of the diameter of the molecule and the viscosity of the electrolyte [100]. The most important properties of the buffer system influencing the electrophoretic separation are ionic strength, viscosity and pH of the buffer [100]. The strength of electric field is dependent on the applied voltage as well as on capillary length. The efficiency is proportional to an applied electric field and a total mobility of a particle [100, 101]. When a higher electric field is applied, an electrolyte migrates faster through the capillary. Therefore, the shorter the analysis time the less analytes may diffuse. Lastly, the charge of capillary surface and its coating contribute to the changes in electroosmotic flow (EOF) [100]. The surface of capillaries can be modified either by covalent binding such as polyvinyl alcohols for analysis of carbohydrates or acrylamide for capillary isoelectric focussing, or by dynamic coating [100, 102]. Using these modifications EOF can be reduced or even completely reversed [103].

Data analysis

With the increased popularity of international and multi-center studies [104-107], high-throughput methods are on the rise [85, 107-111], enabling fast analysis of hundreds of samples simultaneously, thus moving the bottleneck of the scientific procedure towards data analysis. While most analytical procedures were in recent years fully or partially automated [108, 112, 113], the availability of tools enabling fast automated analysis of data to scientists with no to little background in computer science is still limited. While all instruments come equipped with vendor software, their applications are restricted to basic operations and often cannot be performed in batch format. The example of vendor software is Bruker Flex Analysis (Bruker Daltonics, Bremen, Germany) for mass spectrometry instruments and Karat 32 (Beckman Coulter, Fullerton, CA, USA) for Beckman P/ACE MDQ capillary electrophoresis system. Since the demand for more powerful software is quite high, a number of programs have become available, most of them under free or open-source licensing. For example, the analytical software for mass spectrometric data mMass [114]

supports wide range of formats. It provides many features from basic spectrum viewer to more advanced data processing tools, such as calibration, smoothing and baseline subtraction. Additionally, there are options to create average or summed spectra from multiple samples, providing visual comparisons of individual sample groups. Other features include automatic annotations based on custom lists. Similar feature is provided by the software Glycoworkbench [115, 116], which enables spectra annotations with CFG notations, however operates only in single sample format.

While the above mentioned software used in combination provide a complete workflow from raw data import to visualisation, the most versatile option for data sorting, manipulation and visualisation still remains the use of programming languages and environments such as Python [117].

Two Python scripts for targeted peak extraction of MALDI-TOF-MS spectra were published in recent years by Reiding *et al.* [85] and Jansen *et al.* [118]. Both enable fast calculation of areas under the curve based on a list of compositions from hundreds of samples in minutes. The first script utilises standard Python libraries Math [119], Os [120] and Time [121] and enables targeted peak extraction of areas under the curve and noise correction. The second more complex script additionally provides a calibration option based on a list of known masses, in low-mass, mid-mass and high-mass range. This function had been missing in the first script and this step needed to be performed by other software in the past, such as vendor programs, prior to data export. Additionally, the usage is more user-friendly, since the package Tkinter [122] is used and thus a graphical user interface is provided. Other packages used in this script are SciPy [123, 124], NumPy [125] and matplotlib [126]. Results provided by the data analysis include absolute and relative areas of individual glycan peaks (user defined) with and without baseline correction, and multiple quality control scores, such as signal-to-noise (S/N) ratio of the analyte and individual isotopes. In the end, results are exported in a text-file enabling easy processing.

Materials and equipment

Centrifuges

Minifuge (VWR, Germany),

Vacuum centrifuge Univapo 150 ECH (Uniequip, Germany).

Other equipment

Analytical scale (Sartorius, Germany),

Cold trap Unicryo MC2 x 21-60°C (Uniequip, Germany),

Incubator 1000 (Dionex, Germany),

MALDI-TOF/TOF-MS Mass spectrometer Ultraflex III with smartbeam-II TM Laser (Bruker Daltonics, Germany),

pH-Meter pH211 (Hanna Instruments, Germany),

Thermomixer comfort (Eppendorf, Germany),

Ultrasonic bath, Sonorex TK52 (Bandelin, Germany),

Vacuum pump (Vacuubrand, Germany),

Water purification system MilliQ Plus (Millipore, Germany).

Reagents

All aqueous solutions were prepared using Milli-Q grade (18.2 MΩ at 25 °C) water. All used chemicals are listed here:

1-hydroxybenzotriazole (HOBT, Sigma-Aldrich, Germany),

1-ethyl-3-(3-(dimethylamino)propyl)-carbodiimide (EDT, Fluorochem, U.K.),

8-Aminopyrene-1,3,6-trisulfonic acid trisodium salt (APTS, Sigma-Aldrich, Germany),

Disodium phosphate (Carl Roth, Germany),

Dithioerythritol (DTE, Sigma-Aldrich, Germany),

Iodoacetamide (IAA, Sigma-Aldrich, Germany),

Monosodium phosphate (Merck Millipore, Germany),

Nonidet P-40 (NP-40, (Calbiochem, CA, USA)
Sodium chloride (Carl Roth, Germany),
Sodium dodecyl sulphate (SDS, Merck Millipore, Germany),
Sodium hydroxide (Merck Millipore, Germany),
Super-DHB (Sigma-Aldrich, Germany).

Solvents

Acetic acid (Merck Millipore, Germany),
Acetonitrile (ACN, VWR Chemicals, Germany),
Ammonium hydroxide solution (25 %) (Merck Millipore, Germany),
Ammonium hydroxide solution (28-31 %) (Merck Millipore, Germany),
Chloroform (Merck Millipore, Germany),
Dimethyl sulfoxide water free (DMSO, Applichem, Germany),
Ethanol (EtOH, Merck Millipore, Germany),
Methanol (MeOH, Merck Millipore, Germany),
Trifluoroacetic acid (TFA, Merck Millipore, Germany).

Enzymes

Peptide-N⁴-(N-acetyl- β -glucosaminyl)asparagine amidase F (250 mU/mL, Roche Diagnostics, Germany).

Standards

3'-Sialyl-N-acetyllactosamine (Sigma-Aldrich, Germany),
6'-Sialyl-N-acetyllactosamine sodium salt (Sigma-Aldrich, Germany),
Dextran hydrolysate prepared in-house from Dextran (DH, Oxford, UK),
Maltose (Sigma-Aldrich, Germany).
Consumables
C18 Reversed-phase Extract-Clean column (Grace Alltech, IL, USA),
Carboglyph Extract-Clean column (Grace Alltech, IL, USA),
Filter tips (Greiner Bio-One, Germany),

GHP membrane 96-well filter microplate (Pall Corporation, MI, USA).

Methods

Since the methods used in this thesis vary based on the final application, they will be presented separately in each chapter.

Chapter 3

Scientific goal

Changes in glycosylation were reported for malignancies and other pathological conditions and several glycan-based biomarkers were proposed in recent years. In general, *N*-glycans are commonly analysed by MALDI-TOF-MS, CE-LIF and HPLC. While analytical methods are always tested for repeatability and reproducibility, there has been a lack of publications aimed at the influence of preanalytical conditions. In routine laboratories the effect of preanalytical conditions on the results of clinical tests is strictly tested. However, similar experiments were not yet reported for glycomic studies. Thus, the first aim of this thesis was to provide recommendations and standardized protocols for the future use of glycan-based biomarkers. A systematic study of preanalytical conditions was performed on both human plasma and serum. Samples were collected in 11 sample collection tubes and processed to create 16 unique conditions, mimicking possible processing errors and approaches. The changes were introduced exclusively during the preanalytical laboratory phase, while the analytical processes were identical for all conditions. The measurements were performed by MALDI-TOF-MS and CE-LIF.

The findings from this section were applied further in Chapter 4 *The effect of preanalytical conditions on results of N-glycan analysis* of this thesis and were published as recommendations for the preanalytical conditions for glycome analysis in human serum and plasma.

Sialylation is of fundamental importance for understanding the causes and pathological alterations of the serum glycome. In human blood and tissues, sialic acids are either α -2,3- or α -2,6-linked to galactoses. In Chapter 5 *Comparison of methods to determine sialic acid linkages* of this thesis a suitable method had to be selected from a wide range of previously published techniques for the derivatisation of sialic acids enabling the differentiation of linkage type. Since most of the published methods were intended for other use than labelling of released *N*-glycans, modifications were needed to allow measurements of serum *N*-glycome. Three methods were tested and evaluated for use with healthy controls and ovarian cancer samples. The selected method was further validated for both intra- and interday repeatability. Additionally, the technical repeatability of MALDI-TOF-MS measurements was evaluated.

The group of Prof. Blanchard recently identified characteristic changes of the serum glycome that were combined in a score named GLYCOV that could diagnose primary

epithelial ovarian cancer in a better way than CA125 the routine serum marker even for early stage patients. GLYCOV contains seven sialylated *N*-glycans but the type of sialic acid linkage has not been investigated yet. Sialic acids are the most exposed monosaccharides to the outer environment, playing a key role in many biological processes including cancerogenesis. Thus, the method selected in Chapter 5 was applied in Chapter 6 *Sialic acid-linkages in ovarian cancer* to investigate the type of sialylation in the serum of epithelial ovarian cancer patients. A cohort of more than 100 patients in FIGO stages I-IV as well as age-matched healthy controls was enrolled in this study. Labelled samples were measured by MALDI-TOF-MS and *N*-glycan levels as well as the type of sialylation were compared between healthy controls and ovarian cancer patients. Moreover, observed changes in sialylation were evaluated for their potential to improve diagnostic power of routinely used ovarian cancer biomarker CA125.

Chapter 4

The effect of preanalytical conditions on results of *N*-glycan analysis

The content of this chapter has been adapted from the research article:

Dědová T, Grunow D, Kappert K, Flach D, Tauber R, Blanchard V. **The effect of blood sampling and preanalytical processing on human N-glycome.** *PloS one.* 2018 Jul 11;13(7):e0200507.

Licensed under CC BY 4.0. The original version can be found under DOI: [10.1371/journal.pone.0200507](https://doi.org/10.1371/journal.pone.0200507)

Background

Number of studies established that observed changes in N-glycome are not only of pathogenic importance but can be used as diagnostic biomarkers. In particular, some glycome variations are a hallmark of malignancy and certain glycome modulations were reported as cancer-specific or cancer-associated [46, 127-131]. An example of such a biomarker based on glycan traits is the GLYCOV index score, developed in our laboratory, which combines both qualitative and quantitative changes in serum N-glycome of patients suffering from epithelial ovarian cancer [47, 48]. It provided superior accuracy, sensitivity and specificity even for early-stage patients when compared with the established tumour marker CA125.

There are several well-established techniques, which are being used for glycoanalytical studies, such as MALDI-TOF-MS, CE-LIF and HPLC [107, 132]. Over 15,000 PubMed entries in the past ten years can be found for glycan biomarkers, but the preanalytical conditions of MALDI-TOF-MS and CE-LIF glycome analysis have never been reported in detail. As previously reported for peptide profiling, glycome profiles can also be influenced by preanalytical variables and lead to inaccurate results [133-135]. Glycoanalytical investigations of large numbers of samples have been performed in recent years because of newly published methods for high-throughput analysis [47, 108, 132]. These studies often utilise samples from various collection sites and biobanks, therefore increasing the variables in preanalytical processing, such as times and temperatures between blood collection and centrifugation. Moreover, the type of transportation method introduces various physical conditions, such as shaking by pneumatic tube system, which can lead to haemolysis [136, 137].

There were reports about intra-individual stability of the glycome over time, investigating the influence of the lifestyle, medical treatment or environment [138, 139]. Ventham and co-authors [140] reported that there is a very small effect of manufacturing of collection tubes, tube volume and serum tube additives, on results of HPLC measurements of human serum N-glycome. Unfortunately, other more detailed investigations were not available in the literature. It can be assumed that there might be an effect of the temperature, the sample and the time until storage and/or measurement on the activity of enzymes

(exoglycosidases and glycosyltransferases, such as sialidase, mannosidase and sialyltransferase). It can be expected that, similar to proteomics [133, 134], the influence of sample freezing could lead also to glycan degradation. Moreover, additional changes of the serum glycome could occur during the preanalytical phase, since glycoproteins may be released from intracellular organelles or by shedding of the cell surface of leukocytes and erythrocytes. Therefore, in this work, the effect of blood collection, e.g. type of collection tubes as well as time and temperature before sample processing and storage on the N-glycome were evaluated systematically for the first time using blood samples from healthy volunteers and analysed with MALDI-TOF-MS and CE-LIF techniques.

Materials and methods

Sample collection

Ten healthy female donors, aged 20-30 years (median = 25, mean = 25.4) donated blood with the ethical approval of the Charité Medical University EA1/175/14. Collection tubes S-Monovette (Sarstedt, Germany) were used for all samples (Table 2).

Table 2 List of serum and plasma collection tubes.

Tube Nr.	Tube	Separator	Clot activator	Anticoagulant
A-D	S-Monovette® 4.9ml Z	None	Silicate beads	None
E	S-Monovette® 4ml Z-Gel	Polyacrylic ester gel	Silicate beads	None
F	S-Monovette® 9ml Z	None	Silicate beads	None
G-H, K	S-Monovette® 5ml 9NC	None	None	Citrate
I	S-Monovette® 4.9ml K3E	None	None	K3 EDTA
J	S-Monovette® 4.9ml LH	None	None	Lithium heparin

Tubes containing various anti-coagulants were used for plasma collection, namely tripotassium ethylenediaminetetraacetic acid (K3EDTA; n = 1; Tube I), lithium heparin (n = 1; Tube J) trisodium citrate solution (n = 3; Tubes G, H, K) for each donor. Serum samples were all collected in clot-activating tubes, of which five contained silica-covered beads (Tubes A-D) and one silica-covered beads and separation gel (Tube E). Two types of collection methods were used for the citrated plasma samples, namely by free flow (Tubes H and K) and by vacuum collection (Tube G). All other samples were collected by free flow only. Collections were performed in two sets of five donors six months apart.

Preanalytical processing

All samples were kept in an up-right position except for centrifugation. The processing resulted in 16 different conditions per donor (Figure 11). Reference conditions, which represent the ideal handling without delays, were prepared for both serum and plasma by processing tubes F and H, respectively. Samples were kept for 0.5 h at RT. They were then centrifuged for 15 minutes at 1500×g, aliquoted immediately after centrifugation

and stored at -80°C , unless stated otherwise. Multiple conditions were created from tubes F and K.

The influence of delayed processing was inspected by keeping three serum collection tubes at room temperature for 2 h (Tube A) and 6 h (Tube B) and at 4°C for 2 h (Tube C) before centrifugation for 15 min at $1500\times g$ at 4°C . Seven tubes (D-J) were centrifuged using the same centrifugal settings after the recommended storage for 30 min at room temperature. All samples were aliquoted after centrifugation, with the exception of tubes D and E, which additionally stayed at room temperature for 6 h, then were aliquoted and stored.

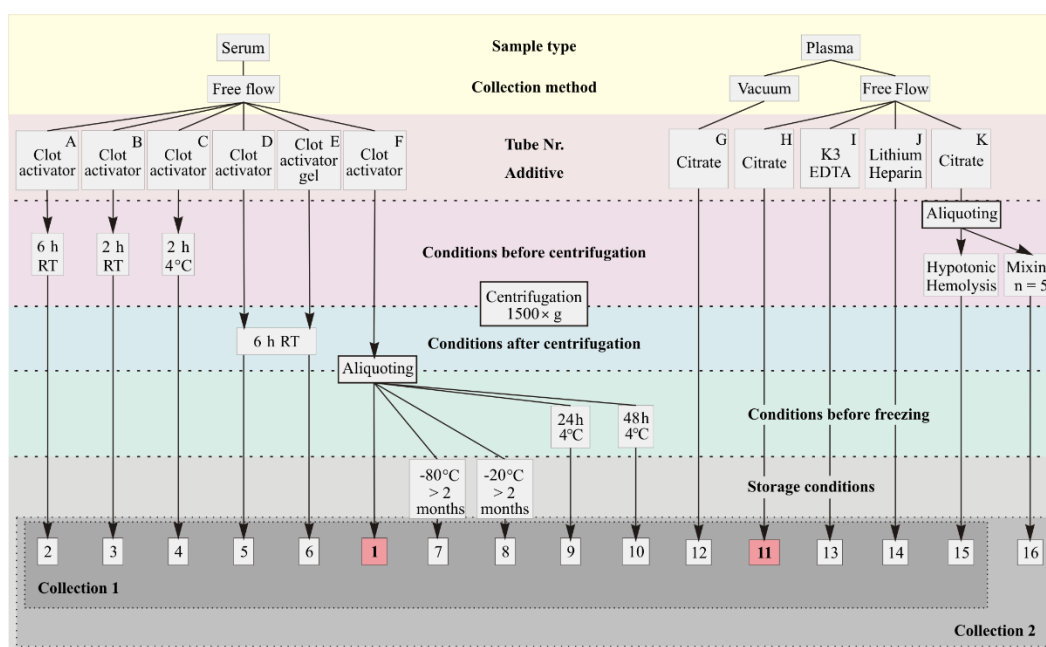


Figure 11 Flowchart showing the preanalytical processing carried out in this study. Standard conditions are marked red.

The remaining Tube K was used to induce two conditions before centrifugation. Whole blood was aliquoted (1 ml) and mixed overnight at room temperature while the remaining citrated blood was hemolysed directly in the collection tube by addition of deionized water (MilliQ, Millipore). The mechanical approach was performed only for the samples in the second collection set ($n = 5$), after initial results from the first set (hemolysed by hypotonic conditions) were obtained. The hypotonic hemolysis was performed on all samples ($n = 10$). Quantitative free haemoglobin measurement was used as an objective

estimate of hemolysis. The aliquoted samples were then stored at -80°C or -20°C until analysis.

Enzymatic N-Glycan release and purification

N-Glycan release was carried out as previously published by Biskup *et al.* [47, 48]. Ten microliters of serum/plasma sample were diluted in phosphate buffer pH 6.8, reduced with dithioerythritol (DTE, Sigma-Aldrich, Germany) for 45 min at 60°C and alkylated with iodoacetamide (IAA, Sigma-Aldrich, Germany) for 1 h at room temperature. The excess of DTE was used to stop the reaction and 100 mU of PNGase F (EC 3.5.152; Roche Applied Science, Indianapolis, IN) were used for enzymatic N-glycan release at 37°C overnight. Released N-glycans were purified using C18 reverse-phase chromatography cartridges and desalted with graphitized carbon columns (both Alltech, Deerfield, IL). Sixty percent of the glycan pool were used for permethylation and MALDI-TOF-MS measurement the rest was desialylated, fluorescently labelled and measured by CE-LIF.

Permethylation and mass spectrometry

Permethylation of purified PNGase F-released N-glycans was performed as previously published by Wedepohl *et al.* [90]. Permethylated glycans were purified by chloroform/water liquid-liquid extraction until the pH of aqueous phase became neutral. After chloroform removal under reduced atmosphere, samples were dissolved in $5\ \mu\text{l}$ 75% aqueous acetonitrile (ACN) and 10% of sample was mixed on a ground steel MALDI target with the equal volume of 10 mg/ml super DHB matrix (2-hydroxy-5-methoxy-benzoic acid / 2,5-dihydroxybenzoic acid, 1:9; Sigma-Aldrich, Germany) prepared in 10% aqueous ACN. MALDI-TOF-MS spectra were recorded on an Ultraflex III mass spectrometer (Bruker Daltonics, Bremen, Germany) equipped with Smartbeam laser (100 Hz laser frequency) in reflectron positive mode as sum of 2000 laser shots in the mass range 1000-5000 Da using 25kV accelerating voltage and ion suppression bellow 990 Da.

N-Glycan identification by MALDI-TOF-MS

All glycans were presumed to have a N2H3 core structure based on the knowledge of N-glycan biosynthetic pathways and on the specificity of PNGase F. The compositions (amount of H, N, F, S) were interpreted based on their m/z values. Annotations of MALDI-TOF-MS spectra, which were exported as ACSII files using the Flexanalysis software (Version 3.0, Build 54, Bruker Daltonics, Bremen, Germany), were carried out using Glycoworkbench (version 1.1.3480) tool and literature [141].

The resulting peak list was used for targeted data extraction of the area under the curve. Firstly, manual recalibration using glycan peaks was performed using known compositions (H3N4F1, H4N4F1, H5N4F1, H5N4S1, H5N5F1S1, H5N4S2, H6N5S3, H6N5F1S3 and H7N6S4). Then baseline detection and subtraction from intensities of all isotopic peaks was done using the Python Script published by Reiding *et al.* [85] with permethylated masses as building blocks (Table 1, Page 32), sodium as charge carrier and a calculation window of 0.49 m/z . SPSS for Windows, version 21 (SPSS Inc, Chicago, Ill) was used for statistical analysis.

Capillary electrophoresis

The protocol, which was previously published by Schwedler *et al.* [88], was used for chemical desialylation with 0.5 M acetic acid (Merck Millipore, Germany) at 80°C for 3h. Then, maltose was used as an internal standard and derivatisation of sample was performed with 8-aminopyrene-1,3,6-trisulfonic acid (APTS, Sigma-Aldrich, USA). All CE-LIF measurements were carried out on a Beckman P/ACE MDQ system, which was equipped with LIF detection ($\lambda_{\text{ex}} = 488 \text{ nm}$, $\lambda_{\text{em}} = 510 \pm 10 \text{ nm}$) (Beckman Coulter, Fullerton, CA, USA).

Separations were performed by reversed polarity in a polyvinyl alcohol-coated capillary (Beckman, 50 μm I.D., total capillary length of 65 cm and 50 cm effective separation length from the injection to the detection window). Injection was done at a pressure of 0.5 psi for 10 s and 30kV applied potential for 20 min at 25°C was used for separation. Signals from CE-LIF measurements were exported as ASCII files and aligned using a Python script HPACED [142], which is based on the highest peak of the spectrum from a certain time

point. The software OpenChrom (Community edition 1.1.0) was used to perform baseline subtraction, Savitzky-Golay signal smoothing and signal integration, performed automatically using the Peak Detector integration function.

Results

N-Glycan profiles obtained with standard conditions

Sixteen different conditions obtained from serum and plasma of 10 healthy women aged 20 - 30 were analysed by MALDI-TOF-MS and CE-LIF to evaluate the influence of preanalytics on *N*-glycan profiles. For both serum and plasma, standard conditions were the time frames between collection and processing as short as possible, thus 30 min between blood withdrawal and centrifugation, followed by aliquoting and immediate storage.

Enzymatic *N*-glycan release from reduced and alkylated proteins was achieved with PNGase F and released *N*-glycans were purified and permethylated before MALDI-TOF-MS measurement (Figure 12) and desialylated then APTS-labelled before CE-LIF measurement.

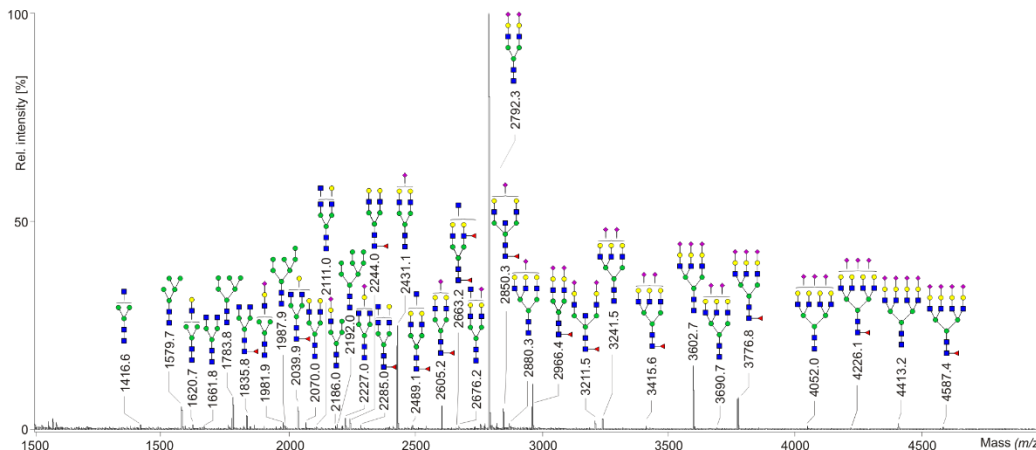


Figure 12 Annotated MALDI-TOF-MS spectrum obtained from a sample processed by the standard procedure.

MALDI-TOF-MS measurement of standard samples

I detected 46 *N*-glycan structures (Figure 13) of which four were of high-mannose type, seven fucosylated asialylated complex-type, fourteen were partially or fully capped with sialic acids and fourteen were fucosylated complex *N*-glycans with sialic acids.

The effect of preanalytical conditions on results of N-glycan analysis

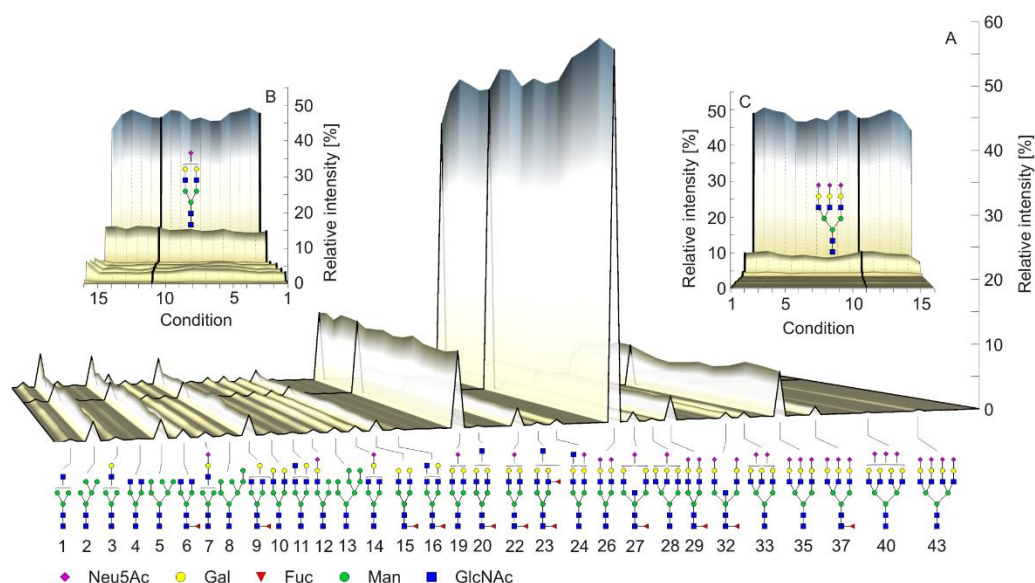


Figure 13 Results of MALDI-TOF-MS analysis. Average MALDI-TOF-MS N-glycan (A) relative intensities from 10 healthy donors under 16 preanalytical conditions (Figure 11). The serum and plasma standard conditions are marked with thick lines. A small increase of N-glycans having low masses (B) can be observed for hemolysed samples (condition 16), while N-glycans having high masses show a small decrease (C).

Relative intensities of 46 glycans (H = hexose, N = N-acetylhexosamine, S = Sialic acid, F = fucose), were normalized to the sum of all glycans and means were calculated for triplicates (n = 465, Table 3).

Table 3 Results of MALDI-TOF-MS analysis obtained using standard conditions.

Sample	Results	Complex-type					High-mannose	Hybrid-type
		Total	Monoant.	Diant.	Triant.	Tetraant.		
Serum	Rel. int., mean [%]	93.6	6.9	72.5	10.1	0.9	5.7	0.7
	SD	3.7	3.1	5.1	3.6	0.3	3.5	0.3
Plasma	Rel. int., mean [%]	93.2	6.9	72.8	9.3	0.7	6.2	0.6
	SD	2.8	3.7	4.2	4.0	0.4	2.6	0.2

The majority of the detected N-glycans was of complex-type, followed by high-mannose and hybrid-type. Further analysis of complex-type N-glycans showed that biantennary N-glycans were the most abundant structures, followed by triantennary, monoantennary and tetraantennary N-glycans.

CE-LIF measurement of standard samples

Ultimately, CE-LIF measurement enabled the identification of N-glycan linkages and positional isomers, which was not possible to achieve by MALDI-TOF-MS analysis alone. However due to the desialylation step, the information about sialylation is lost. Nevertheless, because of co-migration of some glycan structures, 23 glycan peaks were identified (Figure 14). Due to its simplicity even for more complex structures, the standard Oxford notation style was used for CE-LIF results. The Oxford notations are: pentasaccharide core (A0) consists of three mannose residues and two N-acetylglucosamines (GlcNAc); F core fucose; aF antennary fucose; Ax, number GlcNAc attached to the core; B, bisecting GlcNAc; Gx, number of β 1-4 linked galactose (G) on antennae; [3]G1 and [6]G1 indicates that the galactose is on the antenna of the α 1-3 or α 1-6 mannose. The [x] indicates the linkage type: in A2[3]G1 the galactose is linked to the α 1-3 mannose, and in A3[2,2,6] the N-acetylglucosamines are β 1-2-, β 1-2-, and β 1-6-linked to the trimannosyl core. In A3G3[3], the [3] indicates a β 1-3 linkage between terminal G and GlcNAc.

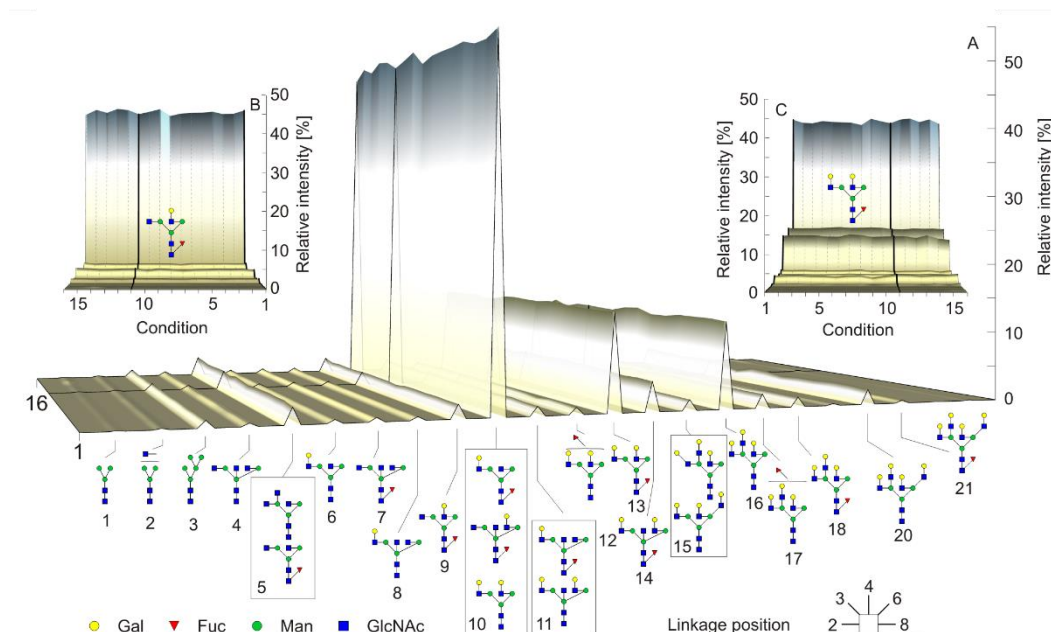


Figure 14 Results of CE-LIF analysis. Average CE-LIF N-glycan profiles (A) from 10 healthy donors under various preanalytical conditions. The conditions are numbered as mentioned on Figure 11. The serum and plasma standard conditions are marked with thick lines. Relative intensities of lower mass (B) and higher mass N-glycans (C) show the similar results throughout various conditions.

N-Glycan profiling of preanalytical deviations by MALDI-TOF-MS and CE-LIF

The Shapiro-Wilk normality test showed non-normal distribution of some glycans, therefore non-parametric tests were further used to assess differences between conditions. Friedman's non-parametric test was used on the complete data set (all conditions from 10 persons) to test if there were differences in relative intensities of individual glycans between different preanalytical conditions and *p* values < 0.05 were considered statistically significant. Data are presented as median relative intensities and interquartile range (IQR), namely 25th percentile (Q1) and 75th percentile (Q3). I detected statistically significant differences in relative intensities of 19 glycans (Table 4). Most of these structures had relative intensities < 1% and only four had relative intensities > 1%. Four of these 19 structures were of high-mannose type and four asialylated were complex-type structures. Eight sialylated structures were significantly different. Five of them were monosialylated, two disialylated and one tetrasialylated. I detected no differences in relative intensities of trisialylated *N*-glycans. Two fucosylated structures and only one from fourteen fucosylated sialylated structures were significantly different. From these results, I can conclude that high-mannose glycans appear to be the most sensitive *N*-glycans throughout all conditions, while fucosylated sialylated structures remain rather stable even during improper pre-analytical processing.

Table 4 Median relative intensities and interquartile range (IQR: 25% Q1, 75% Q3) of all conditions measured by MALDI-TOF-MS and results of Friedman's test statistical analysis.

Glycan type	<i>m/z</i>	Structure	Relative int. [%]			Friedman test	
			Median	IQR		$\chi^2(14)$	<i>p</i> value
				Q1	Q3		
High-mannose	1579.7	N2H5	2.43	1.31	4.25	31.530	0.005
	1783.8	N2H6	2.73	1.65	3.85	28.770	0.011
	1987.9	N2H7	0.45	0.34	0.64	36.470	0.001
	2192.0	N2H8	0.71	0.53	0.99	36.580	0.001
Afucosylated neutral complex	1416.6	N3H3	0.35	0.23	0.56	20.610	0.112
	1620.7	N3H4	0.40	0.22	0.54	36.760	0.001
	1661.8	N4H3	0.11	0.08	0.17	25.970	0.026

The effect of preanalytical conditions on results of N-glycan analysis

Glycan type	m/z	Structure	Relative int. [%]			Friedman test	
			Median	IQR		$\chi^2(14)$	p value
				Q1	Q3		
Afucosylated neutral complex	2070.0	N4H5	0.36	0.28	0.47	24.310	0.042
	2111.0	N5H4	0.19	0.14	0.26	31.090	0.005
	2315.1	N5H5	0.06	0.05	0.09	13.080	0.520
Fucosylated asialylated complex	1835.8	N4H3F1	0.96	0.52	1.50	12.720	0.549
	2039.9	N4H4F1	2.32	1.58	3.52	16.650	0.275
	2244.0	N4H5F1	1.27	0.99	1.80	14.470	0.415
	2285.1	N5H4F1	0.25	0.20	0.32	33.570	0.002
	2489.1	N5H5F1	0.18	0.12	0.24	20.570	0.113
	2663.2	N5H5F2	0.30	0.19	0.44	54.310	< 0.0001
	2693.2	N5H6F1	0.02	0.01	0.03	15.930	0.318
Afucosylated sialylated complex	1981.9	N3H4S1	0.56	0.42	0.78	31.160	0.005
	2227.0	N4H4S1	0.71	0.54	0.89	36.140	0.001
	2431.1	N4H5S1	11.11	9.91	12.82	28.140	0.014
	2676.2	N5H5S1	0.58	0.43	0.88	20.800	0.107
	2792.3	N4H5S2	53.90	50.80	57.09	29.530	0.009
	2880.4	N5H6S1	0.32	0.26	0.38	31.520	0.005
	3037.4	N5H5S2	0.07	0.05	0.11	17.930	0.210
	3241.5	N5H6S2	0.66	0.44	0.97	23.880	0.047
	3602.7	N5H6S3	5.47	3.79	8.79	20.570	0.113
	3690.7	N6H7S2	0.06	0.04	0.09	10.050	0.759
	4052.0	N6H7S3	0.12	0.09	0.17	16.490	0.284
	4413.2	N6H7S4	0.23	0.14	0.35	32.400	0.004
	Fucosylated sialylated complex	2605.2	N4H5S1F1	2.52	1.98	2.86	21.870
2850.3		N5H5S1F1	1.18	0.84	1.75	15.090	0.372
2966.4		N4H5S2F1	3.24	2.52	3.81	20.840	0.106
3054.4		N5H6S1F1	0.09	0.06	0.12	12.000	0.606
3211.5		N5H5S2F1	0.66	0.52	0.88	12.960	0.530
3415.6		N5H6S2F1	0.10	0.06	0.16	13.010	0.526
3776.8		N5H6S3F1	1.03	0.61	1.51	15.830	0.324
3864.8		N6H7S2F1	0.02	0.01	0.03	10.540	0.722
3950.9		N5H6S3F2	0.02	0.01	0.03	10.740	0.706
4226.1		N6H7S3F1	0.03	0.02	0.05	13.600	0.480
4400.2		N6H7S3F2	0.01	0.01	0.02	13.690	0.473
4587.4		N6H7S4F1	0.05	0.03	0.08	24.480	0.040
4761.5		N6H7S4F2	0.02	0.01	0.03	17.110	0.250
4935.7		N6H7S4F3	0.01	0.01	0.02	17.030	0.255
Hybrid		2186.0	N3H5S1	0.45	0.34	0.58	45.260
	2390.1	N3H6S1	0.07	0.05	0.09	16.390	0.290

For the CE-LIF measurements 19 glycan peaks out of 23 were significantly different according to the Friedman's test, ten of those had relative areas > 1% (Table 5).

It should be noted that the Friedman's test detects not only deviations from the standard procedures, but differences between all the tested conditions. Moreover, affected glycans generally had relative intensities below 1%.

Table 5 Median relative intensities and interquartile range (IQR: 25% Q1, 75% Q3) of all conditions measured by CE-LIF and results of Friedman's test statistical analysis.

GU	Structure	Relative int. [%]			Friedman test	
		Median	IQR		$\chi^2(14)$	p value
			Q1	Q3		
4.93	M3	0.11	0.07	0.13	34.331	0.002
5.77	A1	0.13	0.10	0.24	29.730	0.008
6.72	M5	0.97	0.76	1.10	23.210	0.057
7.17	A2B	0.52	0.45	0.60	19.430	0.149
7.62; 7.74	FA2; A3	2.61	2.10	2.99	54.827	< 0.0001
7.95	A2[3]G1	0.54	0.49	0.58	43.170	< 0.0001
8.07	FA2B	0.61	0.57	0.69	47.410	< 0.0001
8.45	A2B[3]G1	0.56	0.52	0.60	48.600	< 0.0001
8.58	FA2[6]G1	1.83	1.65	2.13	49.190	< 0.0001
8.88; 8.91; 8.93	FA2[3]G1; FA2B[6]G1; A2G2	51.18	49.41	52.88	38.220	< 0.0001
9.23; 9.41	FA2B[3]G1; A2BG2	1.71	1.36	1.92	24.905	0.036
9.96	aFA2G2	1.08	0.87	1.43	22.540	0.680
9.82	FA2G2	13.69	13.07	14.41	38.050	0.001
10.14	FA2BG2	4.31	3.87	5.03	36.240	0.001
10.95	A3G3[3]; A3[6]G3	1.55	1.43	1.67	54.980	< 0.0001
11.16	A3G3	12.21	9.99	13.58	36.850	0.001
11.8	aFA3G3	1.87	0.99	2.79	71.270	< 0.0001
12.02	FA3G3	1.21	0.96	1.75	26.490	0.022
12.61	FaFA3G3	0.27	0.16	0.39	28.693	0.011
13	A4G4	2.15	1.91	2.52	52.797	< 0.0001
13.62; 13.77	aFA4G4; FAG4	0.38	0.05	0.71	22.523	0.068
14.22	aF2A4G4	0.03	0.00	0.08	51.396	< 0.0001
14.69	aF3A4G4	0.10	0.07	0.15	71.270	< 0.0001

Post-hoc analysis was performed to further evaluate, which conditions contributed to the results of Friedman's test. For this purpose, all serum and plasma conditions were compared to reference serum and reference plasma, respectively. Wilcoxon signed-rank tests

was performed with a Bonferroni correction applied, therefore significance levels were set at $p \leq 0.0056$ for serum conditions and $p \leq 0.01$ for plasma conditions.

Effect of conditions before centrifugation

Since it is not always possible to perform centrifugation immediately after blood collection, I tested three different conditions to determine the effect of delayed centrifugation. I anticipated changes caused by the activity of enzymes such as sialidases. Samples were kept at up-right position for 2 hours at room temperature and in the fridge (4-8°C) (tubes B and C) and 6 hours at room temperature (tube A). However, I did not detect any statistically significant change in relative intensities of the tested glycans caused by the delays in centrifugation by neither MALDI-TOF-MS nor CE-LIF methods.

Storage time and storage temperature influence

Samples were stored for at least 2 months at -20°C and -80°C, while control conditions were also stored at -80°C but analysed as soon as possible. I observed no statistically significant differences between standard condition and 2 months storage neither at -20°C nor at -80°C. However, by CE-LIF measurements, I observed significant differences between the standard serum and both non-standard conditions, namely structures FA2BG2 for two months long storage at -80°C, and aF3A4G4 for two months storage at -20°C (Table 6).

Table 6 List of glycan structures in serum samples with various storage temperatures measured by CE-LIF, which showed statistically significant differences from the standard condition.

Structure GU	Statistics	ID Nr. Condition		
		1	7	8
		Serum reference	2M -80°C	2M -20°C
FA2BG2	Med(IQR)	3.93(3.76-4.81)	4.54(4.06-5.62)	4.50(3.92-5.32)
10.14	p value(z)	-	0.005 (-2.803)	0.220(-2.293)
aF3A4G4	Med(IQR)	0.11(0.08-0.12)	0.07(0.05-0.09)	0.06(0.05-0.08)
14.69	p value(z)	-	0.013(-2.497)	0.005 (-2.803)

Tubes additives

I observed no statistically significant differences between standard and testing conditions for MALDI-TOF-MS measurement. However, for the CE-LIF measurement, I observed that the peak containing two triantennary galactosylated isoforms A3G3[3] + A3[6]G3 was significantly increased ($p = 0.005$) in the serum gel tube (Table 7).

Table 7 List of glycan structures in serum samples with various additives measured by CE-LIF, which showed statistically significant differences from the standard condition.

Structure GU	Statistics	ID Nr. Condition		
		1	6	7
		Serum reference	6h after	6h after gel
A3G3[3];A3[6]G3	Med(IQR)	1.53(1.40-1.72)	1.53(1.44-1.74)	1.58(1.45-1.73)
10.95	p value(z)	-	0.241(-1.172)	0.005 (-2.803)

MALDI-TOF-MS measurements of plasma samples detected two structures, which were significantly decreased in EDTA and heparin plasma, namely N3H5S1 and N5H5F2 (Table 8).

Table 8 List of glycan structures in plasma samples with various additives measured by MALDI-TOF-MS, which showed statistically significant differences from the standard condition.

Structure m/z	Statistics	ID Nr. Condition			
		11	12	13	14
		Plasma reference	Vacuum	EDTA	Heparin
N3H5S1	Med(IQR)	0.51(0.44-0.90)	0.50(0.33-0.85)	0.43(0.31-0.49)	0.37(0.27-0.49)
2186.0	p value(z)	-	0.959(-0.051)	0.005 (-2.803)	0.005 (-2.803)
N5H5F2	Med(IQR)	0.57(0.44-0.68)	0.40(0.22-0.70)	0.28(0.14-0.43)	0.22(0.18-0.40)
2663.2	p value(z)	-	0.333(-0.968)	0.005 (-2.803)	0.009 (-2.599)

Additionally, six glycan peaks were significantly different between the standard plasma preanalytical condition and heparin for CE-LIF measurements. Three peaks M3; A3G3[3] + A3[6]G3; and aFA3G3 were increased, and three peaks FA2 + A3; A2[3]G1; and FA2B were decreased (Table 9). I observed no difference between the vacuum blood collection method and the free flow.

Table 9 List of glycan structures in plasma samples with various additives measured by MALDI-TOF-MS, which showed statistically significant differences from the standard condition.

Structure GU	Statistics	ID Nr. Condition			
		11	12	13	14
		Plasma reference	Vacuum	EDTA	Heparin
M3	Med(IQR)	0.12(0.08-0.16)	0.12(0.07-0.14)	0.09(0.06-0.12)	0.39(0.21-0.52)
4.93	p value(z)	-	0.386(-0.866)	0.093(-1.682)	0.009 (-2.599)
A3G3[3]; A3[6]G3	Med(IQR)	1.42(1.31-1.57)	1.56(1.45-1.68)	1.51(1.36-1.66)	1.53(1.40-1.70)
10.95	p value(z)	-	0.017(-2.395)	0.013(-2.497)	0.005 (-2.803)
aFA3G3	Med(IQR)	1.71(0.77-2.72)	1.61(0.82-2.18)	1.90(0.83-2.40)	1.82(0.77-2.94)
11.80	p value(z)	-	0.445(-0.764)	0.445(-0.764)	0.007 (-2.701)
FA2; A3	Med(IQR)	2.70(2.10-3.09)	2.63(2.47-3.01)	2.47(2.12-3.02)	2.54(2.04-2.82)
7.62; 7.74	p value(z)	-	0.333(-0.968)	0.047(-1.988)	0.007 (-2.701)
A2[3]G1	Med(IQR)	0.55(0.49-0.60)	0.53(0.48-0.61)	0.56(0.50-0.59)	0.50(0.42-0.54)
7.95	p value(z)	-	0.114(-1.580)	0.575(-0.561)	0.005 (-2.803)
FA2B	Med(IQR)	0.60(0.55-0.71)	0.61(0.56-0.70)	0.62(0.55-0.69)	0.56(0.53-0.64)
8.07	p value(z)	-	0.575(-0.561)	0.241(-1.172)	0.007 (-2.701)

Effect of hypotonic conditions on the N-glycome

Mild hemolysis was induced in samples by addition of deionized water. Using MALDI-TOF-MS, I did not measure any statistically significant differences between hemolysed samples and the reference, however, in the sample hemolysed by hypotonic conditions, there were statistically significant differences from the standard plasma condition in relative areas of A2B3G1, which was significantly increased, and A3G3 which was significantly decreased as determined by CE-LIF.

Table 10 List of structures in plasma samples with various collection methods measured by CE-LIF, which showed statistically significant differences from standard condition.

Structure GU	Statistics	ID Nr. Condition	
		11	15
		Plasma reference	Vacuum
A2B3G1	Med(IQR)	0.54(0.49-0.61)	0.59(0.54-0.62)
8.45	p value(z)	-	0.007 (-2.701)
A3G3	Med(IQR)	12.35(9.92-13.73)	11.30(9.24-13.23)
11.16	p value(z)	-	0.005 (-2.803)

Effect of overnight shaking at RT on the N-glycome

Extreme conditions, *e.g.* mixing at 1400 rpm at RT overnight, were used to induce strong hemolysis in plasma samples from five donors. Wilcoxon signed-rank tests was used with Bonferroni correction applied ($p \leq 0.01$) to compare these samples to standard samples from the same individuals. No statistically significant differences between the relative intensities of glycan structures were observed neither for MALDI-TOF-MS nor for CE-LIF measurements, even though samples were haemolysed (verified by measurement of free haemoglobin).

Correlation between haemolysis and N-glycome

Correlation analysis was performed to assess the relationship between relative intensities of N-glycans as well as calculated traits and the degree of hemolysis, which is presented as the concentration of free haemoglobin in mg/dl. Correlations were described using empirical classifications of interpreting correlation strength using r proposed by Evans *e.g.* $|r| > 0.80$ very strong correlation, $|r| = 0.60 - 0.79$ strong correlation, $|r| = 0.40 - 0.59$ moderate correlation, $|r| = 0.20 - 0.39$ weak correlation, $|r| = 0.00 - 0.19$ very weak correlation [143]. I tested two different types of hemolysis (tube K): hypotonic hemolysis (condition 15, $n = 10$) and hemolysis caused by mixing at 1400 rpm at RT overnight (condition 16, $n = 5$).

A statistically significant very strong negative correlation between relative intensity of N5H6F1 ($r = -0.917$, $n = 5$, $p = 0.028$) and the degree of hemolysis in samples hemolysed by combination of factors was detected. Even though there was no significant correlation

between relative intensities and concentration of free haemoglobin for individual glycan structures, there was a highly significant very strong negative correlation with the value of glycan-based ovarian cancer biomarker (GLYCOV) ($r = -0.958$, $n = 5$, $p = 0.010$). This score developed in our research group is calculated as the ratio: sum of relative intensities of (N5H6S3, N5H6S3F2, N6H7S3F1, N6H7S3F2, N6H7S4F1, N6H7S4F2, N6H7S4F3))/7*4/sum of relative intensities of (N2H5, N2H6, N2H7 and N2H8) (Figure 15). Interestingly, none of the glycan structures that are used to calculate the biomarker GLYCOV showed statistically significant differences between the standard collection method and hemolysed sample when calculated individually. Yet, the values of GLYCOV decreased upon hemolysis, which could lead to false negative measurements in ovarian cancer patients, indicating that hemolysed samples should not be used for biomarker assessments.

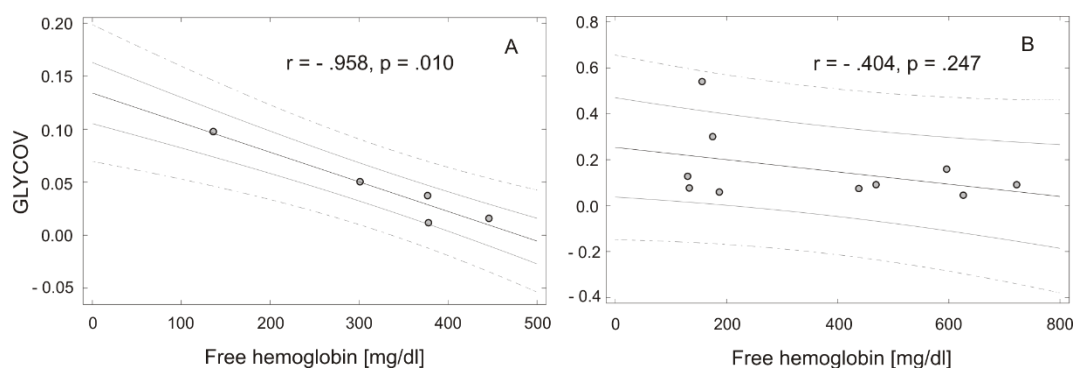


Figure 15 Scatterplot showing the correlation between free haemoglobin concentration and GLYCOV biomarker values. (A) Samples hemolysed by mixing samples, (B) hemolysed by hypotonic conditions. Grey solid and dashed lines indicate the 0.75 and 0.95 confidence intervals, respectively.

Correlation between hemolysis by hypotonic conditions and N-glycome

There was a statistically significant positive correlation in hypotonically hemolysed samples between the concentration of free haemoglobin and relative intensities of two high-mannose structures and four asialylated complex N-glycans (two of these were fucosylated).

There was a very strong positive correlation for N2H5, and a strong positive correlation for N2H6, N3H3, N3H4, N4H3F1 and N4H4F1 (Figure 16), which matches the results observed for GLYCOV. There were also strong negative correlations for two sialylated N-glycans N4H5S1, N5H6S2. However, no statistically significant correlation was found between the GLYCOV value and the degree of hemolysis ($r = -0.404$, $n = 5$, $p = 0.247$),

even though two structures used for its calculation (N2H5 and N2H6) showed strong individual correlation.

When measured by CE-LIF, there was no statistically significant correlation between relative areas of glycan peaks and the degree of hemolysis for neither type of hemolysed samples. It should be noted that, in CE-LIF, most high-mannose structures overlap and therefore cannot be measured.

The effect of preanalytical conditions on results of N-glycan analysis

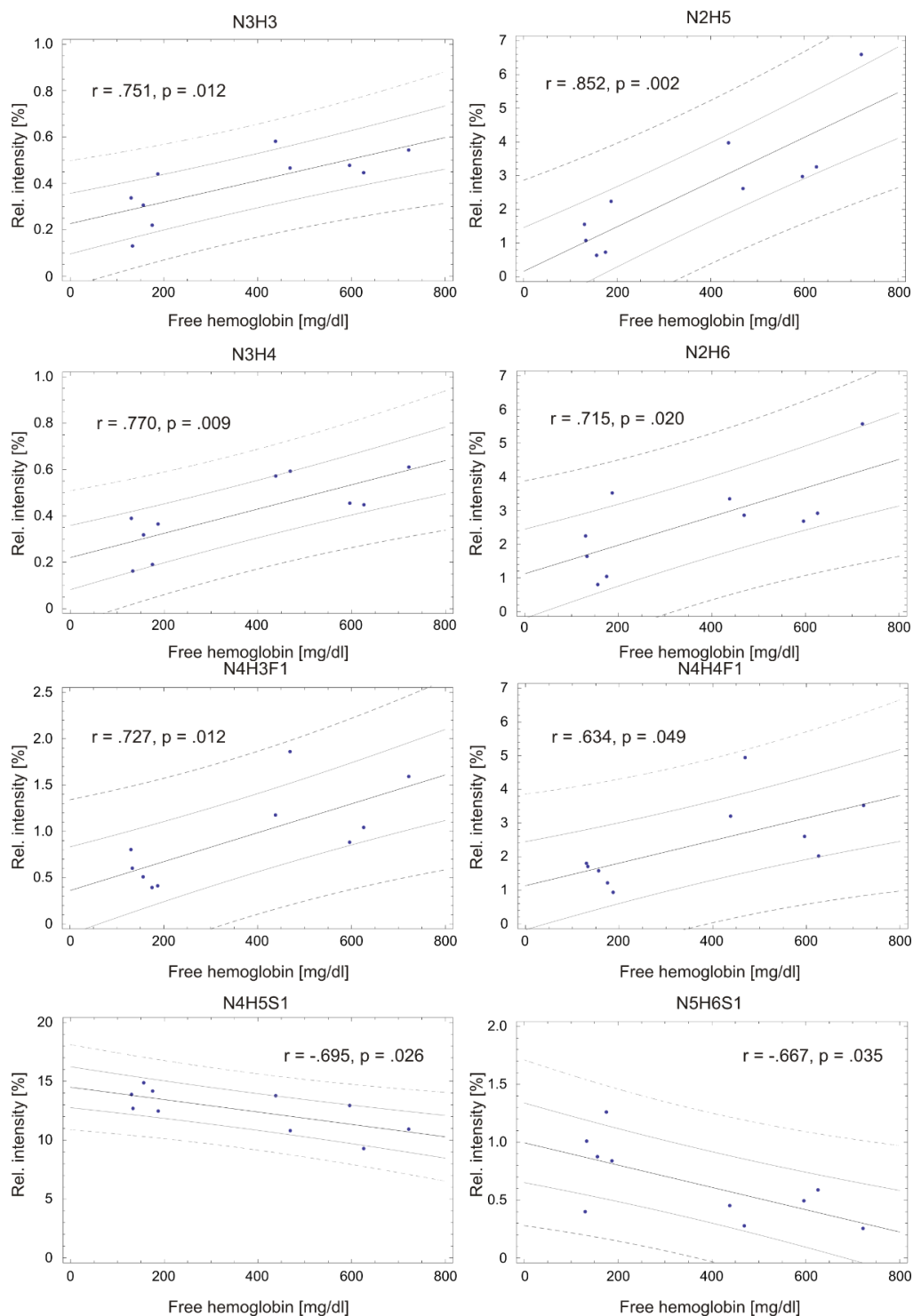


Figure 16 Scatterplot showing the correlation between free haemoglobin concentration and relative intensities of glycan structures. Grey solid and dashed lines indicate the 0.75 and 0.95 confidence intervals, respectively.

Discussion

The effect of sixteen different blood processings prior to *N*-glycan analysis was assessed by MALDI-TOF-MS (n = 465 samples) and CE-LIF (n = 310 samples). As a result, I highlighted some differences that could have influence on the results of glycan-based biomarker studies. There were already studies monitoring methodological robustness, intra-individual and longitudinal stability of the *N*-glycome [107, 138, 139], nevertheless the present study is important prerequisite before transitioning glycan biomarker discovery into clinical biochemistry laboratories.

Using MALDI-TOF-MS, I have shown that, during pre-analytical processing, variation of high-mannose structures can occur, which has influence on the glycan biomarkers such as the GLYCOV score developed in our laboratory [47] as shown in this chapter. The increase of high-mannose structures could result from cell lysis, releasing nascent intracellular glycoproteins [144]. Activity of circulating exoglycosidases could explain the changes observed in abundance of complex-type and sialylated *N*-glycans [145, 146]. Extreme conditions following blood withdrawal were used in this study to induce hemolysis, while no significant *in vivo* hemolysis was observed, since samples were taken from young healthy individuals. It was shown that *in vitro* hemolysis, one of the leading causes of preanalytical errors, is more likely to occur when sampling is performed in tubes filled below halfway in individuals older than 63 years [147, 148].

Using CE-LIF, I observed that long time storage of deep frozen samples at -20°C or -80°C exerted only a negligible influence on the *N*-glycome. Our CE-LIF results differed from those obtained by MALDI-TOF-MS for two reasons. First, sialic acids were removed for the CE-LIF experiments and second, the analysis of most high-mannose *N*-glycans was hindered by co-migration with other human blood *N*-glycans.

This study demonstrated that the glycome is more robust than other analytes such as proteins and peptides, for which preanalytical errors led to non-reproducibility of revolutionary publications [149]. For example, Diamandis and co-workers discovered that lysophosphatidic acid leaking from blood cells, introduced preanalytical biases [150], thus leading to commercial failures as a marker for ovarian cancer [151]. Nonetheless, it should be considered that our data were derived from healthy individuals, therefore preanalytical

analyses, as performed in the present study, are additionally warranted under specified disease conditions.

In this work, it could be shown that the glycome is rather stable in serum and plasma as short time delay between centrifugation at various temperatures seemed to have a no or small effect on the results. After centrifugation and aliquoting, the glycome was stable upon storage at 4°C for at least 48 hours, which is an important information considering future diagnostic applications in clinical laboratories. However, it should be emphasized that hemolysis affects relative intensities of certain glycans, which could lead to false negative (or positive) results in glycan biomarker studies and lead to wrong clinical interpretations.

Author contributions: Data curation, formal analysis, investigation, validation, visualization and manuscript writing were done by me. All authors contributed to the final version of the manuscript.

Chapter 5
**Comparison of methods to determine sialic
acid linkages**

Background

As was already written in the introduction section, sialylation varies between normal and diseased status. Therefore, information about the type of sialylation might prove to be useful in biomarker studies.

Colorimetric assays and fluorometric HPLC analysis are being used for the analysis of free sialic acids and their modifications, additionally, HPLC analysis enables the detection of di-, oligo- and polysialic structures [152]. Sialic acids are released by hydrolysis in mild acidic conditions, labelled with fluorophore 1,2-diamino-4,5-methylenedioxibenzene hydrochloride (DMB) and separated by reversed-phase chromatography. Another way to analyse polysialic acids is to utilise endosialidases, which can specifically cleave polysialic acids of certain type or linkage [153]. Very commonly methods for sialic acid assays are immunochemical methods, which use specific anti-sialic acid antibodies and lectins. These can be applied in immunohistochemistry and lectin histochemistry on tissue sections, enzyme-linked immunosorbent assay (ELISA)[154] or in a form of microarrays [155].

Lectin histochemical methods use lectins to detect the occurrence of sialylated glycoconjugates in tissue sections. The most frequently used lectins are isolated from *Sambucus nigra* (SNA), which is specific for α -2,6-linked Neu5Ac, while lectin from *Maackia amurensis* (MAA) recognises specifically α -2,3-linked Neu5Ac, and slug agglutinin from *Limax flavus* (LFA) is able to bind both Neu5Ac and Neu5Gc [156]. On the other hand, peanut agglutinin (PNA) from *Arachis hypogaea*, recognises non-sialylated sequence Gal- β (1-3)-GalNAc. Lectins are used both in direct and indirect assays, depending on the type of conjugate [157]. For the direct detection methods, lectins are conjugated with fluorescent label or horseradish peroxidase. Indirect methods often utilise antibodies against lectins or biotinylated lectins together with avidin-biotin-peroxidase complex. These methods are useful for tissue and cell analysis, however additional methods needed to be implemented for the analysis of sialic acid linkages from human body fluids that are compatible with MALDI-TOF-MS.

For the successful detection of sialylated glycan structures by MALDI-TOF-MS, the negative charge of sialic acids needs to be neutralised. Permethylation is one of the most used techniques for the neutralisation of sialic acids, however, it has its limitation, since it

does not enable the identification of linkages within the glycan. In the recent years, several methods for the neutralisation and the linkage-specific derivatisation of sialic acids have been published. In this chapter, various methods have been tested and evaluated for their use on released *N*-glycans from human serum, which is a very complex and challenging type of sample.

A fast method for sialic acid linkage-specific labelling was published by Reiding *et al.* in 2014 [85]. In this method sialic acids localized at the termini of *N*-glycans are stabilized utilizing coupling reagents 1-hydroxybenzotriazole (HOBt) and 1-ethyl-3-(3-(dimethylamino)propyl)-carbodiimide (EDT) as activators in ethanol as a solvent. The authors selected this combination of reagents from a wide variety of coupling agents and their respective combinations. Other coupling agents that they tested were 4-(4,6-dimethoxy-1,3,5-triazin-2-yl)-4-methylmorpholinium chloride (DMT-MM), *N,N'*-Dicyclohexylcarbodiimide (DCC) and ethyl-2-cyano-2-(hydroxyimino)acetate (Oxyma Pure), in the combinations DCC + HOBt or Oxyma Pure, and EDC + HOBt or Oxyma Pure. Authors showed that the combination of EDC with HOBt was superior to previously published methods, which utilise DMT-MM [158, 159] and any other of the tested combinations. Additionally, various alkyl donor alcohols were tested, namely methanol, ethanol, 2-propanol and 1-butanol), with ethanol being judged as the best in providing linkage-specific labelling.

While α -2,6-linked sialic acids form ethyl esters (+28 Da), α -2,3-linked sialic acids create a lactone (-18.02 Da) between the carboxylic group of the terminal sialic acid and the C2 hydroxyl group of the sub-terminal galactose. The carboxylic group of sialic acids is first activated by EDC and HOBt catalyses the following conversion to ethyl ester (Figure 17).

Comparison of methods to determine sialic acid linkages

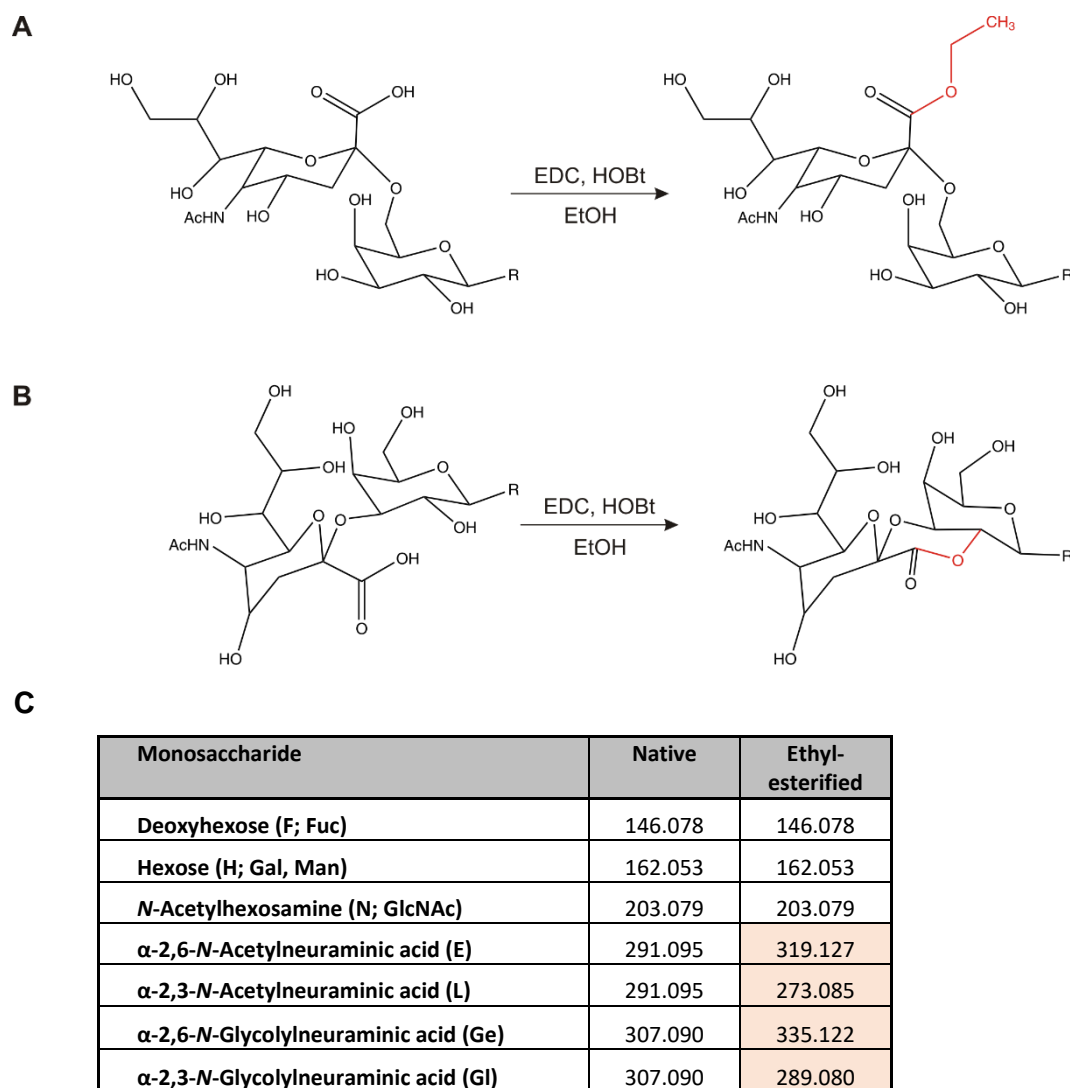


Figure 17 Ethyl esterification (A) and lactonisation (B) reactions catalysed by EDC and HOBT on α -2,6- and α -2,3-linked sialic acids and residue masses of native and labelled monosaccharides (C).

An improved derivatisation method, which uses dimethylamine instead of EtOH as a reagent thus forming more stable amide, was published by de Haan *et al.* in 2015 [160]. This newer method was developed to enable the detection of sialic acid-linkage-labelled N-glycopeptides. The authors compared MALDI-TOF-MS results obtained by ethyl esterification of PNGase F-released IgG N-glycans with those from dimethylamine-labelled glycopeptides. This method was also used on 2-AB labelled N-glycan standards, but authors did not report any application on PNGase F-released human serum N-glycans. The derivatisation reaction by dimethylamidation was performed with HOBT and EDT as activators in dimethylamine (DMA)/dimethylsulfoxide (DMSO). The α -2,3-linked sialic

acids undergo lactonisation and subsequent water loss, causing -18.02 Da shift, as during ethyl esterification reaction. The α -2,6-linked sialic acids are amidated with dimethylamine as nucleophile, which results in $+27.05$ Da shift (Figure 18).

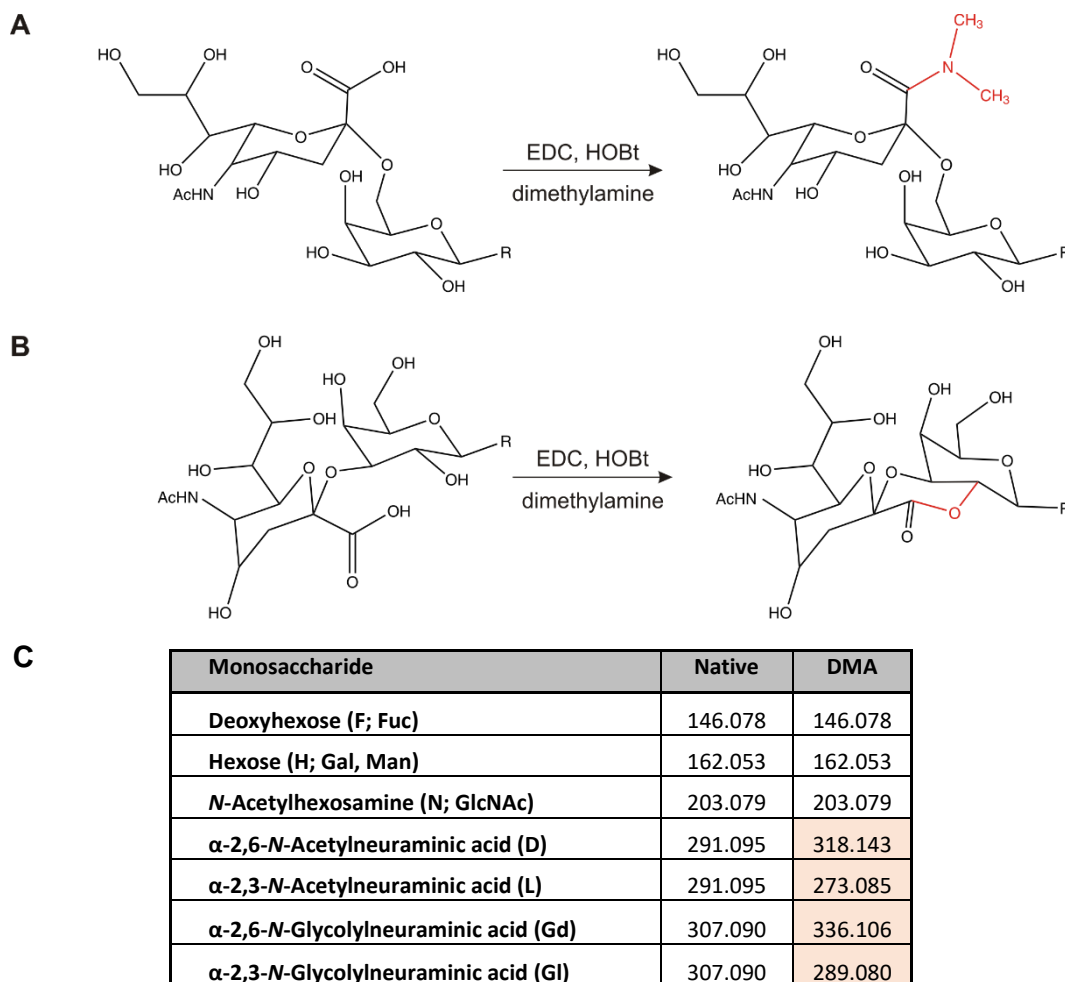


Figure 18 Dimethylamidation reaction of α -2,6-linked sialic acid (A) and lactonisation of α -2,3-linked sialic acid (B) and residue masses of native and dimethylamidated monosaccharides (C).

A new method for the derivatisation of sialic acids from paraffin embedded tissues was published by Holst *et al.* in 2016 [161]. This method was originally applied for *in-situ* reactions on microscopic slides, enabling the detection by MALDI-Imaging technique. In the publication, a dimethylamidation is performed first for 1 h, followed by direct addition of an ammonium hydroxide solution into the reaction and incubation for additional 2 h. The pH change caused by ammonium hydroxide first completely hydrolyses the lactones and the renewed α -2,3-linked sialic acids undergo amidation causing -0.91 Da shift. The α -2,6-linked sialic acids are dimethylamidated, which results in $+27.05$ Da shift (Figure 19).

Comparison of methods to determine sialic acid linkages

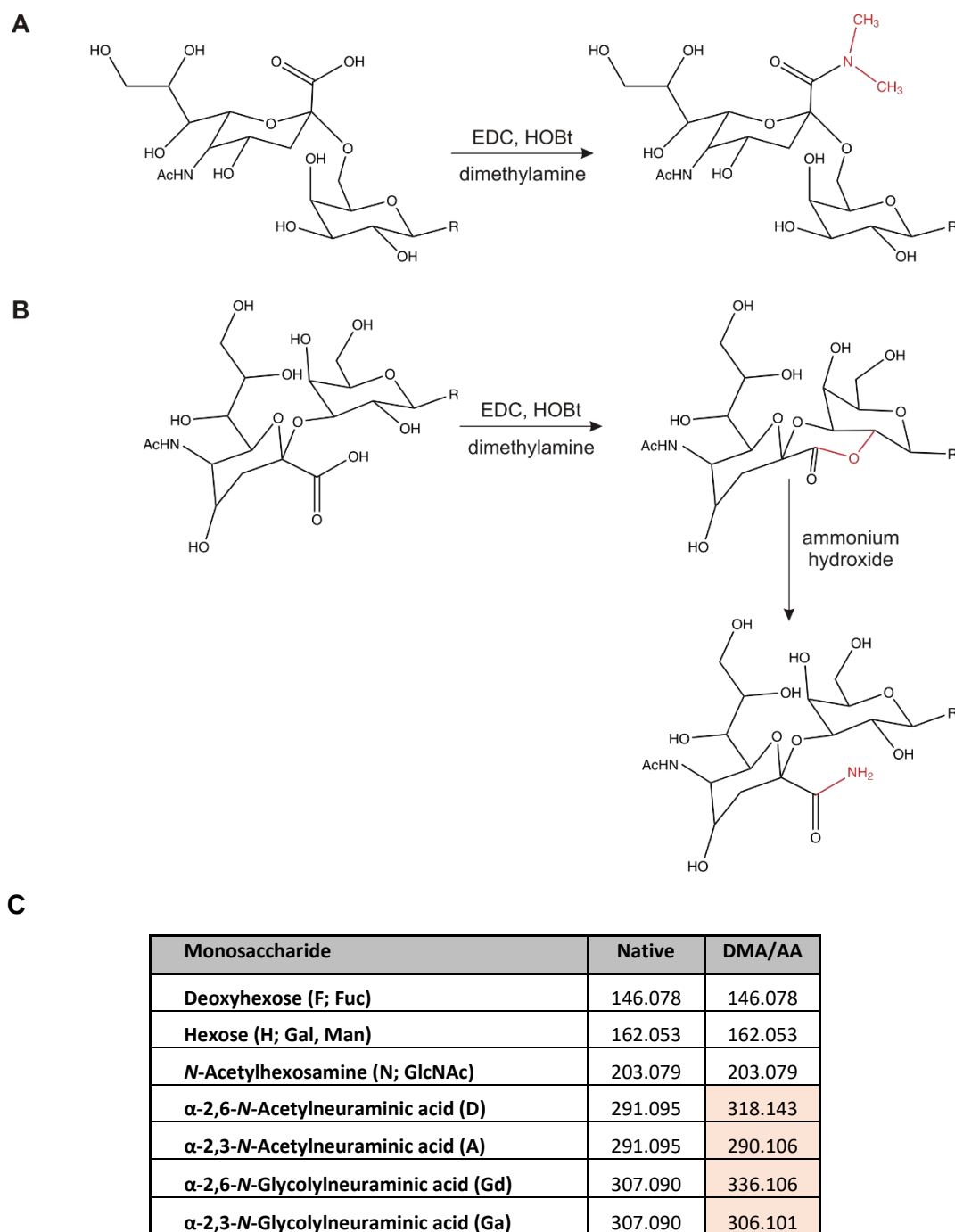


Figure 19 Dimethylamidation reaction of α -2,6-linked sialic acid (A) and lactonisation of α -2,3-linked sialic acid (B), followed by amidation and residue masses of native and double-amidated monosaccharides (C).

Materials and methods

N-Glycan release

The method published by Reiding *et al.* [85] was partially modified and used for the *N*-glycan release as follows: four microliters of 1% SDS (Merck Millipore, Germany) (w/w) solution were used for denaturation of proteins from two microliters of human serum. Samples were incubated for 10 min at 50°C, followed by addition of four microliters release mixture containing 2% NP-40 (Calbiochem, CA, USA) (w/w) and 0.5 mU PNGase F (EC 3.5.152; Roche Applied Science, Indianapolis, IN) in 2.5×PBS and incubated for 5 h at 37°C. The samples were then stored at –20°C until the respective sialic acid labelling method was performed.

Cotton HILIC purification

Cotton HILIC purification was used for samples labelled by the ethyl esterification reaction as published by Reiding *et al.* [85]. Samples were first adjusted to a concentration of 50% ACN and incubated at –20°C for 15 min. The purification was performed in a spin-column format. Each column was conditioned with 3×30 µl MilliQ water, followed by 3×30 µl 80% ACN. Samples were then applied and washed first with 3×30 µl 80% ACN, then with 3×30 µl 80% ACN, 0.1% TFA. The elution was performed using 3×30 µl MilliQ water. Samples were finally dried in a vacuum centrifuge.

HILIC purification with GHP membrane

For reactions performed in DMSO, a 96-well microplate containing a GHP filter membrane was used for sample purification after sialic acid labelling as published by Burnina *et al.* [92]. First, each microplate well was washed with 200 µl of 70% cold ethanol solution, followed by 3×200 µl MilliQ water and 3×200 µl of 96% ACN. Samples, adjusted with 100% ACN to a final concentration of 92% ACN, were then applied and incubated for 10 min, after which a low vacuum was applied to ensure a slow flow through the membrane. Each well was then washed with 3×200 µl of cold 96% ACN. Elution of *N*-

glycans from the plate was performed by addition of 2×50 µl of MilliQ water. Samples were then dried in a vacuum centrifuge and stored until measurement.

MALDI-TOF-MS

For the MALDI-TOF-MS measurement, dried samples were dissolved in 10 µl MilliQ water and 1 µl was applied on a groundsteel MALDI target, dried and then overlaid with 1 µl sDHB matrix (10 mg/ml in 10% aqueous ACN, 1mM NaCl). MALDI-TOF-MS spectra were recorded on an Ultraflex III mass spectrometer (Bruker Daltonics, Bremen, Germany) equipped with a Smartbeam laser (100 Hz laser frequency) in reflectron positive mode as sum of 2500 laser shots in the mass range 1200-5000 Da using 25kV accelerating voltage and ion suppression bellow 1190 Da.

Results

Ethyl esterification and lactonisation of sialic acids

Conditions were tested as originally published by Reiding *et al.* [85]. Glycan standards with defined sialic acid linkages were used, namely 3'-sialyl-N-acetyllactosamine (α -2,3-SiaLacNAc) and 6'-sialyl-N-acetyllactosamine (α -2,6-SiaLacNAc). Ten micrograms of the standards were dried in a vacuum centrifuge, 20 μ l of a solution containing 250 mM EDC, 250 mM HOBt in ethanol were added to the sample and incubated for 1h at 37°C. The same reaction was performed on PNGase F-released N-glycans from human serum. Unfortunately, I was not able to achieve the desired linkage specificity using the original conditions. I observed amidation with ammonia for the α -2,6-SiaLacNAc (m/z 696.2 [M+Na]⁺) when incubated at 37°C. This could be slightly reduced by lowering the temperature to 4°C. Moreover, after incubation at 37°C, non-reacted α -2,3-SiaLacNAc could still be observed (m/z 719.2 [M+2Na-H]⁺), while such peak could not be detected at 4°C. This could be explained by the instability of lactones at higher temperature over time. A similar effect was observed by Li and co-workers [162], who described the decomposition of produced lactones at different pH and noticed decrease of lactones even after water treatment.

Successful labelling with proper linkage specificity was achieved by the extra addition of reaction mixture after 1 h of incubation and by prolongation of the total reaction time to 2 h, while keeping the reaction at 4°C. However, additional side products (such as peaks m/z 696.2 [M+Na]⁺ in α -2,6-SiaLacNAc and m/z 2272.8 [M+Na]⁺ in serum samples) could still be observed in both our data and other publications [162]. For example, the mass m/z 2272.8 [M+Na]⁺ was explained by the authors as amidation with ammonia (released during N-glycan digestion) of one α -2,6-linked sialic acid in N4H5S2 glycan structure. The occurrence of this side reaction was reduced by incubation at 4°C (rather than 37°C), nevertheless could never be fully suppressed, which might cause problems during data analysis.

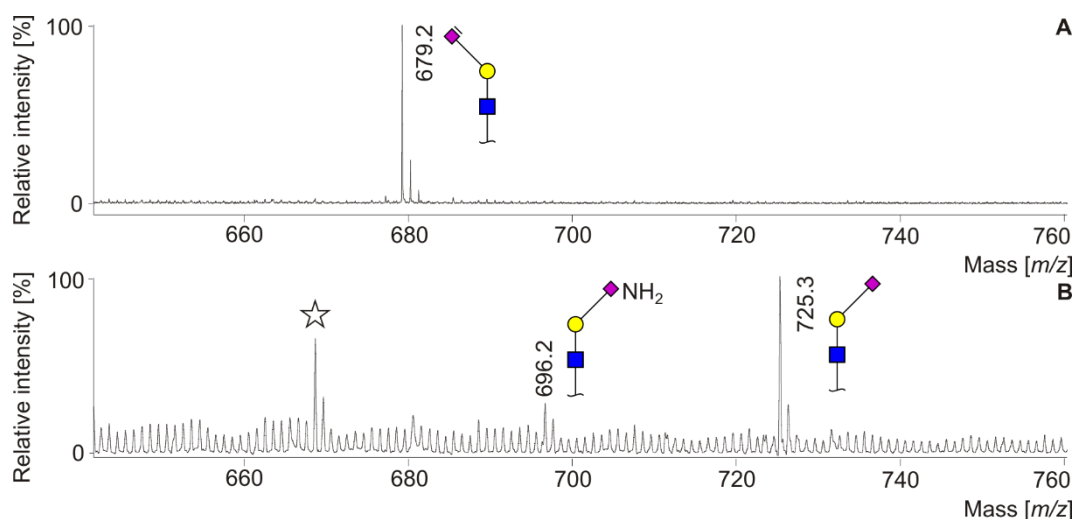


Figure 20 MALDI-TOF-MS results of ethyl esterification and lactonisation reaction. A) Lactonisation of α -2,3-SiaLacNAc and B) Ethyl esterification of α -2,6-SiaLacNAc. Traces of unspecific amidation with ammonia of α -2,6-SiaLacNAc can be detected as m/z 696.2 $[M+Na]^+$. Unidentified modification is marked \star .

The reaction was tested on *N*-glycans released from transferrin standard, but due to poor repeatability and number of side products, I omitted the use of ethyl esterification as a labelling technique for *N*-glycans released from human serum.

Dimethylamidation and lactonisation of sialic acids

I then tested whether dimethylamidation and lactonisation of sialic acids is applicable on PNGase F-released *N*-glycans. Firstly, the reaction was performed on linkage-defined sialyl-lactosamine standards (Figure 21). The reaction originally published by Haan *et al.* [160] for labelling of glycopeptides uses 20 μ l of reaction mixture (250 mM EDC, 500 mM HOBt and 250 mM dimethylamine in DMSO) for 1 μ l of tryptic digest (1 mg/ml IgG, 1:10 enzyme/substrate). After little optimisation of reagent concentration on glycans standards, I established that the best results were achieved when 100 μ g of each standard were incubated with 120 μ l of 250 mM DMA, 250 mM HOBt, 125 mM EDC in DMSO, instead of the original conditions.

Comparison of methods to determine sialic acid linkages

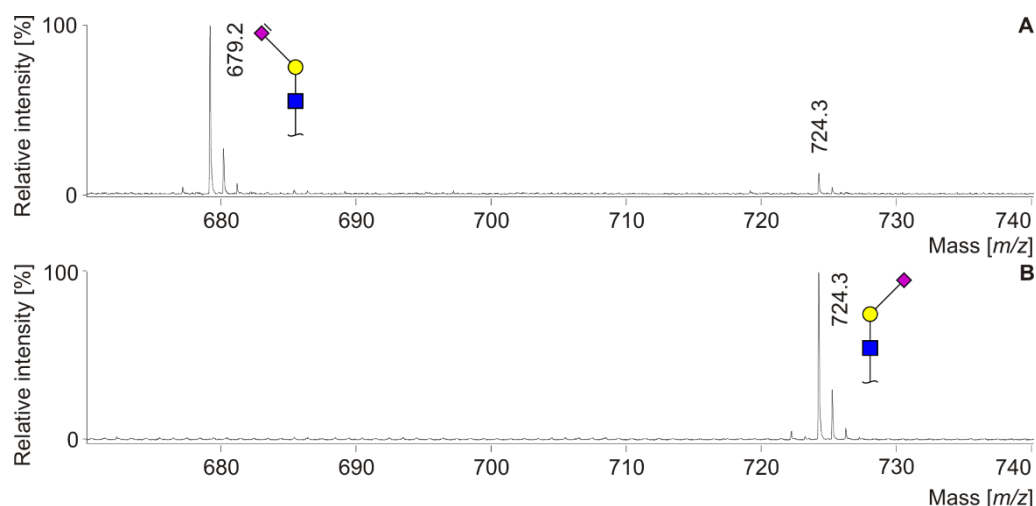


Figure 21 MALDI-TOF-MS spectra of dimethylamidation reaction. A) Lactonisation (m/z 679.2 $[M+Na]^+$) and non-specific dimethylamidation (m/z 724.3 $[M+Na]^+$) of α -2,3-SiaLacNAc and B) Dimethylamidation of α -2,6-SiaLacNAc.

The amidation requires a slightly longer reaction time (3 h) than the ethyl esterification, but the unwanted amidation by ammonia, which was observed after ethyl esterification, was eliminated. Unfortunately, a non-specific dimethylamidation of the α -2,3-linked sialic acid could be observed.

The same conditions were used for the labelling of released *N*-glycans. Unfortunately, I was not able to detect tetraantennary structures, as shown in Figure 22, which could be a result of lactone decomposition as discussed above.

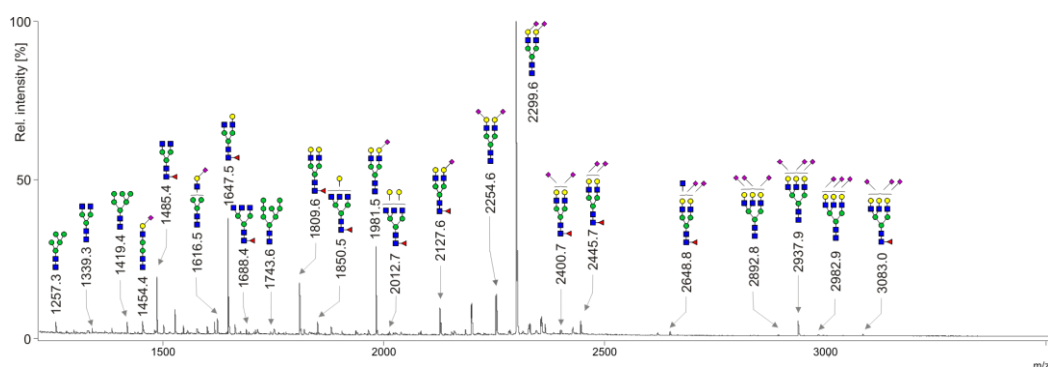


Figure 22 Dimethylamidation reaction of ovarian cancer serum. The position of linkage to the right marks dimethylamidation reaction of α -2,6-linked sialic acid and to the left lactonisation of α -2,3-linked sialic acid.

Double amidation of sialic acids

The reaction was used as published, *e.g.* 250 mM EDC, 500 mM HOBt and 250 mM DMA in DMSO and incubated at 60°C for 1 h, followed by an addition of 25% ammonium hydroxide in ratio 1:2.5. Unfortunately, the incubation for 1 h did not provide linkage-specific result on standards, thus various reaction times were tested. The shortest reaction times providing good results were 2.5 h dimethylamidation, followed by 2.5 h amidation. The linkage specificity of optimised conditions was validated on glycan standards (Figure 23).

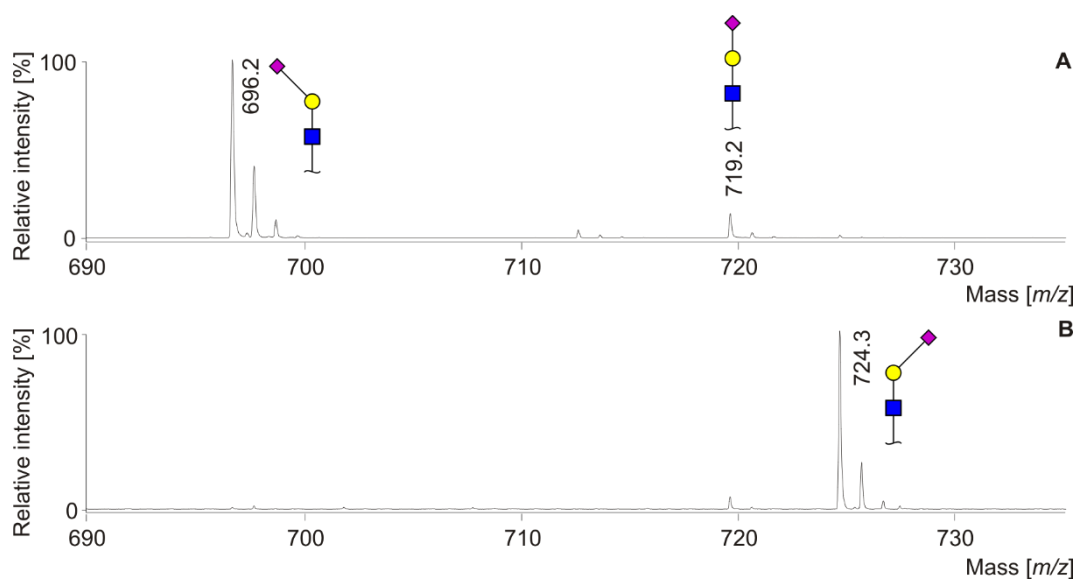


Figure 23 MALDI-TOF-MS results of double-amidation reaction. A) Amidation of α -2,3-SiaLacNAc and B) Dimethylamidation of α -2,6-SiaLacNAc. Traces of re-hydrolysed and/or non-reacted SiaLacNAc can be detected as m/z 719.2 $[M+2Na-H]^+$.

The same reaction was performed on PNGase F-released *N*-glycans from human serum. Serum samples provided complete spectra with detectable tetraantennary structures, as illustrated in Figure 24.

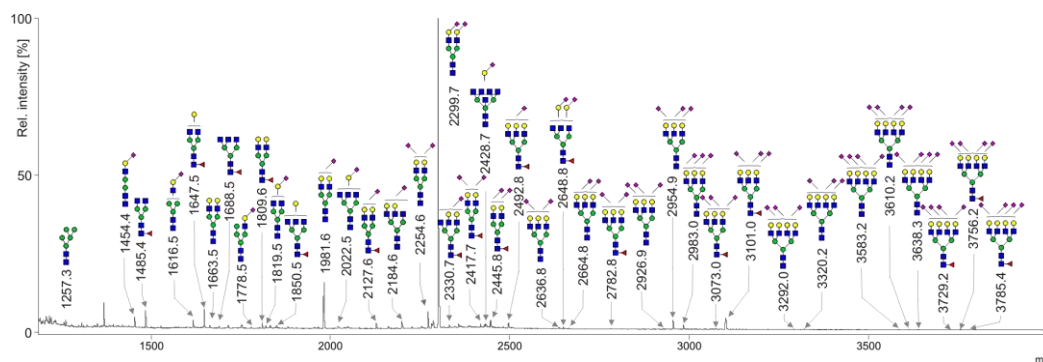


Figure 24 MALDI-TOF-MS spectrum of dimethylamidation and amidation with ammonia. The position of linkage to the right marks dimethylamidation reaction of α -2,6-linked sialic acid and to the left amidation of α -2,3-linked sialic acid.

Repeatability testing

To test inter-, and intra-day repeatability of the method, the *N*-glycan release and derivatisation reaction of pooled serum samples (10 female serum samples, age 20-30 years) were performed on 16 biological replicates (1-16) on three different sets (I-III) (Figure 25).

N-Glycans were released from serum samples and linkage specific sialic acid labelling was performed with the modified double-amidation method published by Holst *et al.* [163]. To one microliter of *N*-glycan release digest were added 10 μ l of reaction mixture (250 mM DMA, 500 mM HOBt, 250 mM EDC in DMSO) and incubated for 2.5 h at 60°C. Then, four microliters of 28% ammonium hydroxide were added and samples were incubated for additional 2.5 h at 60°C. Samples were then adjusted to 92% ACN and transferred to -20°C for 15 min. GHP membrane HILIC purification was then used to clean-up the labelled samples and eluted *N*-glycans were then dried in vacuum centrifuge.

For MALDI-TOF-MS measurements, dried samples were dissolved in 10 μ l MilliQ water and 1 μ l was applied on two different MALDI target spots, dried and then overlaid with 1 μ l sDHB matrix (10 mg/ml in 10% aqueous ACN, 1 mM NaCl). The two-spot application was used to establish instrumentation replicates. For one set of samples, each MALDI spot was measured twice and saved as separate results.

The raw spectra were exported as ASCII files and processed by the Massy Tools python script [118] modified to use residual masses as noted in Figure 19 to extract relative

intensities of 108 glycan structures. Twelve glycan structures had relative intensities > 1%, corresponding to approximately 85% of the total spectrum.

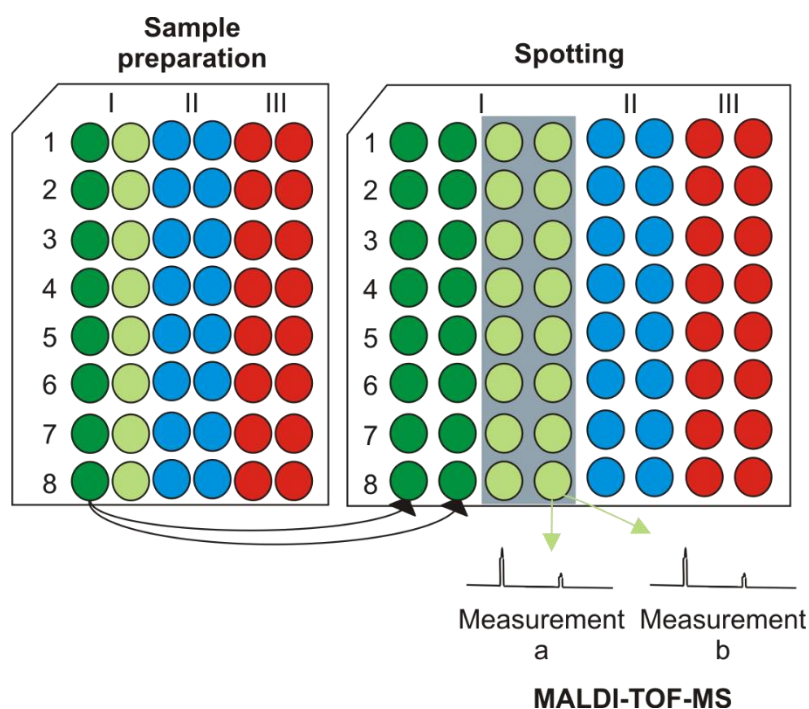


Figure 25 Scheme of repeatability experiments performed on human serum N-glycans by MALDI-TOF-MS. The experiment was performed three times, indicated as I-III. In each set sixteen samples of pooled serum were independently released by PNGase F, labelled, purified by HILIC. For the first set, each sample was then spotted twice on the MALDI target to test a possible influence of crystallisation. For eight samples (sixteen spots) from the first set, two spectra were recorded from each spot (Ma, Mb). Samples from sets II and III were spotted and measured only once.

Relative intensity of these twelve most abundant structures in the MALDI spectra were used to assess intraclass correlation coefficient ($r = 1$ represents perfect reliability with no measurement error) and relative intensities of the two most abundant structures (H5N4D2 and H5N4D1) were used to calculate standard deviations (SD) and coefficients of variation (CV). Firstly, I evaluated instrument repeatability by measuring each target spot twice. There was very strong intraclass correlation ($r = 0.997-1$) between two MALDI measurements from the same target spot and the CV values for individual measurements for H5N4D2 were 0.1-5.2% and for H5N4D1 0.3-14.2% (Table 11).

Table 11 Effect of individual MALDI-TOF-MS measurements on results of two most abundant structures, each sample was measured from two spots twice (Ma, Mb).

Set I		H5N4D2		H5N4D1		H5N4D2			H5N4D1		
		Ma	Mb	Ma	Mb	Mean	SD	CV	Mean	SD	CV
Sample 1	Spot 1	60.2%	57.7%	7.1%	7.8%	58.9%	1.3%	2.1%	7.5%	0.4%	4.7%
	Spot 2	51.8%	52.1%	8.5%	8.8%	52.0%	0.2%	0.3%	8.7%	0.2%	1.9%
Sample 2	Spot 3	49.1%	44.3%	8.3%	8.8%	46.7%	2.4%	5.2%	8.6%	0.3%	3.1%
	Spot 4	52.5%	52.4%	8.3%	8.3%	52.5%	0.0%	0.1%	8.3%	0.0%	0.3%
Sample 3	Spot 5	44.5%	44.8%	7.3%	7.7%	44.7%	0.1%	0.3%	7.5%	0.2%	2.8%
	Spot 6	46.2%	46.4%	7.6%	7.6%	46.3%	0.1%	0.3%	7.6%	0.0%	0.4%
Sample 4	Spot 7	45.9%	50.1%	8.1%	7.2%	48.0%	2.1%	4.3%	7.6%	0.4%	5.7%
	Spot 8	38.0%	39.8%	9.5%	7.1%	38.9%	0.9%	2.4%	8.3%	1.2%	14.2%
Sample 5	Spot 9	49.8%	52.9%	7.3%	6.9%	51.3%	1.6%	3.1%	7.1%	0.2%	2.8%
	Spot 10	44.0%	43.4%	8.1%	8.2%	43.7%	0.3%	0.7%	8.2%	0.0%	0.3%
Sample 6	Spot 11	46.8%	47.5%	7.8%	7.5%	47.2%	0.3%	0.7%	7.7%	0.1%	1.7%
	Spot 12	46.4%	42.8%	7.5%	7.6%	44.6%	1.8%	4.1%	7.6%	0.1%	0.9%
Sample 7	Spot 13	38.9%	38.1%	8.5%	8.5%	38.5%	0.4%	1.1%	8.5%	0.0%	0.2%
	Spot 14	49.7%	49.2%	8.7%	8.5%	49.5%	0.3%	0.6%	8.6%	0.1%	1.0%
Sample 8	Spot 15	47.7%	45.4%	6.4%	6.6%	46.5%	1.1%	2.5%	6.5%	0.1%	1.7%
	Spot 16	42.7%	41.0%	6.6%	6.2%	41.9%	0.9%	2.1%	6.4%	0.2%	3.5%

Secondly, I tested intraclass correlation coefficient between two spots from the same sample to investigate the effect of sample crystallisation. Calculations were performed only from the first measurement of each spot. There was also very strong intraclass correlation between samples measured from different spots ($r = 0.957-1$) and the CV values for different spots of the same sample ranged from 0.5% to 12.2% for H5N4D2 and 0.0% to 8.9% for H5N4D1 (Table 12). It is apparent that the effect of sample spotting is greater than the effect of individual MALDI measurements.

Table 12 Basic repeatability statistics from total data acquired from two spots per sample.

Set I		H5N4D2	H5N4D1	H5N4D2			H5N4D1		
		Ma	Ma	Mean	SD	CV	Mean	SD	CV
Sample 1	Spot 1	60.2%	7.1%	56.0%	4.2%	7.5%	7.8%	0.7%	8.9%
	Spot 2	51.8%	8.5%						
Sample 2	Spot 3	49.1%	8.3%	50.8%	1.7%	3.3%	8.3%	0.0%	0.0%
	Spot 4	52.5%	8.3%						
Sample 3	Spot 5	44.5%	7.3%	45.4%	0.8%	1.8%	7.5%	0.2%	2.3%
	Spot 6	46.2%	7.6%						
Sample 4	Spot 7	45.9%	8.1%	41.9%	3.9%	9.4%	8.8%	0.7%	8.0%
	Spot 8	38.0%	9.5%						
Sample 5	Spot 9	49.8%	7.3%	46.9%	2.9%	6.1%	7.7%	0.4%	5.8%
	Spot 10	44.0%	8.1%						
Sample 6	Spot 11	46.8%	7.8%	46.6%	0.2%	0.5%	7.7%	0.2%	2.0%
	Spot 12	46.4%	7.5%						
Sample 7	Spot 13	38.9%	8.5%	44.3%	5.4%	12.2%	8.6%	0.1%	1.1%
	Spot 14	49.7%	8.7%						
Sample 8	Spot 15	47.7%	6.4%	45.2%	2.5%	5.5%	6.5%	0.1%	2.0%
	Spot 16	42.7%	6.6%						

Similar interclass correlation were observed within individual sets, namely lowest intraclass correlation coefficients were 0.923 for both Set I and II, and 0.978 for Set III, which suggests that the observed differences within sets actually arise from variances between spots, rather than processing of the sample (Table 13).

Intraclass correlation coefficient for all three sets was 0.923 and mean relative intensity values for the highest peak (H5N4D2) was 47.8% (SD \pm 4.6%) across all measurements, with the CV 9.6%, which is acceptable for a semi-quantitative method (Figure 26).

Table 13 Basic repeatability statistics from total data acquired from individual sets of measurements.

Set	Set I			Set II			Set III			Total		
Glycan	Mean	SD	CV	Mean	SD	CV	Mean	SD	CV	Mean	SD	CV
H5N4D2	46.5%	5.2%	11.2%	49.6%	2.7%	5.4%	47.1%	4.8%	10.2%	47.8%	4.6%	9.6%
H5N4D1	7.1%	0.8%	10.8%	7.1%	0.5%	6.7%	6.4%	0.4%	6.1%	6.9%	0.7%	9.4%
H4N4F1	8.0%	2.3%	28.3%	7.2%	1.0%	14.5%	7.5%	1.8%	23.7%	7.6%	1.8%	23.8%
H3N4F1	4.9%	1.6%	32.3%	4.3%	0.7%	15.6%	4.5%	1.2%	25.9%	4.6%	1.2%	26.6%
H5N4D1A1	2.5%	0.7%	28.4%	3.0%	0.4%	13.0%	3.1%	0.4%	12.8%	2.9%	0.6%	20.0%
H5N3A1	2.5%	0.4%	17.8%	2.4%	0.4%	16.2%	3.0%	0.8%	27.5%	2.6%	0.7%	24.7%
H5N4F1	3.0%	0.7%	23.9%	2.7%	0.5%	16.9%	3.0%	0.6%	18.3%	2.9%	0.6%	20.7%
H5N2	2.8%	1.2%	42.6%	2.4%	0.6%	24.1%	2.3%	0.7%	31.0%	2.5%	0.9%	35.8%
H6N5D2A1	2.2%	0.9%	38.9%	2.6%	0.4%	16.1%	2.7%	0.6%	24.2%	2.5%	0.7%	28.0%
H6N2	2.3%	1.0%	42.6%	2.0%	0.5%	22.0%	2.1%	0.6%	28.3%	2.2%	0.7%	33.5%
H5N4F1D2	1.8%	0.5%	28.9%	2.1%	0.2%	11.3%	2.2%	0.4%	18.5%	2.0%	0.4%	21.4%
H5N4F1D1	1.6%	0.3%	16.0%	1.6%	0.1%	7.0%	1.7%	0.2%	13.6%	1.6%	0.2%	12.8%

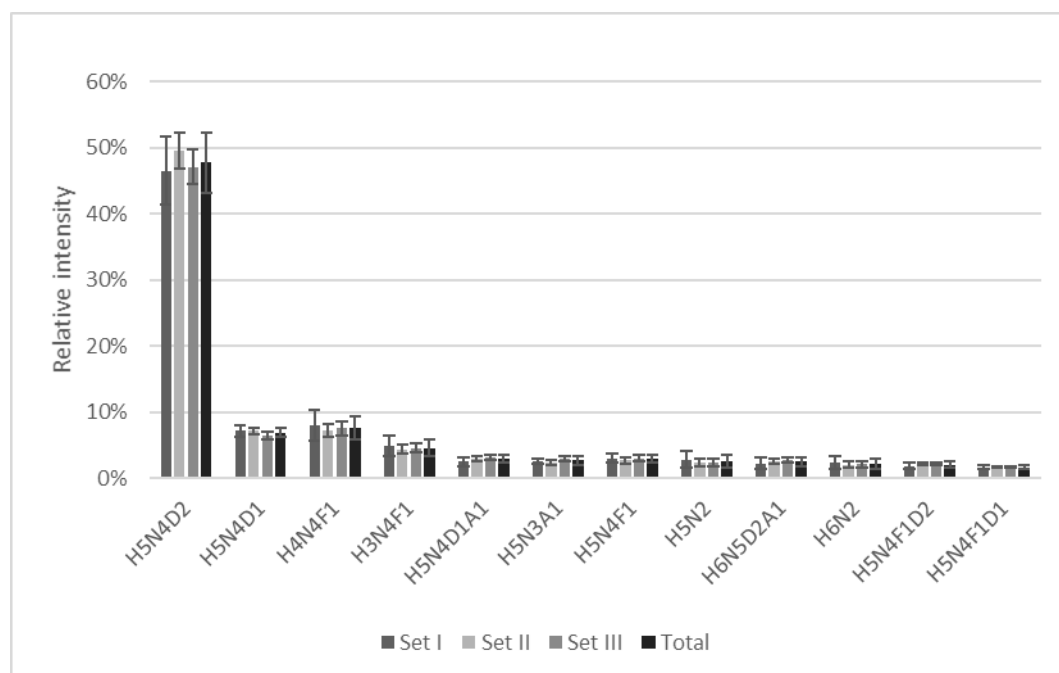


Figure 26 Repeatability of serum N-glycan profiling by MALDI-TOF-MS after double-amidation reaction. Eight samples of pooled serum were independently released by PNGase F, labelled, purified by HILIC and analysed by MALDI-TOF-MS. The experiment was performed three times, indicated as days 1-3. The graph shows the average relative intensities observed for the 12 most abundant structures with error bars for standard deviation.

This information was used for further experiments – each sample was prepared in duplicate from N-glycan release to purification after labelling and then measured by

MALDI-TOF-MS from duplicate spotting, resulting in four spectra per sample, which were then summed together for data analysis, thus reducing influence of both spot-to-spot and sample processing variance.

Conclusion

Three different published methods for linkage-specific sialic acid labelling were tested for their application on PNGase F released serum *N*-glycans. These methods were previously used either on released plasma *N*-glycans [108], IgG glycopeptides [160] or paraffin embedded tissue slides [163]. The ethyl esterification reaction was in recent years referenced in more than 140 publications, however in my experiments, this method proved to be very challenging. I was able to label sialic acids specifically, meaning the α -2,3-linked sialic acids showed only lactonisation and no lactonisation was observed for the α -2,6-linked sialic acids. However, the labelling of α -2,6-linked sialic acids resulted in additional side products, such as amides and others, which could not be identified. There were publications, which addressed similar issues [162, 164] and proposed modifications of this method. Both of these publications utilised protein immobilisation prior labelling, thus enabling removing of derivatisation agents between individual steps. Unfortunately, this setup is more elaborate than the originally proposed one-pot reaction and was not tested.

On the other hand, the dimethylamidation reaction retains the simplicity of one-pot reaction, while providing excellent linkage-specificity for the α -2,6-linked sialic acid and decent linkage-specificity for the α -2,3-linked sialic acid. Unfortunately, when applied on PNGase F-released *N*-glycans from ovarian cancer serum, the detection of tetraantennary structures was not possible. Successful detection of these structures was achieved after labelling with two-step amidation reaction, which also provides good linkage specificity. The method was tested for its repeatability and a protocol was optimised, which will be applied on released *N*-glycans from ovarian cancer patients and healthy control sera.

Repeatability measurements showed that the effect of sample spotting on a MALDI-target is similar to the effect of preparation of biological replicates [85]. Thus, it can be assumed that these changes actually originate from the spotting, rather than sample preparation, which is often reported [85, 160]. It is therefore advisable to perform measurements from duplicate spots on MALDI-target to reduce measurement error. Alternatively, spectra from two spots could be summed directly during MALDI measurement, thus simplifying data analysis.

Chapter 6
Sialic acid-linkages in ovarian cancer

Background

Ovarian cancer was among five leading cancer types in cancer deaths in women in United States in 2017 [165] with estimated 14,800 ovarian cancer deaths and 22,440 new cases. The five-year relative survival rate ranges from of 92% in early stage to only 29% in later stages. Currently, only about 20-25% of ovarian cancer patients are diagnosed in early stages [166]. Early diagnostics is therefore crucial for the long-term survival rate, however 60% of cases in United States between 2006 and 20012 were of late stage [165]. There are three types of cells, from which most of benign and malignant ovarian tumours originate, namely epithelial, stromal and germ, with epithelial being the most common (> 90%) [167].

As discussed in the introduction section, the routinely used tumour marker for ovarian cancer CA125 shows specificity of 94 - 98.5%, but low sensitivity (50 - 62% for early stages of epithelial ovarian cancer) [79]. Since there are no early warning signs, there is a pressing need for improvements in early stage diagnostics [47]. Newer biomarkers have been proposed and used, such as HE4 which shows better sensitivity in terms of distinguishing benign disease from malignant tumour than CA125 [80]. However, the most promising approach seems to be use of multi-factor diagnostics, such as combination of CA125, HE4 and so-called Symptom index (SI) [81], which has sensitivity of 84% and specificity of 98.5% [82]. Alternative methods for early ovarian cancer diagnosis have been proposed in the last decade, such as microRNA [168], protein panel screening [169, 170] and bioinformatic tools [149].

For the potential improvements in ovarian cancer diagnostics, there is a need to understand causes and pathological alterations of this malignancy. Glycosylation plays an important role in biological processes, such as cell recognition, cell-cell interactions, cell-cell communication and adhesion [171]. On human glycoproteins, sialic acids are either α -2,3- or α -2,6-linked to galactoses and are the most exposed monosaccharides to the outer environment, and as such participate in biological processes including cancerogenesis. Correlation has been observed between increased sialylation and ovarian cancer stages, however the linkage type has never been investigated in detail.

Biskup *et al.* recently identified characteristic changes of the serum glycome that were combined in a score named GLYCOV that could diagnose primary epithelial ovarian

cancer in a better way than CA125 [47, 48]. GLYCOV contains seven sialylated *N*-glycans but the type of sialic acid linkage has not been studied yet. A cohort of 110 patients including early (FIGO stages I + II) and late stages (FIGO III and IV) as well as age-matched controls was enrolled in this study. Glycoproteins from serum were released by PNGase F, and the *N*-glycan pool was derivatized using linkage-specific labelling and measured by MALDI-TOF-MS.

Materials and methods

Sample preparation and MALDI-TOF-MS

Serum samples from 110 women aged 32-81 years (mean = 57.1, median = 55.5 years) were used in this study (Table 14). There were 77 samples from primary serous epithelial ovarian cancer patients and 33 healthy controls. For each sample, information about FIGO stage and CA125 measurements were provided. CA125 II immunoassay was used to measure CA125 on a COBAS 6000 analyser (Roche Diagnostics, Germany). Blood was collected as a part of the Tumour Bank Ovarian Cancer project (<http://www.toc-network.de/>). Clot activator serum tubes (Vacutainer, BD, Medical-Pharmaceutical System, NJ, USA) were used for collection. Blood was allowed to clot for minimum of 30 min up to 2 h at room temperature and serum was separated by centrifugation at 1200 g for 15 minutes. Serum was aliquoted and stored at -80°C until the time of analysis.

Table 14 Demographics of samples used in this sialic acid linkage study, CA125 are shown as kU/L.

Stage	Control		Early stage				Late stage			
			FIGO stage I		FIGO stage II		FIGO Stage III		FIGO Stage IV	
Demographics	Age	CA125	Age	CA125	Age	CA125	Age	CA125	Age	CA125
N	33		10		9		43		15	
Mean	52.0	14.5	57.6	514.9	57.4	300.6	59.9	1503.6	59.9	2065.3
Median	50.0	12.0	59.5	28.5	53.0	190.0	60.0	616.0	58.0	1195.0
Range	40-81	6-38	48-67	6-4841	40-78	23-851	35-79	11-8094	32-81	6-14310

Samples were processed exactly as described in Chapter 5. In short, *N*-glycans were released by PNGase F and part of each digest was labelled by double-amidation reaction, after which *N*-glycans were purified by HILIC SPE and dried in vacuum centrifuge. Before measurements, samples were dissolved in 10 μl of MilliQ water and 1 μl of each sample was spotted on two MALDI target spots. Samples were left to dry and each spot was then layered with 1 μl matrix consisting of 10 mg/ml super DHB and 1mM NaCl in 10% aqueous ACN and left to dry.

MALDI-TOF-MS measurements and data processing

MALDI-TOF-MS spectra were recorded on an Ultraflex III mass spectrometer (Bruker Daltonics, Bremen, Germany) equipped with Smartbeam laser (100 Hz laser frequency) in reflectron positive mode as a sum of 2500 laser shots in the mass range 1200-5000 Da using 25kV accelerating voltage and ion suppression bellow 1190 Da. Raw spectra were exported as ASCII text files and Massy Tools script was first used to re-calibrate the obtained spectra using list of 10 glycan masses (N4H3F1, N4H4F1, N4H5D1, N4H5D1F1, N4H5D1A1, N4H5D2, N4H5D2F1, N5H6D2A1, N5H6D2A1F1, N6H7D2A2).

The program mMass was then used to sum all spectra from each sample (n =4) leading to sensitivity increase especially in the high-mass region. The MassyTools Python script [118] was then used on these summed spectra for a targeted peak extraction of background subtracted analyte areas of 100 glycan structures. The output of targeted peak extraction was then processed further, by removing all structures, which had signal-to-noise ratio (S/N) < 9 for more than 90% of all collected spectra. Additionally, all these structures were evaluated for separate sample groups and only structures, which appeared in more than 1/3 of samples in at least a single sample group, were used for statistical analysis, resulting in areas under the curve from 72 glycan peaks. The extracted values were then normalised so that the intensity of the peak at m/z 2299.9 (H4H5D2) was set to 100%. As a result of this approach, variance of this structure could not be statistically tested.

Glycan traits and statistical analysis

Total intensities of various glycan traits, namely high-mannosylation, fucosylation, linkage-specific sialylation and antennarity were calculated as a sum of intensities of all respective structures. For the calculation of sialylation traits, firstly a relative sialylation intensity was calculated for each structure as shown in Equation 1, then total sialylation traits were calculated as a sum of relative sialylation intensities of respective structures. For example, total α -2,3-sialylation of triantennary fucosylated *N*-glycans was calculated according to Equation 2.

Equation 1 Calculation of relative sialylation intensity

$$\begin{aligned}
 \text{S (degree of sialylation)} &= D_n + A_n \\
 \text{relative } \alpha\text{-2,6 sialylation} &= (D_n/S) * (\text{relative intensity } N_n H_n D_n A_n F_n) \\
 \text{relative } \alpha\text{-2,3 sialylation} &= (A_n/S) * (\text{relative intensity } N_n H_n D_n A_n F_n)
 \end{aligned}$$

Equation 2 Calculation of sialylation traits

$$\begin{aligned}
 \text{FUCOSYLATED COMPLEX TRIANTENNARY } \alpha\text{-2,3} &= (1/2) * (N5H5D1A1F1 + N5H6D1A1F1) + (2/3) * (N5H6D1A2F1) \\
 &+ (1/3) * (N5H6D2A1F1)
 \end{aligned}$$

Additionally, a ratio between α -2,3 and α -2,6 sialylation was calculated for each grouped *N*-glycans, which included all complex sialylated structures (Equation 3, Appendix, section Glycan traits calculation, Page 131).

Equation 3 Calculation of relative sialylation

$$\text{FUCOSYLATED COMPLEX TRIANTENNARY} = \frac{\text{FUCOSYLATED COMPLEX TRIANTENNARY } \alpha\text{-2,3}}{\text{FUCOSYLATED COMPLEX TRIANTENNARY } \alpha\text{-2,6}}$$

Means and standard deviations were calculated for FIGO stages and for grouped ovarian cancer stages (healthy controls, early stage = FIGO I + FIGO II, late stage = FIGO III + FIGO IV). The Shapiro-Wilk test showed that the data were not normally distributed and therefore non-parametric tests were used for further statistical evaluation. The Jonckheere-Terpstra test (T_{JT}) was selected since the independent variables consisted of three ordinal groups of cancer progression (healthy control < early stage < late stage), while the dependent variables were measured on continuous level, and there was no relationship between samples in various groups. The T_{JT} was used to test the null hypothesis that the distribution of individual *N*-glycans was the same across ovarian cancer stages. In other words, it was tested if there is a positive or negative trend during cancer progression. The null hypothesis was rejected when $p < 0.05$.

Results

Seventy-one *N*-glycan structures were detected, four were high-mannoses, thirteen were asialylated complex-type structures, of which seven were fucosylated. Due to sialic acid linkage-specific labelling, overall 54 different sialylated *N*-glycans were detected, of which 24 were fucosylated. It should be noted that many of these structures were not observed in early stages of ovarian cancer and/or healthy controls. However, all these structures were included in statistical analysis due to their possible biological significance.

Relative intensities of 71 glycans (H = hexose, N = N-acetylhexosamine, A = α -2,3-linked sialic acid, D = α -2,6-linked sialic acid, F = fucose) were normalized to the base peak intensity. Means and standard deviations (SD) were calculated for healthy controls and all FIGO stages and are presented in Table 15.

Table 15 Mean relative intensities (normalised to the base peak intensity) and SD of all detected structures across ovarian cancer stages measured by MALDI-TOF-MS.

Glycan type	Glycan	Mass [m/z]	Healthy control		Fig0 I		Fig0 II		Fig0 III		Fig0 IV	
			Mean	SD	Mean	SD	Mean	SD	Mean	SD	Mean	SD
High-mannose	N2H5	1257.4	2.06	1.31	2.48	0.69	1.39	0.48	0.86	0.45	0.75	0.44
	N2H6	1419.5	1.46	1.02	1.99	0.72	1.36	0.46	0.95	0.51	0.87	0.58
	N2H7	1581.5	0.19	0.19	0.50	0.25	0.32	0.15	0.25	0.20	0.24	0.20
	N2H8	1743.6	0.37	0.21	0.61	0.37	0.49	0.17	0.40	0.24	0.36	0.24
Complex	N3H4	1298.4	0.18	0.21	0.25	0.24	0.15	0.16	0.07	0.10	0.08	0.09
	N4H3	1339.5	0.37	0.70	0.53	0.34	0.29	0.26	0.23	0.26	0.23	0.24
	N4H5	1663.6	0.73	0.43	0.53	0.12	0.38	0.18	0.24	0.16	0.23	0.15
	N5H4	1704.6	0.16	0.29	0.36	0.18	0.20	0.10	0.23	0.18	0.21	0.16
	N5H5	1866.7	0.04	0.07	0.14	0.17	0.08	0.08	0.09	0.11	0.07	0.09
	N5H6	2028.7	0.00	0.01	0.02	0.06	0.01	0.04	0.02	0.04	0.03	0.05
Complex fucosylated	N4H3F1	1485.5	5.22	3.15	10.49	4.51	8.05	6.05	9.19	12.36	6.20	4.05
	N4H4F1	1647.6	5.19	2.51	8.16	3.93	4.99	3.13	4.45	3.89	3.58	2.37
	N4H5F1	1809.6	1.60	0.89	1.98	1.33	1.23	1.05	0.90	0.84	0.72	0.62
	N5H4F1	1850.7	1.03	0.43	1.42	0.54	0.86	0.40	0.77	0.61	0.63	0.42
	N5H5F1	2012.7	0.15	0.10	0.29	0.20	0.13	0.11	0.14	0.15	0.13	0.10
	N5H5F2	2158.8	0.50	0.13	0.72	0.21	0.54	0.17	0.56	0.26	0.59	0.24
	N5H6F1	2174.8	0.01	0.02	0.07	0.12	-	-	0.03	0.05	0.01	0.02
Complex sialylated	N3H4A1	1588.6	0.01	0.02	0.54	0.79	0.21	0.25	0.46	0.47	0.42	0.48
	N3H4D1	1616.6	1.75	0.51	1.33	0.33	0.89	0.21	0.82	0.33	0.88	0.33
	N3H5A1	1750.6	1.93	0.75	2.03	0.60	1.63	0.46	1.11	0.54	0.85	0.61
	N3H5D1	1778.6	0.47	0.20	0.49	0.08	0.33	0.08	0.26	0.13	0.25	0.10
	N4H4A1	1791.6	0.04	0.16	0.77	1.10	0.32	0.36	0.68	0.70	0.58	0.68
	N4H4D1	1819.7	0.71	0.28	0.73	0.30	0.46	0.12	0.53	0.28	0.52	0.28
	N3H6A1	1912.7	0.02	0.08	0.11	0.15	0.01	0.04	0.05	0.09	0.05	0.10
	N3H6D1	1940.7	0.10	0.08	0.12	0.07	0.05	0.06	0.09	0.07	0.07	0.06
	N4H5A1	1953.7	0.28	0.13	0.54	0.44	0.28	0.16	0.43	0.32	0.37	0.32

Glycan type	Glycan	Mass [m/z]	Healthy control		Figo I		Figo II		Figo III		Figo IV	
			Mean	SD	Mean	SD	Mean	SD	Mean	SD	Mean	SD
Complex sialylated	N4H5D1	1981.7	12.00	2.65	10.52	2.12	8.38	2.60	7.51	2.89	8.32	3.13
	N5H5D1	2184.8	0.36	0.22	0.51	0.20	0.31	0.15	0.25	0.15	0.27	0.13
	N4H5A2	2243.8	0.09	0.10	0.14	0.11	0.04	0.08	0.02	0.05	0.04	0.05
	N4H5D1A1	2271.8	3.77	1.27	3.80	0.64	3.26	1.14	3.09	1.08	2.99	1.02
	N4H5D2	2299.9	100.00	-	100.00	-	100.00	-	100.00	-	100.00	-
	N5H6A1	2318.8	0.16	0.29	-	-	0.12	0.14	0.13	0.22	0.11	0.11
	N5H6D1	2346.9	0.45	0.21	0.44	0.11	0.42	0.15	0.29	0.17	0.32	0.13
	N5H5D2	2502.9	0.27	0.15	0.42	0.11	0.32	0.42	0.21	0.23	0.28	0.28
	N5H6D1A1	2637.0	0.47	0.23	0.49	0.12	0.42	0.22	0.35	0.16	0.32	0.15
	N5H6D2	2665.0	0.64	0.24	0.64	0.16	0.52	0.23	0.39	0.17	0.42	0.11
	N5H6A3	2899.0	-	-	0.04	0.07	-	-	0.03	0.05	0.03	0.05
	N5H6D1A2	2927.1	0.30	0.25	0.32	0.15	0.31	0.21	0.29	0.17	0.26	0.19
	N5H6D2A1	2955.1	6.41	3.07	5.58	2.32	5.22	2.99	4.42	2.35	3.71	2.44
	N5H6D3	2983.1	2.15	0.64	2.93	1.16	2.94	1.65	2.20	0.75	2.28	0.63
	N6H7D1A1	3002.1	0.08	0.10	0.24	0.09	0.22	0.17	0.12	0.09	0.11	0.07
	N6H7D2	3030.1	0.01	0.03	0.07	0.10	0.04	0.08	0.04	0.05	0.05	0.05
	N6H7D1A2	3292.2	0.04	0.06	0.09	0.09	0.09	0.11	0.08	0.09	0.07	0.08
	N6H7D2A1	3320.2	0.05	0.08	0.14	0.12	0.09	0.14	0.09	0.09	0.07	0.06
	N6H7D1A3	3582.3	0.03	0.06	0.05	0.09	0.10	0.14	0.12	0.14	0.11	0.15
	N6H7D2A2	3610.3	0.14	0.12	0.18	0.16	0.24	0.23	0.22	0.17	0.19	0.20
N6H7D3A1	3638.4	0.01	0.04	0.07	0.09	0.08	0.11	0.08	0.09	0.08	0.08	
Complex sialylated fucosylated	N4H5A1F1	2099.7	0.24	0.10	0.23	0.11	0.14	0.12	0.14	0.10	0.17	0.09
	N4H5D1F1	2127.8	2.22	0.84	2.28	1.14	1.55	0.88	1.21	0.75	1.24	0.61
	N5H5D1F1	2330.9	0.94	0.50	1.51	0.89	0.86	0.64	0.67	0.56	0.66	0.31
	N4H5A2F1	2389.9	0.54	0.28	0.62	0.18	0.60	0.20	0.37	0.20	0.22	0.16
	N4H5D1A1F1	2417.9	0.54	0.21	0.66	0.16	0.82	0.55	0.74	0.32	0.91	0.55
	N4H5D2F1	2445.9	4.46	1.15	3.40	1.19	3.56	0.94	2.71	1.05	3.10	1.21
	N5H6D1F1	2492.9	0.05	0.09	0.15	0.15	0.05	0.09	0.02	0.05	0.03	0.05
	N5H5D1A1F1	2621.0	0.01	0.03	0.07	0.10	0.02	0.05	0.03	0.05	0.03	0.04
	N5H5D2F1	2649.0	1.48	0.72	1.55	0.57	1.31	0.80	0.99	0.51	0.93	0.35
	N5H6D1A1F1	2783.0	0.06	0.10	0.18	0.12	0.20	0.14	0.12	0.13	0.19	0.12
	N5H6D2F1	2811.1	0.09	0.10	0.17	0.11	0.17	0.11	0.07	0.09	0.13	0.09
	N5H6D1A2F1	3073.1	0.05	0.07	0.21	0.15	0.25	0.17	0.21	0.13	0.21	0.15
	N5H6D2A1F1	3101.2	2.12	1.06	4.59	2.06	6.37	3.45	5.05	2.46	5.48	2.72
	N5H6D3F1	3129.2	0.12	0.12	0.22	0.14	0.27	0.17	0.15	0.12	0.18	0.11
	N6H7D1A1F1	3148.2	-	-	0.05	0.10	0.06	0.11	0.04	0.07	0.08	0.07
	N5H6D1A2F2	3219.2	-	-	0.01	0.04	0.08	0.12	0.05	0.08	0.08	0.08
	N5H6D2A1F2	3247.2	0.01	0.04	0.04	0.10	0.14	0.14	0.06	0.10	0.11	0.09
	N6H7D1A2F1	3438.3	-	-	-	-	0.07	0.11	0.03	0.06	0.08	0.07
	N6H7D2A1F1	3466.3	-	-	0.01	0.03	0.05	0.11	0.03	0.06	0.06	0.07
	N6H7D1A3F1	3728.4	-	-	-	-	0.11	0.13	0.08	0.12	0.11	0.14
N6H7D2A2F1	3756.4	0.02	0.04	0.08	0.11	0.25	0.20	0.23	0.19	0.22	0.21	
N6H7D3A1F1	3784.4	-	-	0.01	0.03	0.03	0.06	0.06	0.10	0.08	0.08	
N6H7D1A3F2	3874.4	-	-	0.01	0.04	0.03	0.07	0.03	0.06	0.05	0.08	
N6H7D2A2F2	3902.5	-	-	-	-	0.10	0.18	0.07	0.13	0.11	0.11	

Detailed statistics was performed for grouped FIGO stages (early and late stage) and these results will be discussed in the next section.

High-mannose N-glycans

The T_{JT} showed that there was a statistically significant negative trend in mean rank distribution of N2H5 and N2H6, which was observed for both grouped (early and late) and individual FIGO stages (I – IV), however only grouped statistics will be presented (Table 16). The comparisons were performed between healthy controls, early stage and late stage ovarian cancer. Moreover, post-hoc statistical test is reported for total trait only.

Table 16 Results of non-parametric T_{JT} of relative intensities of high-mannose structures and total high-mannosylation. Positive and negative Z values indicate increasing and decreasing trends, respectively. P values < 0.05 were considered statistically significant.

Glycan type	Glycan	m/z	T_{JT}	Z value	p value
High-mannose	N2H5	1257.4	637	-6.764	<0.0001
	N2H6	1419.5	1044	-4.44	<0.0001
	N2H7	1581.5	1885.5	0.367	0.714
	N2H8	1743.6	1634.5	-1.068	0.286
	Total	-	958.0	-4.931	< 0.0001

The post-hoc analysis of the T_{JT} test revealed that there was a highly significant decrease in total high-mannosylation between healthy controls and late stage patients ($T_{JT} = 406.0$, $z = -4.549$, $p < 0.001$), and between early stage and late stage patients ($T_{JT} = 166.0$, $z = -4.620$, $p < 0.001$) (Figure 27).

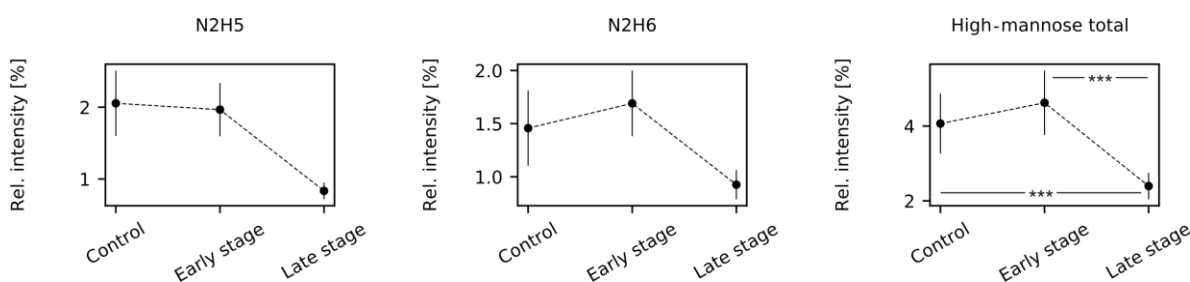


Figure 27 Mean relative intensities and 95% confidence intervals of high-mannose structures.

There was no statistically significant difference between healthy controls and early stage patients.

Complex afucosylated *N*-glycans

There were statistically significant differences for almost all complex asialylated *N*-glycans, namely only N4H3 showed no statistically significant difference. In general, there was a decrease in relative intensity total complex asialylated *N*-glycans (Table 17).

*Table 17 Results of non-parametric T_{JT} of relative intensities of complex asialylated *N*-glycans structures during ovarian cancer progression. Positive and negative Z values indicate increasing and decreasing trends, respectively. P values < 0.05 were considered statistically significant.*

Glycan type	Glycan	m/z	T_{JT}	Z value	p value
Complex	N3H4	1298.4	1478.5	-2.086	0.037
	N4H3	1339.5	1891.5	0.411	0.681
	N4H5	1663.6	434.5	-7.920	< 0.0001
	N5H4	1704.6	2192.5	2.127	0.033
	N5H5	1866.7	2140.5	2.011	0.044
	N5H6	2028.7	2065.0	2.332	0.020
	Total	-	1188.0	-3.618	0.0003

Additionally, there was a statistically significant decrease of monoantennary and biantennary *N*-glycans and increase of triantennary *N*-glycans. These findings do correspond with the published literature, since increased expression of GlcNAcT IV and V leads to increased branching and thus antennarity [172, 173].

Similarly to the high-mannosylation, there was a highly significant decrease in total relative intensity of afucosylated complex-type *N*-glycans. Significant differences were observed between healthy controls and late stage patients ($T_{JT} = 542.0$, $z = -3.426$, $p = 0.001$), and between early stage and late stage patients ($T_{JT} = 291.0$, $z = -3.072$, $p = 0.003$). There was no statistically significant difference between healthy controls and early stage patients (Figure 28).

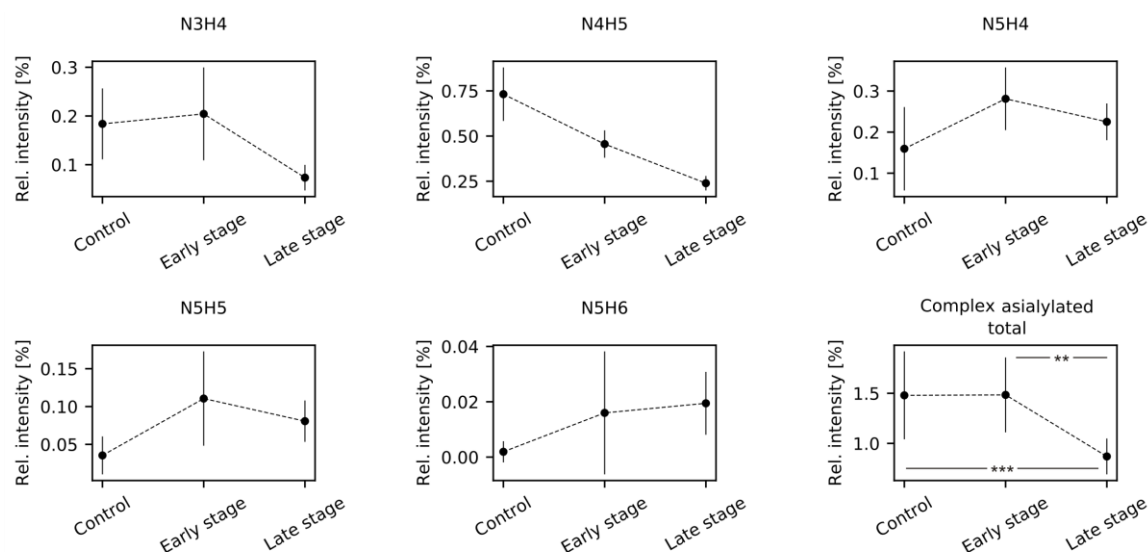


Figure 28 Mean relative intensities and 95% confidence intervals of complex asialylated *N*-glycans during ovarian cancer progression.

Complex-type fucosylated *N*-glycans

There were three complex-type core-fucosylated structures, which showed statistically significant differences in relative intensities between healthy controls and ovarian cancer stages, namely N4H4F1, N4H5F1 and N5H4F1 (Table 18, Figure 29).

Table 18 Results of non-parametric T_{JT} of relative intensities of fucosylated complex-type asialylated *N*-glycans structures during ovarian cancer progression. Positive and negative *Z* values indicate increasing and decreasing trends, respectively. *P* values < 0.05 were considered statistically significant.

Glycan type	Glycan	<i>m/z</i>	T_{JT}	<i>Z</i> value	<i>p</i> value
Complex fucosylated	N4H3F1	1485.5	1919.0	0.557	0.578
	N4H4F1	1647.6	1310.0	-2.921	0.003
	N4H5F1	1809.6	1005.0	-4.662	< 0.0001
	N5H4F1	1850.7	1126.0	-3.972	< 0.0001
	N5H5F1	2012.7	1604.0	-1.246	0.213
	N5H5F2	2158.8	1857.0	0.203	0.839
	N5H6F1	2174.8	1966.5	1.232	0.218
	Total	-	1579.0	-1.385	0.166

These structures are commonly observed on immunoglobulin G (IgG)[174]. Saldova and colleagues [40] showed using ovarian cancer samples, irrespective of FIGO stages, that there was a decrease of IgG galactosylation and an increase of agalactosyl IgG *N*-glycans in ovarian cancer patients. However, it should be noted that our analysis was performed on 110 whole serum *N*-glycome samples and not at the IgG level alone. This is the reason why the observed changes can only be partly explained by the IgG glycosylation alone.

Compared to the above-mentioned publication, our findings suggest an initial increase of relative abundance of total complex fucosylated *N*-glycans in early FIGO stages, followed by a decrease in late stages. This could be explained by inflammation and greater IgG production in early stages, thus greater abundance of glycan structures carried on IgG. Additionally, the expected increase in relative abundance of the agalactosylated structure N4H3F1 was not statistically significant ($p = 0.712$) in this study as shown in Table 18.

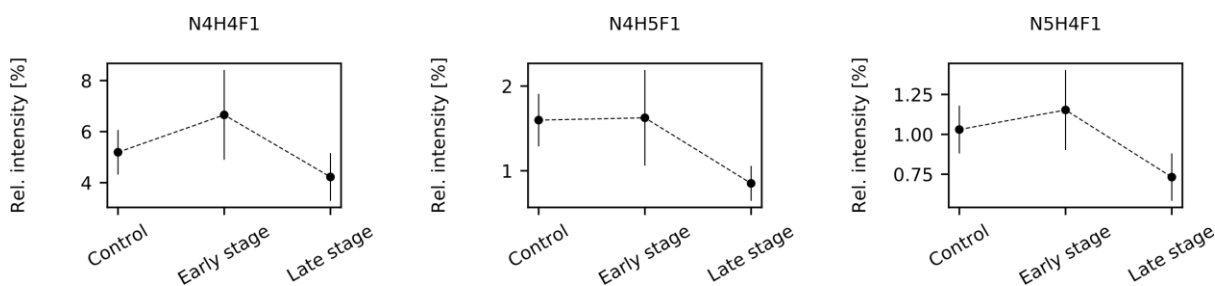


Figure 29 Mean relative intensities and 95% confidence intervals of fucosylated complex asialylated *N*-glycans during ovarian cancer progression.

There was no statistically significant difference in total relative intensity of complex fucosylated *N*-glycans.

Hybrid-type sialylated *N*-glycans

Statistical analysis revealed a significant decrease in both α -2,3- and α -2,6-sialylation forms of hybrid structure N3H5S1. The second hybrid structure N3H6S1 did not show any statistically significant trend for the α -2,6-isomer, however there was a statistically significant increase in relative intensity of the α -2,3-isomer (Table 19). For the total relative intensity of hybrid structures, there was a statistically significant decrease.

Table 19 Results of non-parametric T_{JT} of relative intensities of hybrid N-glycan structures and their total relative intensity during ovarian cancer progression. Positive and negative Z values indicate increasing and decreasing trends, respectively. P values < 0.05 were considered statistically significant.

Glycan type	Glycan	m/z	T_{JT}	Z value	p value
Hybrid-type	N3H5A1	1750.6	783.0	-5.930	< 0.0001
	N3H5D1	1778.6	715.0	-6.319	< 0.0001
	N3H6A1	1912.7	2103.5	2.030	0.042
	N3H6D1	1940.7	1646.5	-1.012	0.312
	Total	-	767.0	-6.022	< 0.0001

The post-hoc analysis revealed that there were statistically significant differences between healthy controls and late stage patients ($T_{JT} = 296.0$, $z = -5.457$, $p < 0.001$), and between early stage and late stage patients ($T_{JT} = 183.0$, $z = -4.348$, $p < 0.001$). There was no statistically significant difference between healthy controls and early stage patients.

Complex-type sialylated N-glycans

The statistical analysis of sialylated complex-type structures was first performed on a single glycan level followed by calculation of glycan traits as explained in the section “Glycan traits and statistical analysis” (page 88). The complex-type sialylated structures are presented here separately based on their fucose content. Additionally, for both fucosylated and afucosylated structures, total glycosylation traits were calculated, such relative antennarity. It should be noted that while total α -2,6-linked sialylation corresponds with a total sialylation relative intensity, the relative α -2,3-linked sialylation shows unique trends (as shown in Appendix, Absolute sialylation, page 133). Therefore, a ratio between α -2,3-linked sialylation and α -2,6-linked sialylation was calculated.

Complex-type sialylated N-glycans - monoantennary

In the monoantennary group, a statistically significant negative trend for the α -2,6-linked isomer and positive trend for α -2,3-linked isomer was observed. The total relative intensity for monoantennary sialylated structures decreased in advanced cancer stages (Table 20).

Table 20 Results of non-parametric T_{IT} of relative intensities of monoantennary sialylated N-glycan structures and their total relative intensity during ovarian cancer progression. Positive and negative Z values indicate increasing and decreasing trends, respectively. P values < 0.05 were considered statistically significant.

Glycan type	Glycan	m/z	T_{IT}	Z value	p value
Complex sialylated monoantennary	N3H4A1	1588.6	2865.0	6.224	< 0.0001
	N3H4D1	1616.6	473.0	-7.700	< 0.0001
	Total	-	1074.0	-4.268	< 0.0001

The post-hoc analysis revealed that there were statistically significant differences between healthy controls and early stage patients ($T_{IT} = 199.0$, $z = -2.176$, $p < 0.044$), and between healthy controls and late stage patients ($T_{IT} = 452.0$, $z = -4.169$, $p < 0.001$). There was no statistically significant difference between early and late stage patients (Figure 30).

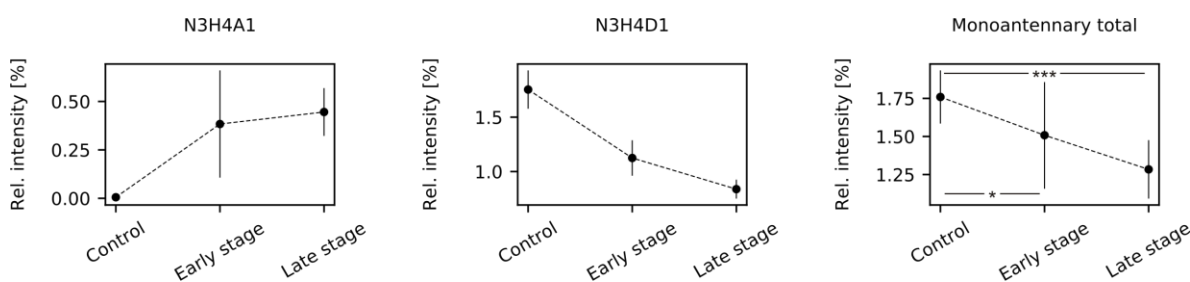


Figure 30 Mean relative intensities and 95% confidence intervals of monoantennary complex sialylated N-glycans during ovarian cancer progression.

Since there were only two structures detected, the analysis of sialic acid linkages corresponds to those of individual N-glycans. There were no fucosylated monoantennary structures detected.

Complex-type sialylated N-glycans - biantennary

The total relative intensity for both fucosylated and afucosylated biantennary glycans decreased in ovarian cancer compared to healthy controls (Table 21). The significant difference was observed for afucosylated structures between healthy controls and late stage patients ($T_{IT} = 337.0$, $z = -5.118$, $p < 0.001$), and between early stage and late stage patients ($T_{IT} = 322.0$, $z = -2.706$, $p = 0.010$). There was no statistically significant difference between healthy controls and early stage patients. For fucosylated structures, there were statistically

significant differences between healthy controls and late stage patients ($T_{JT} = 262.0$, $z = -5.737$, $p < 0.001$), early stage and late stage patients ($T_{JT} = 275.0$, $z = -3.261$, $p = 0.002$), and no differences between healthy controls and early stage.

Table 21 Results of non-parametric T_{JT} of relative intensities of biantennary sialylated N-glycan structures, sialic acid ratio and their total relative intensity during ovarian cancer progression. Positive and negative Z values indicate increasing and decreasing trends, respectively. P values < 0.05 were considered statistically significant.

Glycan type	Glycan	m/z	T_{JT}	Z value	p value
Complex sialylated biantennary	N4H4A1	1791.6	2757.5	5.616	< 0.0001
	N4H4D1	1819.7	1151.0	-3.829	0.0001
	N4H5A1	1953.7	2034.5	1.216	0.224
	N4H5D1	1981.7	758.0	-6.073	< 0.0001
	N4H5A2	2243.8	1338.0	-3.283	0.001
	N4H5D1A1	2271.8	1286.0	-3.058	0.002
	N4H5D2	2299.9	-	-	-
	α -2,3/ α -2,6	-	2947.0	6.427	< 0.0001
	Total	-	879.0	-5.382	< 0.0001
Complex sialylated fucosylated Biantennary	N4H5A1F1	2099.7	1029.0	-4.531	< 0.0001
	N4H5D1F1	2127.8	829.0	-5.668	< 0.0001
	N4H5A2F1	2389.9	1047.0	-4.424	< 0.0001
	N4H5D1A1F1	2417.9	2402.5	3.318	0.001
	N4H5D2F1	2445.9	784.0	-5.924	< 0.0001
	α -2,3/ α -2,6	-	2391.0	3.252	0.0011
	Total	-	750.0	-6.119	< 0.0001

The α -2,3/ α -2,6-sialylation ratio significantly increases for both afucosylated and fucosylated N-glycans in ovarian cancer patients (Figure 31). Post-hoc analysis showed no statistical differences between early stage and late stage for both afucosylated and fucosylated biantennary N-glycans. There were statistically significant differences between healthy control and early stage (afucosylated: $T_{JT} = 544.0$, $z = 4.380$, $p < 0.001$; fucosylated: $T_{JT} = 453.0$, $z = 2.651$, $p = 0.012$) and between healthy control and late stage (afucosylated: $T_{JT} = 1707.0$, $z = 6.191$, $p < 0.001$; fucosylated: $T_{JT} = 1370.0$, $z = 3.409$, $p = 0.001$).

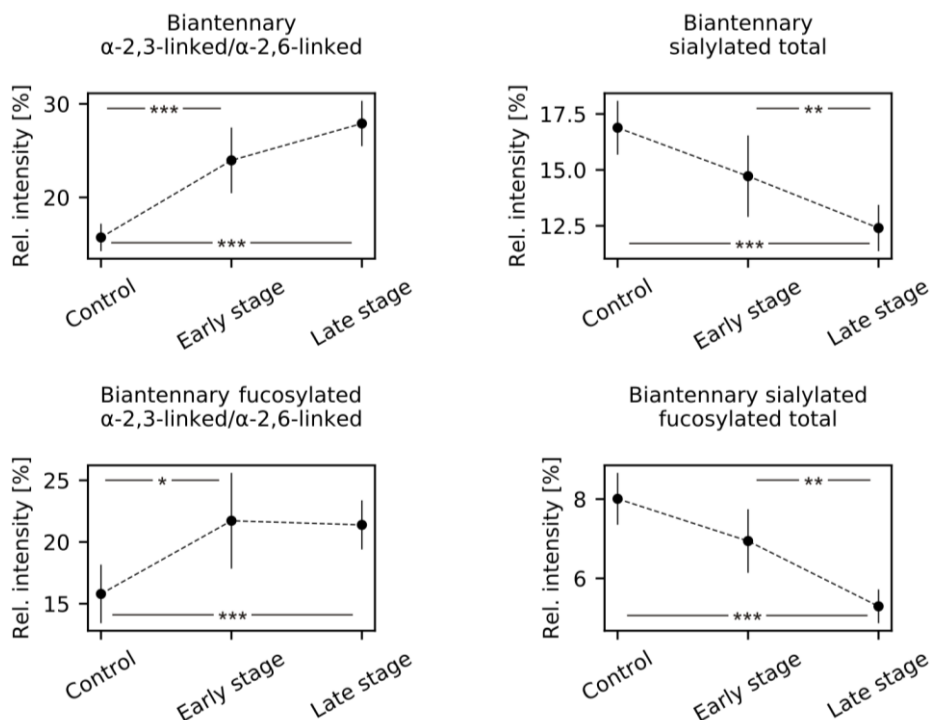


Figure 31 Mean and 95% confidence intervals of sialylation ratio and total relative intensities of biantennary complex sialylated *N*-glycans during ovarian cancer progression.

Complex-type sialylated *N*-glycans – triantennary

There was a statistically significant decrease in total relative intensity of triantennary sialylated *N*-glycans between healthy controls and late stage patients ($T_{JT} = 569.0$, $z = -3.203$, $p = 0.002$), and between early stage and late stage patients ($T_{JT} = 357.0$, $z = -2.292$, $p = 0.033$). There was no statistically significant difference between healthy controls and early stage patients. On the other hand, there was a statistically significant increase in total intensity of fucosylated sialylated triantennary *N*-glycans (Table 22). The observed differences were between healthy controls and early stage patients ($T_{JT} = 531.0$, $z = 4.133$, $p < 0.001$), healthy controls and late stage patients ($T_{JT} = 1480.0$, $z = 4.317$, $p < 0.001$), and no differences between early stage and late stage patients.

Table 22 Results of non-parametric T_{JT} of relative intensities of triantennary sialylated N-glycan structures, sialic acid ratio and their total relative intensity during ovarian cancer progression. Positive and negative Z values indicate increasing and decreasing trends, respectively. P values < 0.05 were considered statistically significant.

Glycan type	Glycan	m/z	T_{JT}	Z value	p value
Complex sialylated Bisect/Triantennary	N5H5D1	2184.8	1307.0	-2.938	0.003
	N5H6A1	2318.8	1905.0	0.550	0.583
	N5H6D1	2346.9	1116.0	-4.030	< 0.0001
	N5H5D2	2502.9	1445.5	-2.165	0.03
	N5H6D1A1	2637.0	1131.5	-3.942	< 0.0001
	N5H6D2	2665.0	876.0	-5.399	< 0.0001
	N5H6A3	2899.0	2247.5	3.618	0.0003
	N5H6D1A2	2927.1	1741.5	-0.458	0.647
	N5H6D2A1	2955.1	1197.0	-3.566	0.0004
	N5H6D3	2983.1	1819.0	-0.014	0.989
	α -2,3/ α -2,6	-	1562.0	-1.482	0.138
	Total	-	1229.0	-3.383	0.001
Complex sialylated fucosylated Triantennary	N5H5D1F1	2330.9	1266.0	-3.172	0.002
	N5H6D1F1	2492.9	1591.0	-1.624	0.104
	N5H5D1A1F1	2621.0	2052.5	1.645	0.100
	N5H5D2F1	2649.0	1194.0	-3.583	0.0003
	N5H6D1A1F1	2783.0	2256.0	2.571	0.01
	N5H6D2F1	2811.1	1675.0	-0.869	0.385
	N5H6D1A2F1	3073.1	2621.0	4.655	< 0.0001
	N5H6D2A1F1	3101.2	2816.0	5.679	< 0.0001
	N5H6D3F1	3129.2	1988.5	0.968	0.333
	N5H6D1A2F2	3219.2	2347.5	3.978	< 0.0001
	N5H6D2A1F2	3247.2	2288.0	3.167	0.002
	α -2,3/ α -2,6	-	2982.0	6.627	< 0.0001
	Total	-	2429.0	3.469	0.001

Similarly to the monoantennary and biantennary complex-type N-glycans, there was an increase in relative intensity of a glycan carrying only α -2,3-linked sialic acid and a decrease in relative intensities of structures with α -2,6 linked sialic acids, however there were no statistically significant differences in the sialylation ratio of triantennary afucosylated structures (Figure 32). On the other hand, there was a statistically significant

increase in sialylation ratio of fucosylated triantennary *N*-glycans, which was observed between the healthy controls and both early stage ($T_{JT} = 517.0$, $z = 3.867$, $p < 0.001$) and late stage ($T_{JT} = 1736.0$, $z = 6.413$, $p < 0.001$) ovarian cancer patients.

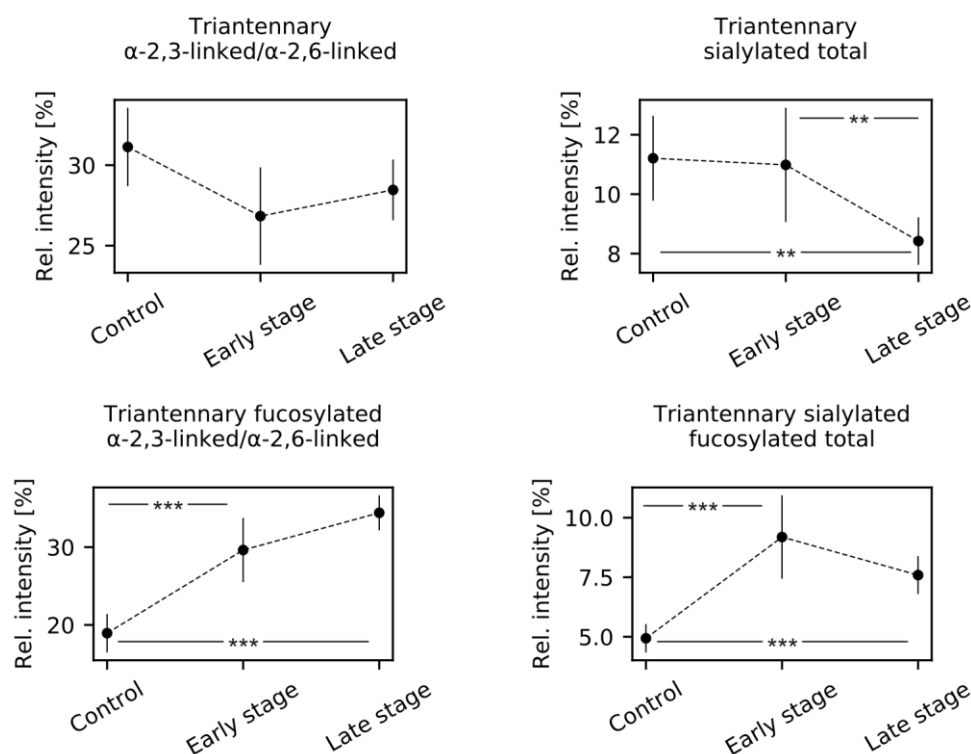


Figure 32 Mean and 95% confidence intervals of sialylation ratio and total relative intensities of triantennary complex sialylated *N*-glycans during ovarian cancer progression.

Complex-type sialylated *N*-glycans - tetraantennary

There was a statistically significant increase in relative intensities of three tetraantennary *N*-glycans, namely N6H7D2, N6H7D1A3 and N6H7D3A1 (Table 23). There was a statistically significant increase in total relative intensity of tetraantennary *N*-glycans between healthy controls and early stage patients ($T_{JT} = 463.0$, $z = 2.861$, $p = 0.006$), and between healthy controls and late stage patients ($T_{JT} = 1299.0$, $z = 2.836$, $p = 0.07$). There was no statistically significant difference between early and late stage patients. Similarly, there was a statistically significant increase in total relative intensity of fucosylated tetraantennary *N*-glycans between healthy controls and early stage ($T_{JT} = 511.0$, $z = 4.421$, $p < 0.001$) and late

stage ($T_{IT} = 1684.0$, $z = 6.274$, $p < 0.001$) ovarian cancer patients. There were no differences between early stage and late stage patients.

Table 23 Results of non-parametric T_{IT} of relative intensities of tetraantennary sialylated N-glycan structures, sialic acid ratio and their total relative intensity during ovarian cancer progression. Positive and negative Z values indicate increasing and decreasing trends, respectively. P values < 0.05 were considered statistically significant.

Glycan type	Glycan	m/z	T_{IT}	Z value	p value
Complex sialylated tetraantennary	N6H7D1A1	3002.1	1880.5	0.345	0.73
	N6H7D2	3030.1	2259.0	3.024	0.002
	N6H7D1A2	3292.2	2112.0	1.804	0.071
	N6H7D2A1	3320.2	2021.0	1.228	0.219
	N6H7D1A3	3582.3	2267.0	2.839	0.005
	N6H7D2A2	3610.3	2149.5	1.901	0.057
	N6H7D3A1	3638.4	2320.5	3.308	0.001
	α -2,3/ α -2,6	-	1726.5	-0.546	0.585
	Total	-	2248.5	2.446	0.014
Complex sialylated fucosylated Tetraantennary	N6H7D1A1F1	3148.2	2346.0	3.865	0.0001
	N6H7D1A2F1	3438.3	2306.5	3.834	0.0001
	N6H7D2A1F1	3466.3	2242.0	3.502	0.0005
	N6H7D1A3F1	3728.4	2428.0	4.366	< 0.0001
	N6H7D2A2F1	3756.4	2746.0	5.565	< 0.0001
	N6H7D3A1F1	3784.4	2390.5	4.364	< 0.0001
	N6H7D1A3F2	3874.4	2224.5	3.423	0.001
	N6H7D2A2F2	3902.5	2318.5	3.929	< 0.0001
	α -2,3/ α -2,6	-	490.5	0.663	0.507
	Total	-	2864.0	6.184	< 0.0001

However, there was no statistically significant difference in relative sialylation for neither afucosylated nor fucosylated N-glycans. Moreover, the ratio between α -2,3 and α -2,6 sialylation was 1:1 for both afucosylated and fucosylated N-glycans in all three cohorts (Figure 33). This could be due to steric hinderance of α -2,3-linkages, which theoretically favours mixed α -2,3 / α -2,6 sialic acid linkages.

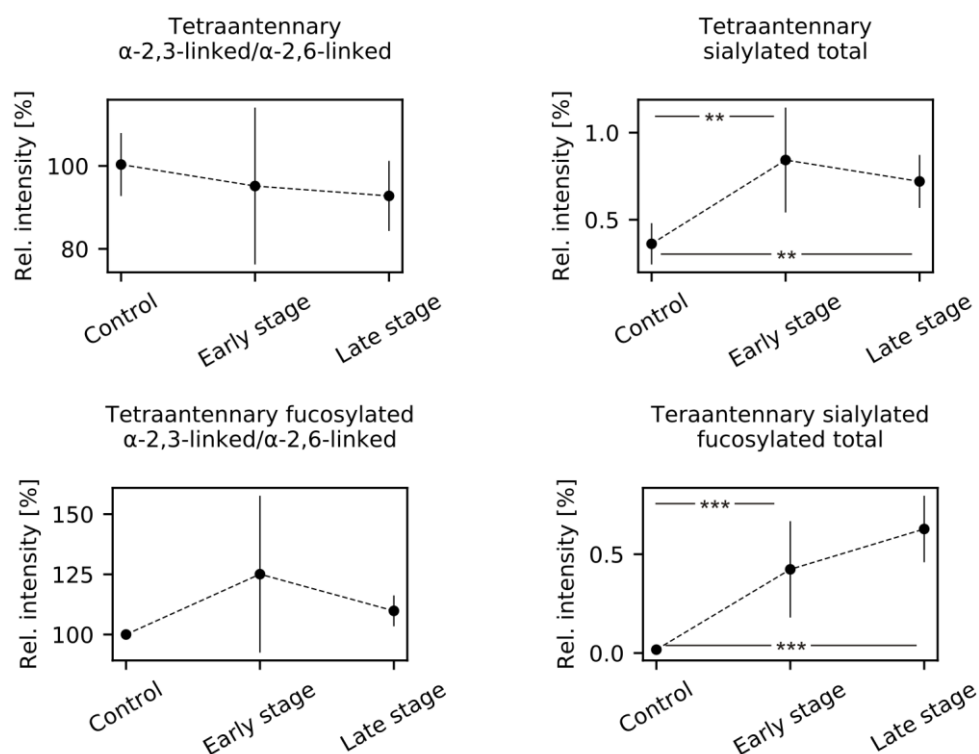


Figure 33 Mean and 95% confidence intervals of sialylation ratio and total relative intensities of tetraantennary complex-type sialylated *N*-glycans during ovarian cancer progression.

Total complex-type sialylated *N*-glycans

The total relative intensities of all sialylated afucosylated and fucosylated *N*-glycans were calculated as a sum of all *N*-glycans carrying sialic acids. There was a statistically significant decrease in total relative intensity of afucosylated sialylated *N*-glycans (Table 24). The observed decrease was statistically significant between late stage ovarian cancer patients and healthy controls ($T_{JT} = 393.0$, $z = -4.656$, $p < 0.001$), and between late stage and early stage ovarian cancer patients ($T_{JT} = 277.0$, $z = -3.237$, $p < 0.001$). There were no statistically significant differences in total relative intensity of fucosylated sialylated *N*-glycans. There were highly significant increases in sialylation ratio for both afucosylated and fucosylated *N*-glycans.

Table 24 Results of non-parametric T_{JT} of sialic acid ratio and total relative intensity of sialylated N-glycan structures during ovarian cancer progression. Positive and negative Z values indicate increasing and decreasing trends, respectively. P values < 0.05 were considered statistically significant.

Glycan type	Fucosylation	Glycan	T_{JT}	Z value	p value
Complex sialylated	Afucosylated	α -2,3/ α -2,6	2705.0	5.045	< 0.0001
		Total	948.0	-4.988	< 0.0001
	Fucosylated	α -2,3/ α -2,6	2934.0	6.353	< 0.0001
		Total	1815.0	-0.037	0.970
	Total	α -2,3/ α -2,6	3057.0	7.055	< 0.0001

Specifically, there were statistically significant differences between healthy control and early stage (afucosylated: $T_{JT} = 458.0$, $z = 2.746$, $p = 0.009$; fucosylated: $T_{JT} = 516.0$, $z = 3.848$, $p < 0.001$) and between healthy control and late stage (afucosylated: $T_{JT} = 1530.0$, $z = 4.730$, $p < 0.001$; fucosylated: $T_{JT} = 1727.0$, $z = 6.356$, $p < 0.001$) (Figure 34).

These changes in sialylation ratio are cancer specific, since in both fucosylated and afucosylated glycans are observed statistically significant differences between healthy controls and cancer stages. Moreover, there were no statistically significant differences between early and late stage ovarian cancer patients, which makes these ratios a possible candidate for improving ovarian cancer diagnostics.

On the total sialylation level, there were statistically significant differences between all three cohorts. There were highly significant increases between healthy controls and both early ($T_{JT} = 552.0$, $z = 4.532$, $p < 0.001$) and late ($T_{JT} = 1762$, $z = 6.645$, $p < 0.001$) stages of ovarian cancer. There was a statistically significant increase in sialylation ratio between early and late stage patients ($T_{JT} = 743$, $z = 2.269$, $p = 0.035$).

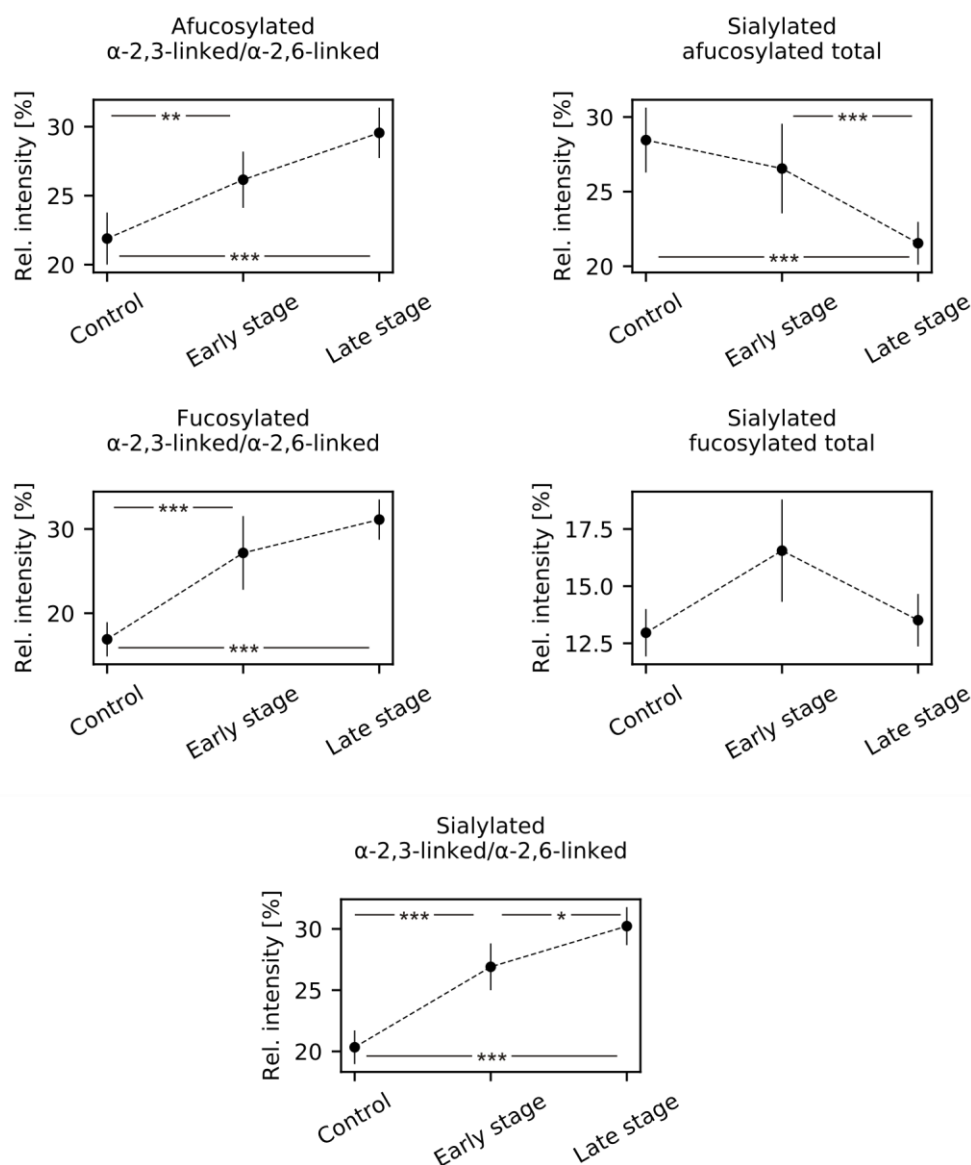


Figure 34 Mean and 95% confidence intervals of sialylation ratio and total relative intensities of complex sialylated N-glycans during ovarian cancer progression.

Sialylation ratio as enhancement of ovarian cancer diagnosis

Since the changes in sialylation ratio showed statistically significant differences between healthy controls and primary serous epithelial ovarian cancer patients, the values were used for construction of receiver operating characteristic (ROC) curves (Figure 35) to evaluate possible application in ovarian cancer diagnostics.

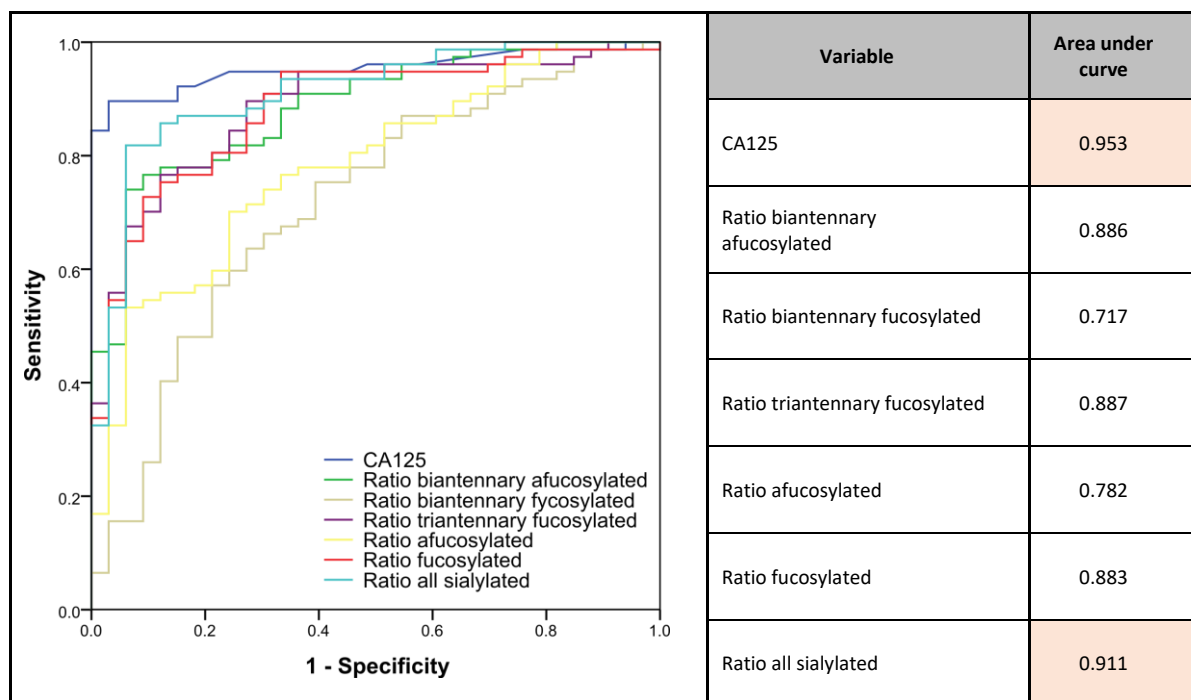


Figure 35 ROC curves of various sialylation ratios and CA125 generated for 33 healthy controls and 77 ovarian cancer patients.

The ratios for separate groups based on antennarity and fucosylation showed ROC curves with areas under the curve (AUC) from 0.717 to 0.887, which is a “good” result. The AUC for total sialylation ratio was 0.911, which is a “very good” classifier, however still lower than for the routinely used CA125 (AUC = 0.953). The software MedCalc (Version 18.6) was then used to evaluate the cut-off value of total sialylation ratio based on Youden index ($J = 0.7576$) and the calculated cut-off value of 0.2424 was estimated (Figure 36).

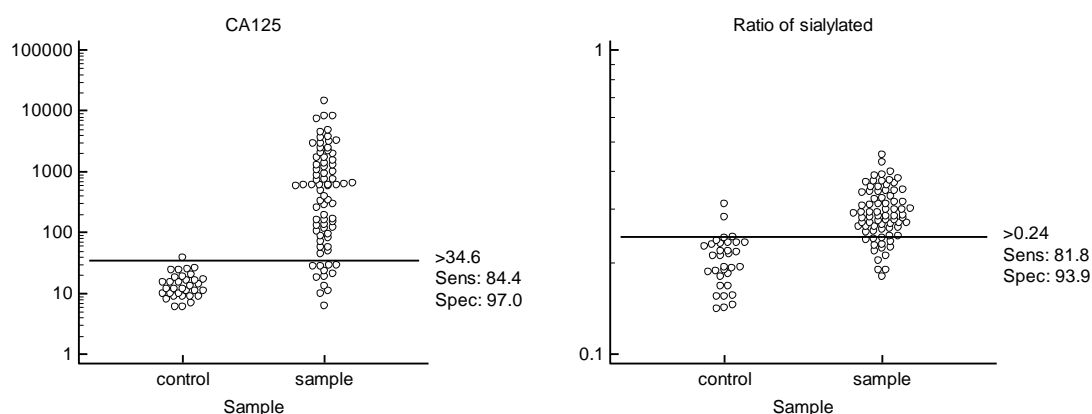


Figure 36 Dot plot of logarithmically transformed values, lines indicate sensitivity and specificity at the calculated cut-off values.

Since the total sialylation ratio showed a “very good” classification (> 0.9), it was tested if the combination of obtained sialylation ratio with CA125 could improve ovarian cancer diagnostic. A logistic regression was performed to evaluate the potential of CA125 and sialylation ratio on the ovarian cancer diagnosis.

The prediction model was as follows:

$$-10.553 + 0.108 \cdot \text{CA125} + 33.062 \cdot \text{ratio}.$$

The logistic regression model was statistically significant ($\chi^2(4) = 101.402$, $p < 0.001$), explained 85.4% (Nagelkerke R^2) of the variance in ovarian cancer and correctly classified 88.2% of cases. Therefore, a ROC curve was plotted for the combined probability results and the final AUC was 0.985, which means a “very good” classification (Figure 37).

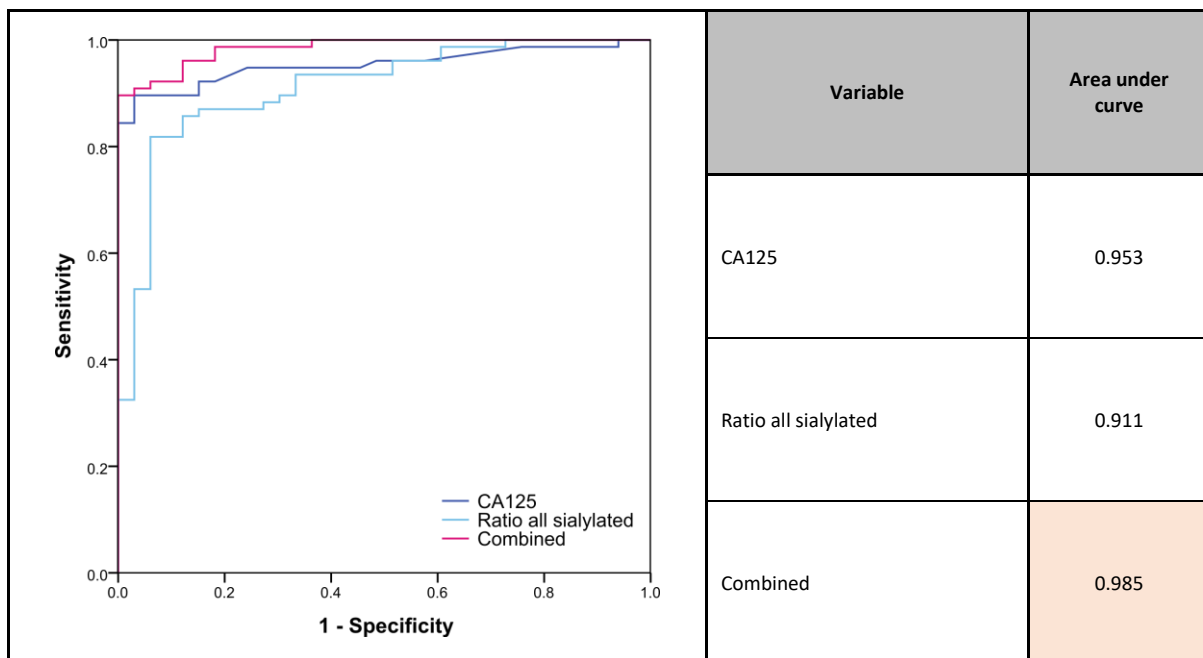


Figure 37 Discovery ROC curve generated for 33 healthy controls and 77 ovarian cancer patients, based on the binary logistic regression model by the combination of CA125 and total sialylation ratio.

The software MedCalc was then used to evaluate the cut-off value of combined probability based on maximal Youden index ($J = 0.8961$) and the calculated optimal cut-off value for the binary logistic regression model was obtained (0.8187), which showed a sensitivity of 89.6% and a specificity of 100% (Figure 38).

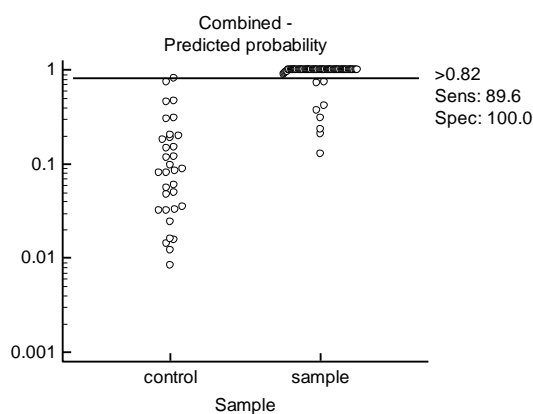


Figure 38 Optimal cut-off value based on the binary logistic regression model.

These results suggest that information about sialylation linkages provides cancer-specific insight. This information alone was inferior in classification to the routinely used biomarker CA125. Nevertheless, the combination of the sialylation ratio and biomarker CA125 resulted in an improvement of both the specificity and the sensitivity.

Discussion

In the present study, I compared the serum *N*-glycome from primary serous epithelial ovarian cancer patients in early (FIGO I + II) and late stages (FIGO III + IV) of the disease to age-matched healthy controls. The main focus of the *N*-glycome analysis was on the changes in sialylation, with regard to sialic acid linkages. The *N*-glycans from serum samples were released by PNGase F and sialic acids were stabilised before MALDI-TOF-MS measurement by linkage-specific labelling [163].

Many glycan traits showed statistically significant differences only between healthy patients and late stage ovarian cancer patients and no differences between healthy controls and early stage patients. In general, the differences in relative intensities of asialylated structures, such as high-mannose and complex asialylated afucosylated structures were statistically significant only between healthy controls and late stage ovarian cancer. Additionally, some relative intensities of total sialylation, thus without information about linkage, also showed differences only between healthy controls and late stage patients, namely, biantennary *N*-glycans both carrying a fucose and no fucose and triantennary afucosylated *N*-glycans.

On the other hand, the majority of sialylation traits showed specificity for ovarian cancer already in early stage, which is desired for potential biomarker use. On the level of total sialylation, regardless of the linkage type, a statistically significant decrease was observed for monoantennary afucosylated *N*-glycans. In contrast, triantennary fucosylated *N*-glycans and tetraantennary *N*-glycans both fucosylated and afucosylated showed statistically significant increase. Since the changes in relative intensities without the focus on sialic acid linkages has been extensively studied in recent years in various malignancies [40, 41, 46-49, 129, 175], these will not be discussed further in this thesis.

More importantly, the information about sialic acid linkage ratios always showed statistically significant differences already for early stage ovarian cancer. When classified according to the antennarity, there was statistically significant increase in α -2,3/ α -2,6 ratio for biantennary afucosylated and fucosylated *N*-glycans, and triantennary fucosylated *N*-glycans. Similarly, there was a statistically significant increase in α -2,3/ α -2,6 ratio of all afucosylated and fucosylated sialylated *N*-glycans. Most importantly, the increase in α -2,3/

α -2,6 ratio of all sialylated *N*-glycans showed statistically significant differences between all three cohorts.

In many publications [46-49], structure N5H6S3F1 was significantly increased in malignancies. This structure has four potential sialylation isomers, namely N5H6A3F1, N5H6A2D1F1, N5H6A1D2F1 and N5H6D3F1. Interestingly, in the present study only structures with mixed sialylation, *e.g.* N5H6A2D1F1, N5H6A1D2F1 show statistically significant increase in ovarian cancer. On the other hand, the structure N5H6D3F1 showed no differences between healthy controls and ovarian cancer patients and N5H6A3F1 could not be detected in any cohort. The increase of N5H6A1D2F1 is accompanied by statistically significant decrease of N5H6A1D2. These changes correlate with findings that synthesis of SLe^x antigen requires first addition of sialic acid, followed by addition of antennary fucose [176].

The observed changes in ovarian cancer serum sialylation agree with findings in other types of cancer. Holst *et al.* showed by MALDI-Imaging in colorectal carcinoma, that the α -2,3-linked sialic acid was increased in stroma, tumour, and necrotic cell regions, while α -2,6-linked sialic acid was more prominent in inflammatory areas, *e.g.* rich in collagen, necrotic regions and red-blood cells [163]. On some colorectal cancer cell lines (HT29, WiDr, SW48, T84, and Lovo) an increased α -2,3-sialylation was observed together with multi-fucosylation [177]. Saldova *et al.* observed increased α -2,3-sialylation in prostate cancer as compared to benign hyperplasia [178]. In the study performed by Wang and colleagues [179], increased mRNA expression of ST3Gal III, ST3Gal IV and ST3Gal VI was observed in ovarian serous carcinoma tissues. Moreover, immunohistochemical staining using MMA showed strong positivity in ovarian epithelial carcinoma part, while normal epithelial part showed strong negativity. Wen, Sung and colleagues then studied expression of ST3Gal I in serous type epithelial ovarian cancer [180] and in clear cell type epithelial ovarian cancer [181]. They proposed α -2,3-sialylation as potential prognostic marker and possible therapy target of ovarian cancer.

The sialylation changes were reported here as a ratio between relative α -2,3-sialylation and α -2,6-sialylation. In general, glycans containing exclusively α -2,3-linked sialic acids were not observed in the samples in high amounts and structures carrying both linkage types were most prominent in tri- and tetraantennary structures. This is most likely

an effect of steric hindrance. However, there was an increase in the relative α -2,3-sialylation in ovarian cancer samples as compared to healthy controls. Moreover, the relative α -2,3-linked sialylation increased with increasing antennarity and cancer stage, reaching its maximum in tetraantennary structures (50%).

Since the increase in total α -2,3/ α -2,6-sialylation ratio was statistically significant for ovarian cancer, ROC curves were generated for the ratio, biomarker CA125 and for binary logistic regression model by the combination of CA125 and total sialylation ratio. The proposed model could improve the classification of ovarian cancer patients compared to CA125 alone. While CA125 alone showed sensitivity of 84.4% and specificity of 97%, in combination with sialylation ratio the sensitivity and specificity increased to 89.6% and 100%, respectively.

The advantage of such an approach lies in the utilisation of a biomarker, which is already used all over the world in clinical laboratories, whose sensitivity and specificity could be improved by an additional measurement of glycosylation. Such a measurement could be proposed in unclear cases and/or cases below certain cut-off value of CA125. Since the results observed here were obtained from the whole serum N-glycome, it is unclear, which glycoproteins contributed to the changes, however the increased α -2,3-sialylation clearly correlated with ovarian cancer stage. A further study of sialylation of specific proteins, such as acute-phase proteins, could shed light on the pathogenesis of ovarian cancer and maybe serve as better biomarker than a total serum N-glycome.

Chapter 7

General conclusion

Glycans have been proposed as potential biomarkers or prognostic markers before [40, 46-48, 131, 182-187]. However, introduction of glycobiology into a clinical environment brings the same challenges as other disciplines. One of the main issues with clinical biomarker testing is repeatability and reproducibility [188-190]. This is the reason why this work focussed on tasks necessary to achieve a successful application of glycoanalytical methods to clinical diagnostic.

To this end, the first aim of this thesis was to perform a systematic study of blood sampling and sample pre-processing on the stability of the human N-glycome. The standard sample processing, its challenges and possible variations were considered. Firstly, the type of blood collection tubes was evaluated to assess if samples from various sources could be used. This is important an information for potential use of samples from biobanks. Secondly, the effect of delayed processing after blood collection and after centrifugation together with variations in storage temperature were tested. Lastly and most importantly, hemolysis, which is a phenomenon commonly observed in clinical laboratories, was introduced and its effect on the N-glycome was evaluated. The study showed that the effect of preanalytical conditions was minor even for very serious deviations from standard sampling procedures, such as six-hour delay in centrifugation. Only hemolysis, which is easily identified, considerably influenced the outcome of glycan measurement. As a result, these samples can be simply excluded.

The second aim of this thesis was to evaluate the changes in sialylation of ovarian cancer patients. Firstly, a method for linkage-specific sialic acid labelling has been selected from a range of previously published techniques. Since the majority of the original publications applied these techniques on different sample types, the methods were modified for application on PNGase F released serum N-glycans. Once the optimal method has been selected, a repeatability testing was performed together with the development of analytical and data-analytical protocols, which allowed high-throughput processing. Secondly, the optimised protocol was applied to analyse 110 serum samples of primary epithelial ovarian cancer patients and healthy controls. It was possible to identify changes in sialylation that were unique for ovarian cancer patients when compared to healthy controls. Specifically, there was an increase of relative α -2,3-sialylation in ovarian cancer patients. Even though the sialylation deviations alone were inferior to the routinely used biomarker CA125 in sample

classification, it was possible to improve the diagnostic power of CA125, when the two tests were combined.

List of references

1. Spiro RG. **Protein glycosylation: nature, distribution, enzymatic formation, and disease implications of glycopeptide bonds.** *Glycobiology*. 2002; 12(4):43R-56R. DOI: 10.1093/glycob/12.4.43R.
2. Varki A. **Biological roles of oligosaccharides: all of the theories are correct.** *Glycobiology*. 1993; 3(2):97-130, <https://www.ncbi.nlm.nih.gov/pubmed/8490246>.
3. Varki A. **Biological roles of glycans.** *Glycobiology*. 2017; 27(1):3-49. DOI: 10.1093/glycob/cww086.
4. Schnaar RL. **Glycans and glycan-binding proteins in immune regulation: A concise introduction to glycobiology for the allergist.** *J Allergy Clin Immunol*. 2015; 135(3):609-15. DOI: 10.1016/j.jaci.2014.10.057.
5. Amon R, Reuven EM, Leviatan Ben-Arye S, Padler-Karavani V. **Glycans in immune recognition and response.** *Carbohydr Res*. 2014; 389:115-22. DOI: 10.1016/j.carres.2014.02.004.
6. Varki A, Gagneux P. **Multifarious roles of sialic acids in immunity.** *Ann N Y Acad Sci*. 2012; 1253(1):16-36. DOI: 10.1111/j.1749-6632.2012.06517.x.
7. Johnson JL, Jones MB, Ryan SO, Cobb BA. **The regulatory power of glycans and their binding partners in immunity.** *Trends Immunol*. 2013; 34(6):290-8. DOI: 10.1016/j.it.2013.01.006.
8. Bochner BS, Zimmermann N. **Role of siglecs and related glycan-binding proteins in immune responses and immunoregulation.** *J Allergy Clin Immunol*. 2015; 135(3):598-608. DOI: 10.1016/j.jaci.2014.11.031.
9. Pearce OM, Laubli H. **Sialic acids in cancer biology and immunity.** *Glycobiology*. 2016; 26(2):111-28. DOI: 10.1093/glycob/cwv097.
10. Wormald MR, Dwek RA. **Glycoproteins: glycan presentation and protein-fold stability.** *Structure*. 1999; 7(7):R155-60. DOI: 10.1016/S0969-2126(99)80095-1.
11. Stanley P, Schachter H, Taniguchi N. **N-Glycans.** In: nd, Varki A, Cummings RD, Esko JD, Freeze HH, Stanley P, *et al.*, editors. *Essentials of Glycobiology*. Cold Spring Harbor (NY)2009.
12. Kasturi L, Eshleman JR, Wunner WH, Shakin-Eshleman SH. **The hydroxy amino acid in an Asn-X-Ser/Thr sequon can influence N-linked core glycosylation efficiency and the level of expression of a cell surface glycoprotein.** *J Biol Chem*. 1995; 270(24):14756-61.
13. Mellquist JL, Kasturi L, Spitalnik SL, Shakin-Eshleman SH. **The amino acid following an asn-X-Ser/Thr sequon is an important determinant of N-linked core glycosylation efficiency.** *Biochemistry*. 1998; 37(19):6833-7. DOI: 10.1021/bi972217k.
14. Gavel Y, Heijne Gv. **Sequence differences between glycosylated and non-glycosylated Asn-X-Thr/Ser acceptor sites: implications for protein engineering.** *Protein Engineering, Design and Selection*. 1990; 3(5):433-42. DOI: 10.1093/protein/3.5.433.
15. Samraj AN, Laubli H, Varki N, Varki A. **Involvement of a non-human sialic Acid in human cancer.** *Front Oncol*. 2014; 4:33. DOI: 10.3389/fonc.2014.00033.

16. Varki A, Cummings RD, Esko JD, Freeze HH, Stanley P, Marth JD, Bertozzi CR, Hart GW, Etzler ME. **Symbol nomenclature for glycan representation.** *Proteomics*. 2009; 9(24):5398-9. DOI: 10.1002/pmic.200900708.
17. Marek KW, Vijay IK, Marth JD. **A recessive deletion in the GlcNAc-1-phosphotransferase gene results in peri-implantation embryonic lethality.** *Glycobiology*. 1999; 9(11):1263-71. DOI: 10.1093/glycob/9.11.1263.
18. Rush JS. **Role of Flippases in Protein Glycosylation in the Endoplasmic Reticulum.** *Lipid Insights*. 2015; 8(Suppl 1):45-53. DOI: 10.4137/LPI.S31784.
19. Schauer R. **Chemistry, Metabolism, and Biological Functions of Sialic Acids.** In: Horton RST, Derek, editors. *Advances in Carbohydrate Chemistry and Biochemistry*. 40: Academic Press; 1982. p. 131-234.
20. Varki A, Schauer R. **Sialic Acids.** In: nd, Varki A, Cummings RD, Esko JD, Freeze HH, Stanley P, *et al.*, editors. *Essentials of Glycobiology*. Cold Spring Harbor (NY)2009.
21. Tanner ME. **The enzymes of sialic acid biosynthesis.** *Bioorg Chem*. 2005; 33(3):216-28. DOI: 10.1016/j.bioorg.2005.01.005.
22. Sundaram AK, Pitts L, Muhammad K, Wu J, Betenbaugh M, Woodard RW, Vann WF. **Characterization of N-acetylneuraminic acid synthase isoenzyme 1 from Campylobacter jejuni.** *Biochem J*. 2004; 383(Pt 1):83-9. DOI: 10.1042/BJ20040218.
23. Hinderlich S, Weidemann W, Yardeni T, Horstkorte R, Huizing M. **UDP-GlcNAc 2-Epimerase/ManNAc Kinase (GNE): A Master Regulator of Sialic Acid Synthesis.** *Top Curr Chem*. 2015; 366:97-137. DOI: 10.1007/128_2013_464.
24. Harduin-Lepers A, Vallejo-Ruiz V, Krzewinski-Recchi MA, Samyn-Petit B, Julien S, Delannoy P. **The human sialyltransferase family.** *Biochimie*. 2001; 83(8):727-37, <https://www.ncbi.nlm.nih.gov/pubmed/11530204>.
25. Brockhausen I. **Mucin-type O-glycans in human colon and breast cancer: glycodynamics and functions.** *EMBO Rep*. 2006; 7(6):599-604. DOI: 10.1038/sj.embor.7400705.
26. Brockhausen I. **Pathways of O-glycan biosynthesis in cancer cells.** *Biochimica et biophysica acta*. 1999; 1473(1):67-95. DOI: 10.1016/S0304-4165(99)00170-1.
27. Crocker PR, Varki A. **Siglecs, sialic acids and innate immunity.** *Trends Immunol*. 2001; 22(6):337-42. DOI: 10.1016/S1471-4906(01)01930-5.
28. Macauley MS, Crocker PR, Paulson JC. **Siglec-mediated regulation of immune cell function in disease.** *Nat Rev Immunol*. 2014; 14(10):653-66. DOI: 10.1038/nri3737.
29. Boldt DH, Armstrong JP. **Rosette formation between human lymphocytes and sheep erythrocytes. Inhibition of rosette formation by specific glycopeptides.** *J Clin Invest*. 1976; 57(4):1068-78, <http://www.ncbi.nlm.nih.gov/pmc/articles/PMC436751/>.
30. Stamenkovic I, Seed B. **The B-cell antigen CD22 mediates monocyte and erythrocyte adhesion.** *Nature*. 1990; 345(6270):74-7. DOI: 10.1038/345074a0.

31. Freeman SD, Kelm S, Barber EK, Crocker PR. **Characterization of CD33 as a new member of the sialoadhesin family of cellular interaction molecules.** *Blood*. 1995; 85(8):2005-12.
32. Crocker PR, Mucklow S, Bouckson V, McWilliam A, Willis AC, Gordon S, Milon G, Kelm S, Bradfield P. **Sialoadhesin, a macrophage sialic acid binding receptor for haemopoietic cells with 17 immunoglobulin-like domains.** *The EMBO Journal*. 1994; 13(19):4490-503. DOI: 10.1002/j.1460-2075.1994.tb06771.x.
33. Kelm S, Pelz A, Schauer R, Filbin MT, Tang S, de Bellard ME, Schnaar RL, Mahoney JA, Hartnell A, Bradfield P, *et al.* **Sialoadhesin, myelin-associated glycoprotein and CD22 define a new family of sialic acid-dependent adhesion molecules of the immunoglobulin superfamily.** *Curr Biol*. 1994; 4(11):965-72, <https://www.ncbi.nlm.nih.gov/pubmed/7533044>.
34. Murphy K, Weaver C. **Janeway's immunobiology:** Garland Science; 2016.
35. Meri S, Pangburn MK. **Discrimination between activators and nonactivators of the alternative pathway of complement: regulation via a sialic acid/polyanion binding site on factor H.** *PNAS*. 1990; 87(10):3982-6. DOI: 10.1073/pnas.87.10.3982.
36. Michalek MT, Mold C, Bremer EG. **Inhibition of the alternative pathway of human complement by structural analogues of sialic acid.** *The Journal of Immunology*. 1988; 140(5):1588, <http://www.jimmunol.org/content/140/5/1588.abstract>.
37. Schmidt CQ, Ederveen ALH, Harder MJ, Wuhrer M, Stehle T, Blaum BS. **Biophysical analysis of sialic acid recognition by the complement regulator Factor H.** *Glycobiology*. 2018; 1:9.
38. Fujita T, Satomura A, Hidaka M, Ohsawa I, Endo M, Ohi H. **Inhibitory effect of free sialic acid on complement activation and its significance in hypocomplementemic glomerulonephritis.** *J Clin Lab Anal*. 1999; 13(4):173-9, <https://www.ncbi.nlm.nih.gov/pubmed/10414597>.
39. Gout E, Garlatti V, Smith DF, Lacroix M, Dumestre-Perard C, Lunardi T, Martin L, Cesbron JY, Arlaud GJ, Gaboriaud C, *et al.* **Carbohydrate recognition properties of human ficolins: glycan array screening reveals the sialic acid binding specificity of M-ficolin.** *J Biol Chem*. 2010; 285(9):6612-22. DOI: 10.1074/jbc.M109.065854.
40. Saldova R, Royle L, Radcliffe CM, Abd Hamid UM, Evans R, Arnold JN, Banks RE, Hutson R, Harvey DJ, Antrobus R, *et al.* **Ovarian cancer is associated with changes in glycosylation in both acute-phase proteins and IgG.** *Glycobiology*. 2007; 17(12):1344-56. DOI: 10.1093/glycob/cwm100.
41. Saldova R, Haakensen VD, Rodland E, Walsh I, Stockmann H, Engebraaten O, Borresen-Dale AL, Rudd PM. **Serum N-glycome alterations in breast cancer during multimodal treatment and follow-up.** *Mol Oncol*. 2017; 11(10):1361-79. DOI: 10.1002/1878-0261.12105.
42. Dennis JW, Laferte S, Waghorne C, Breitman ML, Kerbel RS. **Beta 1-6 branching of Asn-linked oligosaccharides is directly associated with metastasis.** *Science*. 1987; 236(4801):582, <http://science.sciencemag.org/content/236/4801/582.abstract>.

43. Fernandes B, Sagman U, Auger M, Demetrio M, Dennis J. **β 1-6 branched oligosaccharides as a marker of tumor progression in human breast and colon neoplasia.** *Cancer Res.* 1991; 51(2):718-23.
44. Miyoshi E, Moriwaki K, Nakagawa T. **Biological Function of Fucosylation in Cancer Biology.** *The Journal of Biochemistry.* 2008; 143(6):725-9. DOI: 10.1093/jb/mvn011.
45. Miyoshi E, Uozumi N, Noda K, Hayashi N, Hori M, Taniguchi N. **Expression of α 1-6 fucosyltransferase in rat tissues and human cancer cell lines.** *International Journal of Cancer.* 1998; 72(6):1117-21. DOI: 10.1002/(SICI)1097-0215(19970917)72:6<1117::AID-IJC29>3.0.CO;2-#.
46. Kyselova Z, Mechref Y, Kang P, Goetz JA, Dobrolecki LE, Sledge GW, Schnaper L, Hickey RJ, Malkas LH, Novotny MV. **Breast cancer diagnosis and prognosis through quantitative measurements of serum glycan profiles.** *Clin Chem.* 2008; 54(7):1166-75. DOI: 10.1373/clinchem.2007.087148.
47. Biskup K, Braicu EI, Sehouli J, Fotopoulou C, Tauber R, Berger M, Blanchard V. **Serum glycome profiling: a biomarker for diagnosis of ovarian cancer.** *J Proteome Res.* 2013; 12(9):4056-63. DOI: 10.1021/pr400405x.
48. Biskup K, Braicu EI, Sehouli J, Tauber R, Blanchard V. **The serum glycome to discriminate between early-stage epithelial ovarian cancer and benign ovarian diseases.** *Dis Markers.* 2014; 2014:238197. DOI: 10.1155/2014/238197.
49. Biskup K, Braicu EI, Sehouli J, Tauber R, Blanchard V. **The ascites N-glycome of epithelial ovarian cancer patients.** *Journal of Proteomics.* 2017; 157:33-9. DOI: <https://doi.org/10.1016/j.jprot.2017.02.001>.
50. de Leoz MLA, Young LJT, An HJ, Kronewitter SR, Kim J, Miyamoto S, Borowsky AD, Chew HK, Lebrilla CB. **High-Mannose Glycans are Elevated during Breast Cancer Progression.** *Molecular & Cellular Proteomics.* 2011; 10(1), <http://www.mcponline.org/content/10/1/M110.002717.abstract>.
51. Dall'Olio F, Chiricolo M. **Sialyltransferases in cancer.** *Glycoconj J.* 2001; 18(11-12):841-50. DOI: 10.1023/A:1022288022969.
52. Skacel PO, Edwards AJ, Harrison CT, Watkins WM. **Enzymic control of the expression of the X determinant (CD15) in human myeloid cells during maturation: the regulatory role of 6-sialyltransferase.** *Blood.* 1991; 78(6):1452-60, <https://www.ncbi.nlm.nih.gov/pubmed/1679356>.
53. Kaneko Y, Yamamoto H, Kersey DS, Colley KJ, Leestma JE, Moskal JR. **The expression of Gal β 1,4GlcNAc α 2,6 sialyltransferase and α 2,6-linked sialoglycoconjugates in human brain tumors.** *Acta Neuropathol.* 1996; 91(3):284-92. DOI: 10.1007/s004010050427.
54. Recchi MA, Hebbbar M, Hornez L, Harduin-Lepers A, Peyrat JP, Delannoy P. **Multiplex reverse transcription polymerase chain reaction assessment of sialyltransferase expression in human breast cancer.** *Cancer Res.* 1998; 58(18):4066-70, <https://www.ncbi.nlm.nih.gov/pubmed/9751611>.
55. Wang PH, Li YF, Juang CM, Lee YR, Chao HT, Tsai YC, Yuan CC. **Altered mRNA expression of sialyltransferase in squamous cell carcinomas of the cervix.** *Gynecol Oncol.* 2001; 83(1):121-7. DOI: 10.1006/gyno.2001.6358.

56. Fukushima K, Hara-Kuge S, Seko A, Ikehara Y, Yamashita K. **Elevation of α 2→6 Sialyltransferase and α 1→2 Fucosyltransferase Activities in Human Choriocarcinoma.** *Cancer Res.* 1998; 58(19):4301-6, <http://www.ncbi.nlm.nih.gov/pubmed/9766657>.
57. Olio FD, Malagolini N, di Stefano G, Minni F, Marrano D, Serafini-Cessi F. **Increased CMP-NeuAc:Gal β 1,4GlcNAc-R α 2,6 sialyltransferase activity in human colorectal cancer tissues.** *International Journal of Cancer.* 1989; 44(3):434-9. DOI: 10.1002/ijc.2910440309.
58. Hedlund M, Ng E, Varki A, Varki NM. **alpha 2-6-Linked sialic acids on N-glycans modulate carcinoma differentiation in vivo.** *Cancer Res.* 2008; 68(2):388-94. DOI: 10.1158/0008-5472.CAN-07-1340.
59. Lu J, Gu J. **Significance of beta-Galactoside alpha2,6 Sialyltransferase 1 in Cancers.** *Molecules.* 2015; 20(5):7509-27. DOI: 10.3390/molecules20057509.
60. Schultz MJ, Swindall AF, Bellis SL. **Regulation of the metastatic cell phenotype by sialylated glycans.** *Cancer Metastasis Rev.* 2012; 31(3-4):501-18. DOI: 10.1007/s10555-012-9359-7.
61. Christie DR, Shaikh FM, Lucas JAt, Lucas JA, 3rd, Bellis SL. **ST6Gal-I expression in ovarian cancer cells promotes an invasive phenotype by altering integrin glycosylation and function.** *J Ovarian Res.* 2008; 1(1):3. DOI: 10.1186/1757-2215-1-3.
62. Britain CM, Holdbrooks AT, Anderson JC, Willey CD, Bellis SL. **Sialylation of EGFR by the ST6Gal-I sialyltransferase promotes EGFR activation and resistance to gefitinib-mediated cell death.** *J Ovarian Res.* 2018; 11(1):12. DOI: 10.1186/s13048-018-0385-0.
63. Cui H, Yang S, Jiang Y, Li C, Zhao Y, Shi Y, Hao Y, Qian F, Tang B, Yu P. **The glycosyltransferase ST6Gal-I is enriched in cancer stem-like cells in colorectal carcinoma and contributes to their chemo-resistance.** *Clin Transl Oncol.* 2018:1-10. DOI: 10.1007/s12094-018-1840-5.
64. Takada A, Ohmori K, Yoneda T, Tsuyuoka K, Hasegawa A, Kiso M, Kannagi R. **Contribution of carbohydrate antigens sialyl Lewis A and sialyl Lewis X to adhesion of human cancer cells to vascular endothelium.** *Cancer Res.* 1993; 53(2):354-61, <https://www.ncbi.nlm.nih.gov/pubmed/7678075>.
65. Ugorski M, Laskowska A. **Sialyl Lewis(a): a tumor-associated carbohydrate antigen involved in adhesion and metastatic potential of cancer cells.** *Acta Biochim Pol.* 2002; 49(2):303-11, <https://www.ncbi.nlm.nih.gov/pubmed/12362971>.
66. Cui HX, Wang H, Wang Y, Song J, Tian H, Xia C, Shen Y. **ST3Gal III modulates breast cancer cell adhesion and invasion by altering the expression of invasion-related molecules.** *Oncol Rep.* 2016; 36(6):3317-24. DOI: 10.3892/or.2016.5180.
67. Ricardo S, Marcos-Silva L, Valente C, Coelho R, Gomes R, David L. **Mucins MUC16 and MUC1 are major carriers of SLe(a) and SLe(x) in borderline and malignant serous ovarian tumors.** *Virchows Arch.* 2016; 468(6):715-22. DOI: 10.1007/s00428-016-1929-6.
68. Springer GF. **T and Tn, general carcinoma autoantigens.** *Science.* 1984; 224(4654):1198-206, <https://www.ncbi.nlm.nih.gov/pubmed/6729450>.
69. Miles DW, Happerfield LC, Smith P, Gillibrand R, Bobrow LG, Gregory WM, Rubens RD. **Expression of sialyl-Tn predicts the effect of adjuvant chemotherapy in node-positive**

- breast cancer.** *Br J Cancer.* 1994; 70(6):1272-5, <https://www.ncbi.nlm.nih.gov/pubmed/7981088>.
70. Battula VL, Shi Y, Evans KW, Wang RY, Spaeth EL, Jacamo RO, Guerra R, Sahin AA, Marini FC, Hortobagyi G, *et al.* **Ganglioside GD2 identifies breast cancer stem cells and promotes tumorigenesis.** *J Clin Invest.* 2012; 122(6):2066-78. DOI: 10.1172/JCI59735.
71. Guo Z, Wang Q. **Recent development in carbohydrate-based cancer vaccines.** *Curr Opin Chem Biol.* 2009; 13(5-6):608-17. DOI: 10.1016/j.cbpa.2009.08.010.
72. Xu Y, Sette A, Sidney J, Gendler SJ, Franco A. **Tumor-associated carbohydrate antigens: a possible avenue for cancer prevention.** *Immunol Cell Biol.* 2005; 83(4):440-8. DOI: 10.1111/j.1440-1711.2005.01347.x.
73. Hutchins LF, Makhoul I, Emanuel PD, Pennisi A, Siegel ER, Jousheghany F, Guo X, Pashov AD, Monzavi-Karbassi B, Kieber-Emmons T. **Targeting tumor-associated carbohydrate antigens: a phase I study of a carbohydrate mimetic-peptide vaccine in stage IV breast cancer subjects.** *Oncotarget.* 2017; 8(58):99161-78. DOI: 10.18632/oncotarget.21959.
74. Strassburger D, Glaffig M, Stergiou N, Bialas S, Besenius P, Schmitt E, Kunz H. **Synthetic MUC1 Antitumor Vaccine with Incorporated 2,3-Sialyl-T Carbohydrate Antigen Inducing Strong Immune Responses with Isotype Specificity.** *ChemBioChem.* 2018. DOI: 10.1002/cbic.201800148.
75. Varki A. **Colloquium paper: uniquely human evolution of sialic acid genetics and biology.** *Proc Natl Acad Sci U S A.* 2010; 107 Suppl 2:8939-46. DOI: 10.1073/pnas.0914634107.
76. Samraj AN, Pearce OM, Laubli H, Crittenden AN, Bergfeld AK, Banda K, Gregg CJ, Bingman AE, Secrest P, Diaz SL, *et al.* **A red meat-derived glycan promotes inflammation and cancer progression.** *Proc Natl Acad Sci U S A.* 2015; 112(2):542-7. DOI: 10.1073/pnas.1417508112.
77. Hedlund M, Padler-Karavani V, Varki NM, Varki A. **Evidence for a human-specific mechanism for diet and antibody-mediated inflammation in carcinoma progression.** *Proc Natl Acad Sci U S A.* 2008; 105(48):18936-41. DOI: 10.1073/pnas.0803943105.
78. Felder M, Kapur A, Gonzalez-Bosquet J, Horibata S, Heintz J, Albrecht R, Fass L, Kaur J, Hu K, Shojaei H, *et al.* **MUC16 (CA125): tumor biomarker to cancer therapy, a work in progress.** *Mol Cancer.* 2014; 13:129. DOI: 10.1186/1476-4598-13-129.
79. Soletormos G, Duffy MJ, Othman Abu Hassan S, Verheijen RH, Tholander B, Bast RC, Jr., Gaarenstroom KN, Sturgeon CM, Bonfrer JM, Petersen PH, *et al.* **Clinical Use of Cancer Biomarkers in Epithelial Ovarian Cancer: Updated Guidelines From the European Group on Tumor Markers.** *Int J Gynecol Cancer.* 2016; 26(1):43-51. DOI: 10.1097/IGC.0000000000000586.
80. Li J, Dowdy S, Tipton T, Podratz K, Lu WG, Xie X, Jiang SW. **HE4 as a biomarker for ovarian and endometrial cancer management.** *Expert Rev Mol Diagn.* 2009; 9(6):555-66. DOI: 10.1586/erm.09.39.
81. Goff BA, Mandel LS, Drescher CW, Urban N, Gough S, Schurman KM, Patras J, Mahony BS, Andersen MR. **Development of an ovarian cancer symptom index: possibilities for earlier detection.** *Cancer.* 2007; 109(2):221-7. DOI: 10.1002/cncr.22371.

82. Goff BA, Agnew K, Neradilek MB, Gray HJ, Liao JB, Urban RR. **Combining a symptom index, CA125 and HE4 (triple screen) to detect ovarian cancer in women with a pelvic mass.** *Gynecol Oncol.* 2017; 147(2):291-5. DOI: 10.1016/j.ygyno.2017.08.020.
83. Patel T, Bruce J, Merry A, Bigge C, Wormald M, Jaques A, Parekh R. **Use of hydrazine to release in intact and unreduced form both N- and O-linked oligosaccharides from glycoproteins.** *Biochemistry.* 1993; 32(2):679-93, <https://www.ncbi.nlm.nih.gov/pubmed/8422375>.
84. Song X, Ju H, Lasanajak Y, Kudelka MR, Smith DF, Cummings RD. **Oxidative release of natural glycans for functional glycomics.** *Nat Methods.* 2016; 13(6):528-34. DOI: 10.1038/nmeth.3861.
85. Reiding KR, Blank D, Kuijper DM, Deelder AM, Wuhrer M. **High-throughput profiling of protein N-glycosylation by MALDI-TOF-MS employing linkage-specific sialic acid esterification.** *Anal Chem.* 2014; 86(12):5784-93. DOI: 10.1021/ac500335t.
86. Trimble RB, Maley F. **Optimizing hydrolysis of N-linked high-mannose oligosaccharides by endo- β -N-acetylglucosaminidase H.** *Analytical Biochemistry.* 1984; 141(2):515-22. DOI: [https://doi.org/10.1016/0003-2697\(84\)90080-0](https://doi.org/10.1016/0003-2697(84)90080-0).
87. Maley F, Trimble RB, Tarentino AL, Plummer TH. **Characterization of glycoproteins and their associated oligosaccharides through the use of endoglycosidases.** *Analytical Biochemistry.* 1989; 180(2):195-204. DOI: [https://doi.org/10.1016/0003-2697\(89\)90115-2](https://doi.org/10.1016/0003-2697(89)90115-2).
88. Schwedler C, Kaup M, Weiz S, Hoppe M, Braicu EI, Sehouli J, Hoppe B, Tauber R, Berger M, Blanchard V. **Identification of 34 N-glycan isomers in human serum by capillary electrophoresis coupled with laser-induced fluorescence allows improving glycan biomarker discovery.** *Anal Bioanal Chem.* 2014; 406(28):7185-93. DOI: 10.1007/s00216-014-8168-y.
89. Blanchard V, Liu X, Eigel S, Kaup M, Rieck S, Janciauskiene S, Sandig V, Marx U, Walden P, Tauber R, *et al.* **N-glycosylation and biological activity of recombinant human alpha1-antitrypsin expressed in a novel human neuronal cell line.** *Biotechnology and Bioengineering.* 2011; 108(9):2118-28. DOI: 10.1002/bit.23158.
90. Wedepohl S, Kaup M, Riese SB, Berger M, Dervede J, Tauber R, Blanchard V. **N-glycan analysis of recombinant L-Selectin reveals sulfated GalNAc and GalNAc-GalNAc motifs.** *J Proteome Res.* 2010; 9(7):3403-11. DOI: 10.1021/pr100170c.
91. Selman MH, Hemayatkar M, Deelder AM, Wuhrer M. **Cotton HILIC SPE microtips for microscale purification and enrichment of glycans and glycopeptides.** *Anal Chem.* 2011; 83(7):2492-9. DOI: 10.1021/ac1027116.
92. Burnina I, Hoyt E, Lynaugh H, Li H, Gong B. **A cost-effective plate-based sample preparation for antibody N-glycan analysis.** *J Chromatogr A.* 2013; 1307:201-6. DOI: 10.1016/j.chroma.2013.07.104.
93. Buszewski B, Noga S. **Hydrophilic interaction liquid chromatography (HILIC)--a powerful separation technique.** *Anal Bioanal Chem.* 2012; 402(1):231-47. DOI: 10.1007/s00216-011-5308-5.
94. Ciucanu I, Kerek F. **A simple and rapid method for the permethylation of carbohydrates.** *Carbohydrate research.* 1984; 131(2):209-17.

95. Morelle W, Faïd V, Chirat F, Michalski JC. **Analysis of N- and O-linked glycans from glycoproteins using MALDI-TOF mass spectrometry.** *Methods Mol Biol.* 2009; 534:5-21. DOI: 10.1007/978-1-59745-022-5_1.
96. Struwe WB, Cosgrave EFJ, Byrne JC, Saldova R, Rudd PM. **Glycoproteomics in Health and Disease.** In: Owens R, Nettleship J, editors. *Functional and Structural Proteomics of Glycoproteins.* Dordrecht: Springer Netherlands; 2011. p. 1-38.
97. Cotter RJ. **Time-of-Flight Mass Spectrometry.** *Time-of-Flight Mass Spectrometry.* ACS Symposium Series. 549: American Chemical Society; 1993. p. 16-48.
98. Han L, Costello CE. **Mass spectrometry of glycans.** *Biochemistry (Mosc).* 2013; 78(7):710-20. DOI: 10.1134/S0006297913070031.
99. Harvey DJ. **Structural determination of N-linked glycans by matrix-assisted laser desorption/ionization and electrospray ionization mass spectrometry.** *Proteomics.* 2005; 5(7):1774-86. DOI: 10.1002/pmic.200401248.
100. Landers JP. **Handbook of capillary and microchip electrophoresis and associated microtechniques.** 3rd ed. Boca Raton: CRC Press; 2008. 1567 p.
101. Tagliaro F, Manetto G, Crivellente F, Smith FP. **A brief introduction to capillary electrophoresis.** *Forensic Science International.* 1998; 92(2):75-88. DOI: [https://doi.org/10.1016/S0379-0738\(98\)00010-3](https://doi.org/10.1016/S0379-0738(98)00010-3).
102. Gilges M, Kleemiss MH, Schomburg G. **Capillary Zone Electrophoresis Separations of Basic and Acidic Proteins Using Poly(vinyl alcohol) Coatings in Fused Silica Capillaries.** *Analytical Chemistry.* 1994; 66(13):2038-46. DOI: 10.1021/ac00085a019.
103. Galceran MT, Puignou L, Diez M. **Comparison of different electroosmotic flow modifiers in the analysis of inorganic anions by capillary electrophoresis.** *Journal of Chromatography A.* 1996; 732(1):167-74. DOI: [https://doi.org/10.1016/0021-9673\(95\)01248-6](https://doi.org/10.1016/0021-9673(95)01248-6).
104. Huffman JE, Knezevic A, Vitart V, Kattla J, Adamczyk B, Novokmet M, Igl W, Pucic M, Zgaga L, Johannson A, *et al.* **Polymorphisms in B3GAT1, SLC9A9 and MGAT5 are associated with variation within the human plasma N-glycome of 3533 European adults.** *Hum Mol Genet.* 2011; 20(24):5000-11. DOI: 10.1093/hmg/ddr414.
105. Knezevic A, Gornik O, Polasek O, Pucic M, Redzic I, Novokmet M, Rudd PM, Wright AF, Campbell H, Rudan I, *et al.* **Effects of aging, body mass index, plasma lipid profiles, and smoking on human plasma N-glycans.** *Glycobiology.* 2010; 20(8):959-69. DOI: 10.1093/glycob/cwq051.
106. Rudan I, Marusic A, Jankovic S, Rotim K, Boban M, Lauc G, Grkovic I, Dogas Z, Zemunik T, Vataavuk Z, *et al.* **"10001 Dalmatians:" Croatia launches its national biobank.** *Croat Med J.* 2009; 50(1):4-6, <https://www.ncbi.nlm.nih.gov/pubmed/19260138>.
107. Huffman JE, Pucic-Bakovic M, Klaric L, Hennig R, Selman MH, Vuckovic F, Novokmet M, Kristic J, Borowiak M, Muth T, *et al.* **Comparative performance of four methods for high-throughput glycosylation analysis of immunoglobulin G in genetic and epidemiological research.** *Mol Cell Proteomics.* 2014; 13(6):1598-610. DOI: 10.1074/mcp.M113.037465.

108. Bladergroen MR, Reiding KR, Hipgrave Ederveen AL, Vreeker GC, Clerc F, Holst S, Bondt A, Wuhrer M, van der Burgt YE. **Automation of High-Throughput Mass Spectrometry-Based Plasma N-Glycome Analysis with Linkage-Specific Sialic Acid Esterification.** *J Proteome Res.* 2015; 14(9):4080-6. DOI: 10.1021/acs.jproteome.5b00538.
109. Zoldos V, Horvat T, Lauc G. **Glycomics meets genomics, epigenomics and other high throughput omics for system biology studies.** *Curr Opin Chem Biol.* 2013; 17(1):34-40. DOI: 10.1016/j.cbpa.2012.12.007.
110. Aich U, Lakkub J, Liu A. **State-of-the-art technologies for rapid and high-throughput sample preparation and analysis of N-glycans from antibodies.** *ELECTROPHORESIS.* 2016; 37(11):1468-88. DOI: 10.1002/elps.201500551.
111. Dědová T, Grunow D, Kappert K, Flach D, Tauber R, Blanchard V. **The effect of blood sampling and preanalytical processing on human N-glycome.** *PloS one.* 2018; 13(7):e0200507. DOI: 10.1371/journal.pone.0200507.
112. Shubhakar A, Reiding KR, Gardner RA, Spencer DI, Fernandes DL, Wuhrer M. **High-Throughput Analysis and Automation for Glycomics Studies.** *Chromatographia.* 2015; 78(5-6):321-33. DOI: 10.1007/s10337-014-2803-9.
113. Varadi C, Lew C, Guttman A. **Rapid magnetic bead based sample preparation for automated and high throughput N-glycan analysis of therapeutic antibodies.** *Anal Chem.* 2014; 86(12):5682-7. DOI: 10.1021/ac501573g.
114. Strohal M, Hassman M, Kosata B, Kodicek M. **mMass data miner: an open source alternative for mass spectrometric data analysis.** *Rapid Commun Mass Spectrom.* 2008; 22(6):905-8. DOI: 10.1002/rcm.3444.
115. Damerell D, Ceroni A, Maass K, Ranzinger R, Dell A, Haslam SM. **Annotation of glycomics MS and MS/MS spectra using the GlycoWorkbench software tool.** *Methods Mol Biol.* 2015; 1273:3-15. DOI: 10.1007/978-1-4939-2343-4_1.
116. Damerell D, Ceroni A, Maass K, Ranzinger R, Dell A, Haslam SM. **The GlycanBuilder and GlycoWorkbench glycoinformatics tools: updates and new developments.** *Biol Chem.* 2012; 393(11):1357-62. DOI: 10.1515/hsz-2012-0135.
117. **Welcome to Python.org** [Available from: <https://www.python.org/>].
118. Jansen BC, Reiding KR, Bondt A, Hipgrave Ederveen AL, Palmblad M, Falck D, Wuhrer M. **MassyTools: A High-Throughput Targeted Data Processing Tool for Relative Quantitation and Quality Control Developed for Glycomic and Glycoproteomic MALDI-MS.** *J Proteome Res.* 2015; 14(12):5088-98. DOI: 10.1021/acs.jproteome.5b00658.
119. **9.2. math — Mathematical functions — Python 2.7.15 documentation** [Available from: <https://docs.python.org/2/library/math.html>].
120. **15.1. os — Miscellaneous operating system interfaces — Python 2.7.15 documentation** [Available from: <https://docs.python.org/2/library/os.html>].
121. **15.3. time — Time access and conversions — Python 2.7.15 documentation** [Available from: <https://docs.python.org/2/library/time.html>].
122. **24.1. Tkinter — Python interface to Tcl/Tk — Python 2.7.15 documentation** [Available from: <https://docs.python.org/2/library/tkinter.html>].

123. Oliphant TE. **Python for Scientific Computing**. *Computing in Science & Engineering*. 2007; 9(3):10-20. DOI: 10.1109/mcse.2007.58.
124. Millman KJ, Aivazis M. **Python for Scientists and Engineers**. *Computing in Science & Engineering*. 2011; 13(2):9-12. DOI: 10.1109/mcse.2011.36.
125. Walt Svd, Colbert SC, Varoquaux G. **The NumPy array: a structure for efficient numerical computation**. *Computing in Science & Engineering*. 2011; 13(2):22-30.
126. Hunter JD. **Matplotlib: A 2D graphics environment**. *Computing in science & engineering*. 2007; 9(3):90-5.
127. Anugraham M, Jacob F, Nixdorf S, Everest-Dass AV, Heinzelmann-Schwarz V, Packer NH. **Specific glycosylation of membrane proteins in epithelial ovarian cancer cell lines: glycan structures reflect gene expression and DNA methylation status**. *Mol Cell Proteomics*. 2014; 13(9):2213-32. DOI: 10.1074/mcp.M113.037085.
128. Balog CI, Stavenhagen K, Fung WL, Koeleman CA, McDonnell LA, Verhoeven A, Mesker WE, Tollenaar RA, Deelder AM, Wuhler M. **N-glycosylation of colorectal cancer tissues: a liquid chromatography and mass spectrometry-based investigation**. *Mol Cell Proteomics*. 2012; 11(9):571-85. DOI: 10.1074/mcp.M111.011601.
129. Abd Hamid UM, Royle L, Saldova R, Radcliffe CM, Harvey DJ, Storr SJ, Pardo M, Antrobus R, Chapman CJ, Zitzmann N, *et al*. **A strategy to reveal potential glycan markers from serum glycoproteins associated with breast cancer progression**. *Glycobiology*. 2008; 18(12):1105-18. DOI: 10.1093/glycob/cwn095.
130. Liu XE, Desmyter L, Gao CF, Laroy W, Dewaele S, Vanhooren V, Wang L, Zhuang H, Callewaert N, Libert C, *et al*. **N-glycomic changes in hepatocellular carcinoma patients with liver cirrhosis induced by hepatitis B virus**. *Hepatology*. 2007; 46(5):1426-35. DOI: 10.1002/hep.21855.
131. Vuckovic F, Theodoratou E, Thaci K, Timofeeva M, Vojta A, Stambuk J, Pucic-Bakovic M, Rudd PM, Derek L, Servis D, *et al*. **IgG Glycome in Colorectal Cancer**. *Clin Cancer Res*. 2016; 22(12):3078-86. DOI: 10.1158/1078-0432.CCR-15-1867.
132. Trbojevic-Akmacic I, Vilaj M, Lauc G. **High-throughput analysis of immunoglobulin G glycosylation**. *Expert Rev Proteomics*. 2016; 13(5):523-34. DOI: 10.1080/14789450.2016.1174584.
133. Lista S, Faltraco F, Hampel H. **Biological and methodical challenges of blood-based proteomics in the field of neurological research**. *Progress in neurobiology*. 2013; 101-102:18-34. DOI: 10.1016/j.pneurobio.2012.06.006.
134. Sogawa K, Noda K, Umemura H, Seimiya M, Kuga T, Tomonaga T, Nishimura M, Kanai F, Imazeki F, Takizawa H, *et al*. **Serum fibrinogen alpha C-chain 5.9 kDa fragment as a biomarker for early detection of hepatic fibrosis related to hepatitis C virus**. *Proteomics Clinical applications*. 2013; 7(5-6):424-31. DOI: 10.1002/prca.201200094.
135. Leichtle AB, Dufour JF, Fiedler GM. **Potentials and pitfalls of clinical peptidomics and metabolomics**. *Swiss Med Wkly*. 2013; 143:w13801. DOI: 10.4414/smww.2013.13801.

136. Kara H, Bayir A, Ak A, Degirmenci S, Akinici M, Agacayak A, Marcil E, Azap M. **Hemolysis associated with pneumatic tube system transport for blood samples.** *Pak J Med Sci.* 2014; 30(1):50-8. DOI: 10.12669/pjms.301.4228.
137. Sodi R, Darn SM, Stott A. **Pneumatic tube system induced haemolysis: assessing sample type susceptibility to haemolysis.** *Ann Clin Biochem.* 2004; 41(Pt 3):237-40. DOI: 10.1258/000456304323019631.
138. Knezevic A, Polasek O, Gornik O, Rudan I, Campbell H, Hayward C, Wright A, Kolcic I, O'Donoghue N, Bones J, *et al.* **Variability, heritability and environmental determinants of human plasma N-glycome.** *J Proteome Res.* 2009; 8(2):694-701. DOI: 10.1021/pr800737u.
139. Saldova R, Huffman JE, Adamczyk B, Muzinic A, Kattla JJ, Pucic M, Novokmet M, Abrahams JL, Hayward C, Rudan I, *et al.* **Association of medication with the human plasma N-glycome.** *J Proteome Res.* 2012; 11(3):1821-31. DOI: 10.1021/pr2010605.
140. Ventham NT, Gardner RA, Kennedy NA, Shubhakar A, Kalla R, Nimmo ER, Consortium I-B, Fernandes DL, Satsangi J, Spencer DI. **Changes to serum sample tube and processing methodology does not cause Intra-Individual [corrected] variation in automated whole serum N-glycan profiling in health and disease.** *PLoS One.* 2015; 10(4):e0123028. DOI: 10.1371/journal.pone.0123028.
141. Klein A. **Chapter 2 Human Total Serum N - Glycome.** In: Chemistry BTAiC, editor. 46: Elsevier; 2008. p. 51-85.
142. Streck A. **GitHub - xstreck1/HPACED: Highest Peak Alignment for Capillary Electrophoresis Data** [Available from: <https://github.com/xstreck1/HPACED>].
143. Evans JD. **Straightforward statistics for the behavioral sciences.** Pacific Grove: Brooks/Cole Pub. Co; 1996 1996. 600 p.
144. Hamouda H, Kaup M, Ullah M, Berger M, Sandig V, Tauber R, Blanchard V. **Rapid analysis of cell surface N-glycosylation from living cells using mass spectrometry.** *J Proteome Res.* 2014; 13(12):6144-51. DOI: 10.1021/pr5003005.
145. Alhadeff JA, Janowsky AJ. **Human serum alpha-L-fucosidase.** *Clin Chim Acta.* 1978; 82(1-2):133-40, <https://www.ncbi.nlm.nih.gov/pubmed/618676>.
146. Schauer R, Veh RW, Wember M. **Demonstration of neuraminidase activity in human blood serum and human milk using a modified, radioactively labelled alpha1-glycoprotein as substrate.** *Hoppe Seylers Z Physiol Chem.* 1976; 357(4):559-66, <https://www.ncbi.nlm.nih.gov/pubmed/964915>.
147. Berger-Achituv S, Budde-Schwartzman B, Ellis MH, Shenkman Z, Erez I. **Blood sampling through peripheral venous catheters is reliable for selected basic analytes in children.** *Pediatrics.* 2010; 126(1):e179-86. DOI: 10.1542/peds.2009-2920.
148. Wollowitz A, Bijur PE, Esses D, John Gallagher E. **Use of butterfly needles to draw blood is independently associated with marked reduction in hemolysis compared to intravenous catheter.** *Acad Emerg Med.* 2013; 20(11):1151-5. DOI: 10.1111/acem.12245.

149. Petricoin EF, Ardekani AM, Hitt BA, Levine PJ, Fusaro VA, Steinberg SM, Mills GB, Simone C, Fishman DA, Kohn EC, *et al.* **Use of proteomic patterns in serum to identify ovarian cancer.** *Lancet.* 2002; 359(9306):572-7. DOI: 10.1016/S0140-6736(02)07746-2.
150. Diamandis EP. **Cancer biomarkers: can we turn recent failures into success?** *J Natl Cancer Inst.* 2010; 102(19):1462-7. DOI: 10.1093/jnci/djq306.
151. Xu Y, Shen Z, Wiper DW, Wu M, Morton RE, Elson P, Kennedy AW, Belinson J, Markman M, Casey G. **Lysophosphatidic acid as a potential biomarker for ovarian and other gynecologic cancers.** *JAMA.* 1998; 280(8):719-23, <https://www.ncbi.nlm.nih.gov/pubmed/9728644>.
152. Kitajima K, Varki N, Sato C. **Advanced technologies in sialic acid and sialoglycoconjugate analysis.** *SialoGlyco Chemistry and Biology II*: Springer; 2013. p. 75-103.
153. Jakobsson E, Schwarzer D, Jokilammi A, Finne J. **Endosialidases: versatile tools for the study of polysialic acid.** *SialoGlyco Chemistry and Biology II*: Springer; 2012. p. 29-73.
154. Kumada Y, Ohigashi Y, Emori Y, Imamura K, Omura Y, Kishimoto M. **Improved lectin ELISA for glycosylation analysis of biomarkers using PS-tag-fused single-chain Fv.** *J Immunol Methods.* 2012; 385(1-2):15-22. DOI: 10.1016/j.jim.2012.07.021.
155. Hirabayashi J, Kuno A, Tateno H. **Development and applications of the lectin microarray.** *SialoGlyco Chemistry and Biology II*: Springer; 2014. p. 105-24.
156. Cummings RD, Etzler ME. **Antibodies and Lectins in Glycan Analysis.** In: nd, Varki A, Cummings RD, Esko JD, Freeze HH, Stanley P, *et al.*, editors. *Essentials of Glycobiology.* Cold Spring Harbor (NY)2009.
157. Walker R. **The use of lectins in histopathology.** *Pathology-Research and Practice.* 1989; 185(6):826-35.
158. Alley WR, Jr., Novotny MV. **Glycomic analysis of sialic acid linkages in glycans derived from blood serum glycoproteins.** *J Proteome Res.* 2010; 9(6):3062-72. DOI: 10.1021/pr901210r.
159. Wheeler SF, Domann P, Harvey DJ. **Derivatization of sialic acids for stabilization in matrix-assisted laser desorption/ionization mass spectrometry and concomitant differentiation of alpha(2 --> 3)- and alpha(2 --> 6)-isomers.** *Rapid Commun Mass Spectrom.* 2009; 23(2):303-12. DOI: 10.1002/rcm.3867.
160. de Haan N, Reiding KR, Habegger M, Reusch D, Falck D, Wuhrer M. **Linkage-specific sialic acid derivatization for MALDI-TOF-MS profiling of IgG glycopeptides.** *Anal Chem.* 2015; 87(16):8284-91. DOI: 10.1021/acs.analchem.5b02426.
161. Holst S, Wuhrer M, Rombouts Y. **Glycosylation Characteristics of Colorectal Cancer.** In: Research BTAiC, editor.: Academic Press.
162. Li H, Gao W, Feng X, Liu BF, Liu X. **MALDI-MS analysis of sialylated N-glycan linkage isomers using solid-phase two step derivatization method.** *Anal Chim Acta.* 2016; 924:77-85. DOI: 10.1016/j.aca.2016.04.023.
163. Holst S, Heijs B, de Haan N, van Zeijl RJ, Briaire-de Bruijn IH, van Pelt GW, Mehta AS, Angel PM, Mesker WE, Tollenaar RA, *et al.* **Linkage-Specific in Situ Sialic Acid**

Derivatization for N-Glycan Mass Spectrometry Imaging of Formalin-Fixed Paraffin-Embedded Tissues. *Anal Chem.* 2016; 88(11):5904-13. DOI: 10.1021/acs.analchem.6b00819.

164. Yang S, Jankowska E, Kosikova M, Xie H, Cipollo J. **Solid-Phase Chemical Modification for Sialic Acid Linkage Analysis: Application to Glycoproteins of Host Cells Used in Influenza Virus Propagation.** *Anal Chem.* 2017; 89(17):9508-17. DOI: 10.1021/acs.analchem.7b02514.

165. Siegel RL, Miller KD, Jemal A. **Cancer Statistics, 2017.** *CA Cancer J Clin.* 2017; 67(1):7-30. DOI: 10.3322/caac.21387.

166. Mathieu KB, Bedi DG, Thrower SL, Qayyum A, Bast RC, Jr. **Screening for ovarian cancer: imaging challenges and opportunities for improvement.** *Ultrasound Obstet Gynecol.* 2018; 51(3):293-303. DOI: 10.1002/uog.17557.

167. Reid BM, Permuth JB, Sellers TA. **Epidemiology of ovarian cancer: a review.** *Cancer Biol Med.* 2017; 14(1):9-32. DOI: 10.20892/j.issn.2095-3941.2016.0084.

168. Taylor DD, Gercel-Taylor C. **MicroRNA signatures of tumor-derived exosomes as diagnostic biomarkers of ovarian cancer.** *Gynecol Oncol.* 2008; 110(1):13-21. DOI: 10.1016/j.ygyno.2008.04.033.

169. Visintin I, Feng Z, Longton G, Ward DC, Alvero AB, Lai Y, Tenthorey J, Leiser A, Flores-Saaib R, Yu H, *et al.* **Diagnostic markers for early detection of ovarian cancer.** *Clin Cancer Res.* 2008; 14(4):1065-72. DOI: 10.1158/1078-0432.CCR-07-1569.

170. Mor G, Visintin I, Lai Y, Zhao H, Schwartz P, Rutherford T, Yue L, Bray-Ward P, Ward DC. **Serum protein markers for early detection of ovarian cancer.** *Proc Natl Acad Sci U S A.* 2005; 102(21):7677-82. DOI: 10.1073/pnas.0502178102.

171. Kim YJ, Varki A. **Perspectives on the significance of altered glycosylation of glycoproteins in cancer.** *Glycoconj J.* 1997; 14(5):569-76. DOI: 10.1023/A:1018580324971.

172. Arnold JN, Saldova R, Hamid UMA, Rudd PM. **Evaluation of the serum N-linked glycome for the diagnosis of cancer and chronic inflammation.** *Proteomics.* 2008; 8(16):3284-93. DOI: 10.1002/pmic.200800163.

173. Brockhausen I, Narasimhan S, Schachter H. **The biosynthesis of highly branched N-glycans: studies on the sequential pathway and functional role of N-actylglucosaminyltransferases I, II, III, IV, V and VI.** *Biochimie.* 1988; 70(11):1521-33. DOI: [https://doi.org/10.1016/0300-9084\(88\)90289-1](https://doi.org/10.1016/0300-9084(88)90289-1).

174. Huhn C, Selman MH, Ruhaak LR, Deelder AM, Wuhrer M. **IgG glycosylation analysis.** *Proteomics.* 2009; 9(4):882-913. DOI: 10.1002/pmic.200800715.

175. Haakensen VD, Steinfeld I, Saldova R, Shehni AA, Kifer I, Naume B, Rudd PM, Borresen-Dale AL, Yakhini Z. **Serum N-glycan analysis in breast cancer patients--Relation to tumour biology and clinical outcome.** *Mol Oncol.* 2016; 10(1):59-72. DOI: 10.1016/j.molonc.2015.08.002.

176. Ogawa J-i, Inoue H, Koide S. **α -2,3-sialyltransferase type 3N and α -1,3-fucosyltransferase type VII are related to sialyl Lewisx synthesis and patient survival from lung carcinoma.** *Cancer.* 2000; 79(9):1678-85. DOI: 10.1002/(SICI)1097-0142(19970501)79:9<1678::AID-CNCR7>3.0.CO;2-8.

177. Holst S, Deuss AJM, van Pelt GW, van Vliet SJ, Garcia-Vallejo JJ, Koeleman CAM, Deelder AM, Mesker WE, Tollenaar RA, Rombouts Y. **N-glycosylation profiling of colorectal cancer cell lines reveals association of fucosylation with differentiation and CDX1/villin mRNA expression.** *Mol Cell Proteomics*. 2015:mcp-M115.
178. Saldova R, Fan Y, Fitzpatrick JM, Watson RW, Rudd PM. **Core fucosylation and alpha2-3 sialylation in serum N-glycome is significantly increased in prostate cancer comparing to benign prostate hyperplasia.** *Glycobiology*. 2011; 21(2):195-205. DOI: 10.1093/glycob/cwq147.
179. Wang PH, Lee WL, Juang CM, Yang YH, Lo WH, Lai CR, Hsieh SL, Yuan CC. **Altered mRNA expressions of sialyltransferases in ovarian cancers.** *Gynecol Oncol*. 2005; 99(3):631-9. DOI: 10.1016/j.ygyno.2005.07.016.
180. Wen KC, Sung PL, Hsieh SL, Chou YT, Lee OK, Wu CW, Wang PH. **alpha2,3-sialyltransferase type I regulates migration and peritoneal dissemination of ovarian cancer cells.** *Oncotarget*. 2017; 8(17):29013-27. DOI: 10.18632/oncotarget.15994.
181. Sung PL, Wen KC, Horng HC, Chang CM, Chen YJ, Lee WL, Wang PH. **The role of alpha2,3-linked sialylation on clear cell type epithelial ovarian cancer.** *Taiwan J Obstet Gynecol*. 2018; 57(2):255-63. DOI: 10.1016/j.tjog.2018.02.015.
182. Weiz S, Wiczorek M, Schwedler C, Kaup M, Braicu EI, Sehouli J, Tauber R, Blanchard V. **Acute-phase glycoprotein N-glycome of ovarian cancer patients analyzed by CE-LIF.** *ELECTROPHORESIS*. 2016; 37(11):1461-7. DOI: 10.1002/elps.201500518.
183. Kanoh Y, Mashiko T, Danbara M, Takayama Y, Ohtani S, Egawa S, Baba S, Akahoshi T. **Changes in serum IgG oligosaccharide chains with prostate cancer progression.** *Anticancer Res*. 2004; 24(5B):3135-9, <https://www.ncbi.nlm.nih.gov/pubmed/15510601>.
184. Ruhaak LR, Miyamoto S, Lebrilla CB. **Developments in the identification of glycan biomarkers for the detection of cancer.** *Mol Cell Proteomics*. 2013; 12(4):846-55. DOI: 10.1074/mcp.R112.026799.
185. Kailemia MJ, Park D, Lebrilla CB. **Glycans and glycoproteins as specific biomarkers for cancer.** *Analytical and Bioanalytical Chemistry*. 2017; 409(2):395-410. DOI: 10.1007/s00216-016-9880-6.
186. Adamczyk B, Tharmalingam T, Rudd PM. **Glycans as cancer biomarkers.** *Biochimica et biophysica acta*. 2012; 1820(9):1347-53. DOI: 10.1016/j.bbagen.2011.12.001.
187. Mechref Y, Hu Y, Garcia A, Hussein A. **Identifying cancer biomarkers by mass spectrometry-based glycomics.** *ELECTROPHORESIS*. 2012; 33(12):1755-67. DOI: 10.1002/elps.201100715.
188. O'Bryant SE, Gupta V, Henriksen K, Edwards M, Jeromin A, Lista S, Bazenet C, Soares H, Lovestone S, Hampel H, *et al.* **Guidelines for the standardization of preanalytic variables for blood-based biomarker studies in Alzheimer's disease research.** *Alzheimer's & Dementia*. 2015; 11(5):549-60. DOI: <https://doi.org/10.1016/j.jalz.2014.08.099>.
189. Dakappagari N, Zhang H, Stephen L, Amaravadi L, Khan MU. **Recommendations for clinical biomarker specimen preservation and stability assessments.** *Bioanalysis*. 2017; 9(8):643-53. DOI: 10.4155/bio-2017-0009.

190. Kellogg MD, Ellervik C, Morrow D, Hsing A, Stein E, Sethi AA. **Preanalytical Considerations in the Design of Clinical Trials and Epidemiological Studies.** *Clinical Chemistry*. 2015; 61(6):797, <http://clinchem.aaccjnl.org/content/61/6/797.abstract>.

Appendix

Glycan trait calculation

$$\text{HIGH-MANNOSE} = N2H5 + N2H6 + N2H7 + N2H8$$

$$\text{COMPLEX ASIALO} = N3H4 + N4H3 + N4H5 + N5H4 + N5H5 + N5H6$$

$$\text{COMPLEX ASIALO FUCOSYLATED} = N4H3F1 + N4H4F1 + N4H5F1 + N5H4F1 + N5H5F1 + N5H5F2 + N5H6F1$$

$$\text{HYBRID} = N3H5A1 + N3H6A1 + N3H5D1 + N3H6D1$$

$$\text{COMPLEX MONOANTENNARY} = N3H4A1 + N3H4D1$$

$$\text{COMPLEX BIANTENNARY} = N4H4A1 + N4H4D1 + N4H5A1 + N4H5D1 + N4H5A2 + N4H5D1A1 + N4H5D2$$

$$\text{COMPLEX TRIANTENNARY} = N5H5D1 + N5H6A1 + N5H6D1 + N5H5D2 + N5H6D1A1 + N5H6D2 + N5H6A3 + N5H6D1A2 + N5H6D2A1 + N5H6D3$$

$$\text{COMPLEX TETRAANTENNARY} = N6H7D1A1 + N6H7D2 + N6H7D1A2 + N6H7D2A1 + N6H7D1A3 + N6H7D2A2 + N6H7D3A1$$

$$\text{FUCOSYLATED COMPLEX BIANTENNARY} = N4H5A1F1 + N4H5D1F1 + N4H5A2F1 + N4H5D1A1F1 + N4H5D2F1$$

$$\text{FUCOSYLATED COMPLEX TRIANTENNARY} = N5H5D1F1 + N5H6D1F1 + N5H5D1A1F1 + N5H5D2F1 + N5H6D1A1F1 + N5H6D2F1 + N5H6D1A2F1 + N5H6D2A1F1 + N5H6D3F1 + N5H6D1A2F2 + N5H6D2A1F2$$

$$\text{FUCOSYLATED COMPLEX TETRAANTENNARY} = N6H7D1A1F1 + N6H7D1A2F1 + N6H7D2A1F1 + N6H7D1A3F1 + N6H7D2A2F1 + N6H7D3A1F1 + N6H7D1A3F2 + N6H7D2A2F2$$

$$\text{BIANTENNARY } \alpha\text{-2,3} = N4H4A1 + N4H5A1 + N4H5A2 + (1/2) * (N4H5D1A1)$$

$$\text{BIANTENNARY } \alpha\text{-2,6} = N4H4D1 + N4H5D1 + (1/2) * (N4H5D1A1)$$

$$\text{TRIANTENNARY } \alpha\text{-2,3} = N5H6A1 + N5H6A3 + (1/2) * (N5H6D1A1) + (2/3) * (N5H6D1A2) + (1/3) * (N5H6D2A1)$$

$$\text{TRIANTENNARY } \alpha\text{-2,6} = N5H5D1 + N5H6D1 + N5H5D2 + N5H6D2 + N5H6D3 + (1/2) * (N5H6D1A1) + (1/3) * (N5H6D1A2) + (2/3) * (N5H6D2A1)$$

$$\text{TETRAANTENNARY } \alpha\text{-2,3} = (1/2) * (N6H7D1A1 + N6H7D2A2) + (2/3) * (N6H7D1A2) + (1/3) * (N6H7D2A1) + (3/4) * (N6H7D1A3) + (1/4) * (N6H7D3A1)$$

TETRAANTENNARY α -2,6 = (1/2) * (N6H7D1A1 + N6H7D2A2) + (1/3) * (N6H7D1A2) + (2/3) * (N6H7D2A1) + (1/4) * (N6H7D1A3) + (3/4) * (N6H7D3A1) + N6H7D2

FUCOSYLATED COMPLEX BIANTENNARY α -2,3 = N4H5A1F1 + N4H5A2F1 + (1/2) * (N4H5D1A1F1)

FUCOSYLATED COMPLEX BIANTENNARY α -2,6 = N4H5D1F1 + N4H5D2F1 + (1/2) * (N4H5D1A1F1)

FUCOSYLATED COMPLEX TRIANTENNARY α -2,3 = (1/2) * (N5H5D1A1F1 + N5H6D1A1F1) + (2/3) * (N5H6D1A2F1) + (1/3) * (N5H6D2A1F1)

FUCOSYLATED COMPLEX TRIANTENNARY α -2,6 = N5H5D1F1 + N5H6D1F1 + N5H5D2F1 + N5H6D2F1 + N5H6D3F1 + (1/2) * (N5H5D1A1F1 + N5H6D1A1F1) + (1/3) * (N5H6D1A2F1) + (2/3) * (N5H6D2A1F1)

FUCOSYLATED COMPLEX TETRAANTENNARY α -2,3 = (1/2) * (N6H7D1A1F1 + N6H7D2A2F1 + N6H7D2A2F2) + (2/3) * (N6H7D1A2F1) + (1/3) * (N6H7D2A1F1) + (3/4) * (N6H7D1A3F1 + N6H7D1A3F2) + (1/4) * (N6H7D3A1F1)

FUCOSYLATED COMPLEX TETRAANTENNARY α -2,6 = (1/2) * (N6H7D1A1F1 + N6H7D2A2F1 + N6H7D2A2F2) + (1/3) * (N6H7D1A2F1) + (2/3) * (N6H7D2A1F1) + (1/4) * (N6H7D1A3F1 + N6H7D1A3F2) + (3/4) * (N6H7D3A1F1)

FUCOSYLATED COMPLEX α -2,3 = FUCOSYLATED COMPLEX BIANTENNARY α -2,3 + FUCOSYLATED COMPLEX TRIANTENNARY α -2,3 + FUCOSYLATED COMPLEX TETRAANTENNARY α -2,3

FUCOSYLATED COMPLEX α -2,6 = FUCOSYLATED COMPLEX BIANTENNARY α -2,6 + FUCOSYLATED COMPLEX TRIANTENNARY α -2,6 + FUCOSYLATED COMPLEX TETRAANTENNARY α -2,6

AFUCOSYLATED COMPLEX α -2,3 = COMPLEX BIANTENNARY α -2,3 + COMPLEX TRIANTENNARY α -2,3 + COMPLEX TETRAANTENNARY α -2,3

AFUCOSYLATED COMPLEX α -2,6 = COMPLEX BIANTENNARY α -2,6 + COMPLEX TRIANTENNARY α -2,6 + COMPLEX TETRAANTENNARY α -2,6

COMPLEX α -2,3 = FUCOSYLATED COMPLEX α -2,3 + AFUCOSYLATED COMPLEX α -2,3

COMPLEX α -2,6 = FUCOSYLATED COMPLEX α -2,6 + AFUCOSYLATED COMPLEX α -2,6

α -2,3/ α -2,6 RATIO = X α -2,3 / X α -2,6

Absolute sialylation

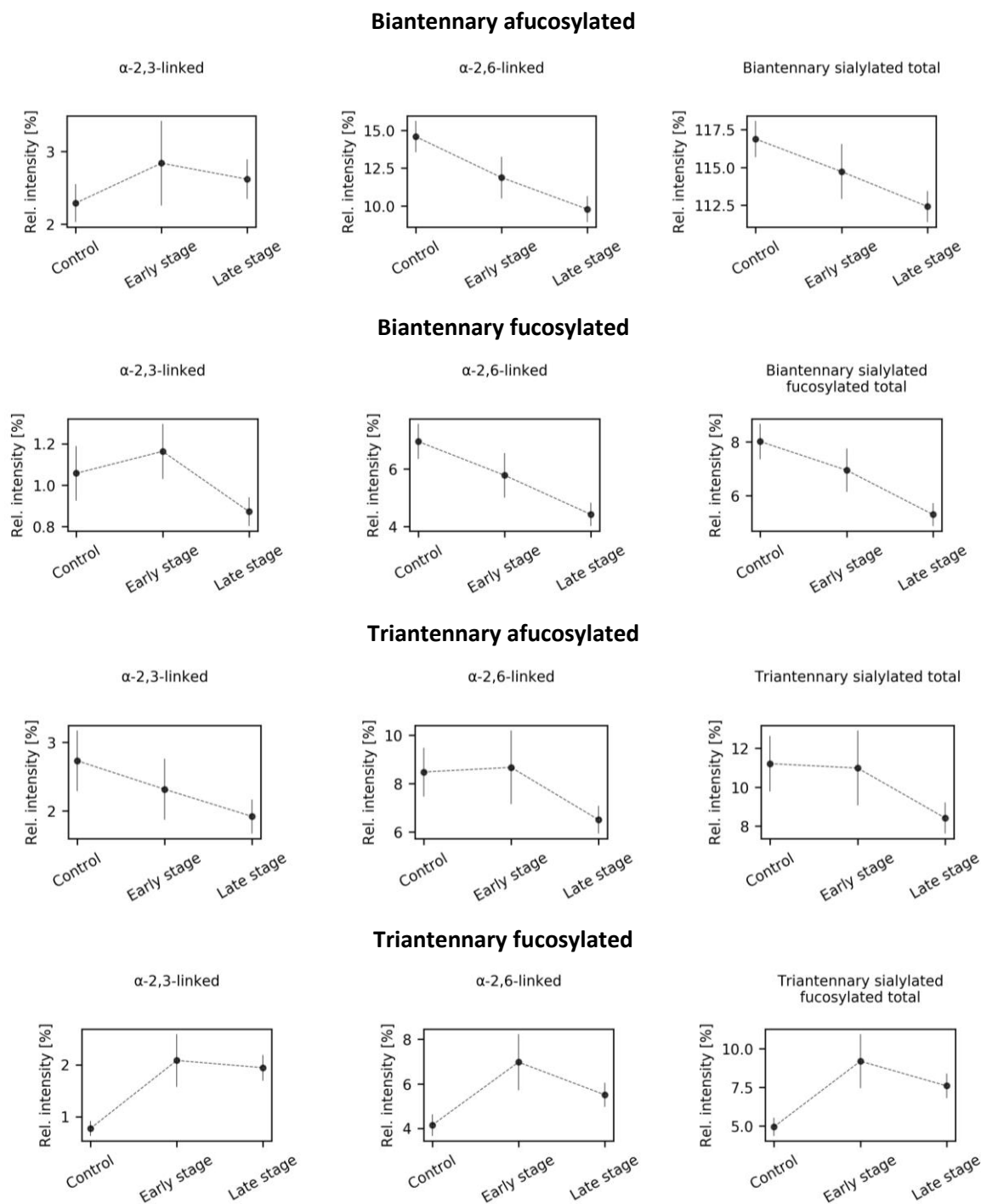


Figure A1 Mean and 95% confidence intervals of linkage-specific sialylation and total relative intensities of complex sialylated N-glycans during ovarian cancer progression.

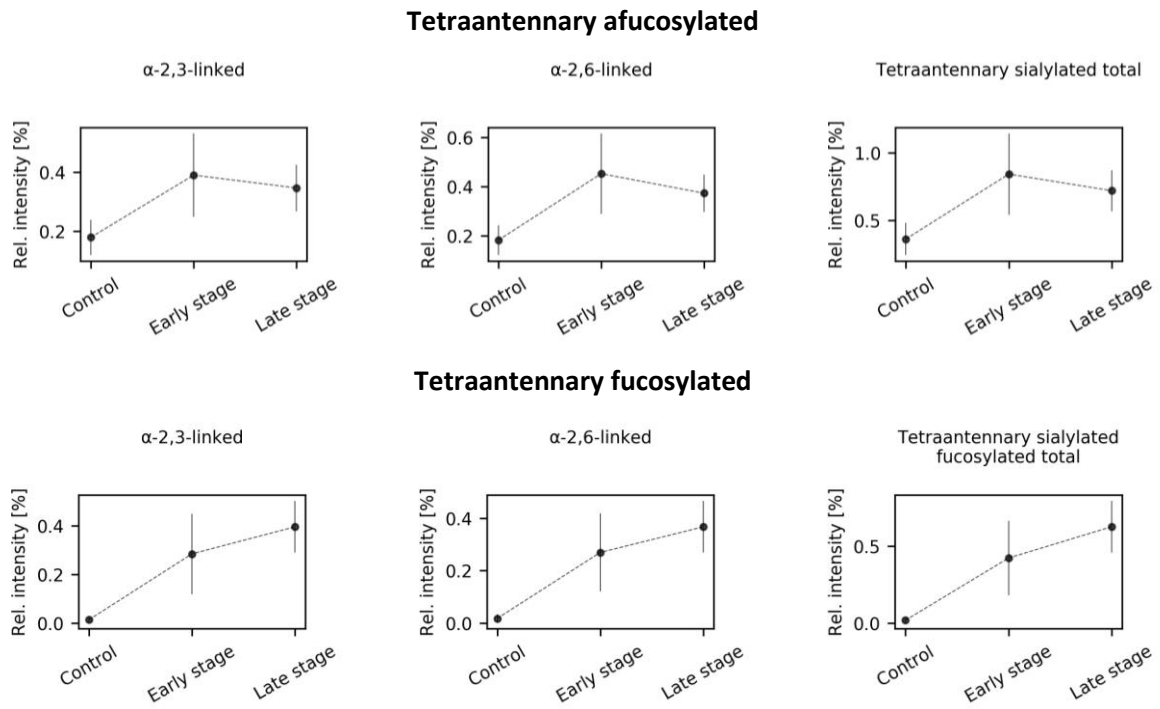


Figure A2 Mean and 95% confidence intervals of linkage-specific sialylation and total relative intensities of complex sialylated N-glycans during ovarian cancer progression.

List of publications and conferences

Publications

Dědová T, Grunow D, Kappert K, Flach D, Tauber R, Blanchard V. **The effect of blood sampling and preanalytical processing on human N-glycome.** *PloS one*. 2018 Jul 11;13(7):e0200507. DOI: <https://doi.org/10.1371/journal.pone.0200507>

Montacir, H., Freyer, N., Knöspel, F., Urbaniak, T., Dědová, T., Berger, M., Damm, G., Tauber, R., Zeilinger, K., Blanchard, V., 2017. **The Cell-Surface N-Glycome of Human Embryonic Stem Cells and Differentiated Hepatic Cells thereof.** *ChemBioChem*. doi:10.1002/cbic.201700001

Celá, A., Mádr, A., Dědová, T., Pelcová, M., Jeřeta, M., Žáková, J., Crha, I., Glatz, Z., 2016. **MEKC-LIF method for analysis of amino acids after on-capillary derivatization by transverse diffusion of laminar flow profiles mixing of reactants for assessing developmental capacity of human embryos after in vitro fertilization.** *Electrophoresis* 37, 2305-2312.

Conference posters

Dědová, T., Tauber, R., and Véronique Blanchard. Congress: »Biotechnology 2020+«, Berlin, Germany, **Sialic acid linkages in ovarian cancer: A tool for improved diagnostics.** 2018

Dědová, T., Grunow, D., Kappert, K., Flach, D., Tauber, R. and Véronique Blanchard. Congress: „new and emerging technologies“, Potsdam-Golm, Germany, **The effect of preanalytics on human N-glycome analysis.** 2017

Dědová, T., Blanchard, V. and Rudolf Tauber. **The effect of preanalytical conditions on human serum N-glycome.** 13th International Interdisciplinary Meeting on Bioanalysis (CECE2016). Brno, Czech Republic: Institute of Analytical Chemistry of the CAS, v. v. i., Brno, Czech Republic, 2016. p. 113-115, 3 pp. ISBN 978-80-904959-4-4. 2015

Dědová, T., Grunow, D., Blanchard, V. and Rudolf Tauber. Deutsche Vereinte Gesellschaft für Klinische Chemie und Laboratoriumsmedizin (DGKL2015), Leipzig, **The Effect of preanalytical conditions on Human serum N-glycome as judged by MALDI-TOF-MS.** 2013

Dědová, T., Celá, A., Mádr, A. and Zdeněk Glatz. **Naphthalene-2,3-dicarbaldehyde derivatization of amino acids - an improved technique for minimization of benzoin condensation.** 10th International Interdisciplinary Meeting on Bioanalysis (CECE2013) *Chemické listy*, Praha: Česká společnost chemická, 2013, vol. 107, S3, p. "S351" - "S352". ISSN 0009-2770.

Curriculum Vitae

Education

2014-present

PhD candidate in Biochemistry Freie Universität Berlin, Germany *Serum glycome in health and disease*. - Supervisor Prof. Dr. V. Blanchard

2012-2014

Mgr. in Analytical Biochemistry, GPA 1.1/1 Masaryk University, Brno, Czech Republic *Determination of Amino Acids by Capillary Electrophoresis with Fluorescence Detection for Metabolomic Studies*. - Supervisor Prof. RNDr. Z. Glatz, CSc.

2009-2012

Bc. in Medical Laboratory Technician, GPA 1.39/1 Masaryk University, Brno, Czech Republic *Options in laboratory measurement of T lymphocyte activation*. – Supervisor prof. MUDr. Vojtěch Thon, Ph.D.

2005-2009

Gymnasium Broumov (High School) Broumov, Czech Republic Final exams in Czech, English, Biology and Chemistry.

Awards and scholarships

2015-2017

Sonnenfeld-Stiftung Scholarship.

2014

Merit scholarship for outstanding results at Masaryk University Brno, Faculty of Science, Czech Republic.

Experience

2017-2018

Labor Berlin - Charité Vivantes GmbH, Berlin, Germany

2014-2018

Institute of Laboratory Medicine, Clinical Chemistry and Pathobiochemistry, Charité Medical University, Berlin, Germany

2010

Clinical laboratories of Faculty hospital Brno, Brno, Czech Republic